School of Chemical Engineering

Investigation into Ash Related Issues during Co-combustion of Coal and Biomass: Development of a Co-firing Advisory Tool

Veena Doshi Arun Kumar

This thesis is presented for the Degree of
Doctor of Philosophy
of
Curtin University of Technology

April 2007

Declaration

To the best of my knowledge and belief this thesis contains no material previously published by any other person except where due acknowledgment has been made.

This thesis contains no material which has been accepted for the award of any other degree or diploma in any university.

Signature: .....

Date: 26/04/07 .....

Abstract

The co-firing technology of coal with biomass has been implemented to enhance the usage of biomass in power generation, thus reducing the release of greenhouse gas emissions. This study deals with the fireside issues, namely ash-related issues that arise during co-combustion of coal and biomass takes place. Ash release from biomass can lead to ash deposition problems such as fouling and slagging on surfaces of power generation boilers. The scope of this work includes the development of a conceptual model that predicts the ash release behaviour and chemical composition of inorganics in coal and biomass when combusted. An advanced analytical method was developed and introduced in this work to determine the speciation of biomass. The method known as pH extraction analysis was used to determine the inorganic speciation in three biomass samples, namely wood chips, wood bark and straw. The speciation of biomass and coal was used as an input to the model to predict the behaviour and release of ash. It was found that the main gas phases during the combustion of biomass are KCl, NaCl, K_2SO_4 and Na_2SO_4. Gas-to-particle formation calculations were carried out to determine the chemical composition of coal and biomass when cooling takes place in the boiler. The results obtained in this work can be used in future work to determine the ash deposition of coal and biomass in boilers.

Acknowledgment

Firstly, I wish to acknowledge Dr Hari Babu Vuthaluru, my Supervisor for giving me the opportunity to pursue my PhD in this interesting 'ever-green' field of renewable energy. His confidence in my ability and his continuous guide throughout the last four years is greatly appreciated. I am also hugely grateful to my Industrial Supervisor, Dr Rob Korbee, for his on-going support and concern for the progress of my thesis. His deep knowledge in this field of research has never failed to amaze me; whilst his strong interest to perform his best is definitely infectious and appreciated.

This PhD would not have been possible without the joint scholarship set up by Dr Hari Vuthaluru of the Chemical Engineering Department, Curtin University of Technology and Dr Jaap Kiel of the Biomass Department of the Energy Research Centre of Netherlands (ECN), as part of their on going collaboration. I feel truly privileged to have been given the opportunity to carry out my research work at ECN as I have gained extensive knowledge and experience that goes beyond the scope of this thesis. A deep acknowledgement also goes to Prof Moses Tade, for both the financial support and also his genuine care for the well being of his students.

I am also gratified to the Environmental Risk Assessment Team of ECN, namely Dr Rob Comans, Andre van Zomeren and Dr Hans Meeussen for their valuable input in the experimental and modelling related work. A heart felt gratitude also goes to Jasper Lensselink , Paul de Wild and Dr Christine Bertrand for their help during the course of this thesis. I also wish to acknowledge Associate Professor Raj Gupta of University of Newcastle for his mentorship and ideas on the coal ash modelling work. The input of undergraduates involved in this research, namely Sarah Vorster, Stacey Pereira, Angus Addison and John Layfield is duly acknowledged.

Finally, I am truly indebted to my parents and siblings for their continuous encouragement, inspiring words (through long distance conversations) and their faith in me throughout these years. Gratitude also goes out for my friends in Perth and Alkmaar and my unlimited family for their wonderful company and constant motivation. To my Eternal Friend, thank you for your constant love and care.

Table of Contents

Acknowledgment ..... **I**

List of Figures ..... **V**

List of Tables ..... **IX**

Nomenclature ..... **X**

CHAPTER 1

Introduction and Objectives **1**

1.1 Objective 2

1.2 Outline of thesis 3

CHAPTER 2

Literature Review **4**

2.1 Co-combustion of Biomass with Coal 4

2.1.2 Challenges in Co-firing of Biomass 5

2.2 Ash Formation during Coal Combustion 6

2.2.1 Coal Characteristics 6

2.2.2 Ash formation 7

2.2.3 Ash Formation Models 8

2.3 Ash Formation during Biomass Combustion 10

2.3.1 Biomass Characterisation 10

2.3.2 Ash Forming Elements 14

2.3.3 Behaviour of Inorganic matter 15

2.3.4 Ash formation Mechanisms 16

2.5 Summary of Literature Review 22

CHAPTER 3

Biomass Speciation Modeling **24**

3.1 Inorganic Matter in Biomass 25

3.2 Determination of Biomass Speciation 27

3.3 Experimental Procedures 30

3.3.1 Coal/Biomass Selection 30

3.3.2 pH dependent leaching 31

3.3.3 ICP analysis 32

3.3.4 Ion Chromatography 32
3.3.5 HFO extraction 33
3.3.6 SHA Extraction 33
3.3.7 Kinetic Experiments 34
3.3.8 Lab Scale Combustion Simulator 34
3.4 Speciation model development 37
3.4.1 MINTEQA2Thermochemical Model 37
3.4.2 LeachXS Thermochemical Model 41

CHAPTER 4

Speciation Results and Validation 44

4.1 pH extraction analysis 44
4.2 MINTEQA2 Modeling Results 52
4.3 LeachXS Results 56
4.4 Comparison between pH Extraction and CF Method 67
4.5 Ash release results 73

CHAPTER 5

Ash Formation Modeling 80

5.1 High Temperature Thermochemistry 81
5.1.1 Application of FACTSAGE 81
5.2 Gas-to-Particle Conversion Modeling 87
5.2.1 Homogeneous and Heterogeneous Condensation 89
5.2.2 Ash particle formation 91
5.2.3 Overall Model 94

CHAPTER 6

Practical Implications 96
6.1 Determination of biomass speciation 97
6.3 Ash release behaviour 99
6.4 Interaction between coal and biomass ash 100
6.5 Gas-to-particle formation 101

CHAPTER 7

Conclusion and Recommendations 102

7.1 Characterisation of fuel 102
7.2 Ash Formation Modelling 103
7.3 Recommendations for future work 104

APPENDICES

Appendix A

Summary of coal and biomass composition 106

Appendix B

Chemical Fractionation Experimental Method 107

Appendix C

pH Extraction Method 108

Appendix D

Speciation Modelling 111

Appendix E

High temperature thermochemistry 119

Appendix F

Condensation calculations 124

References 128

List of Publications…… 133

List of Figures

Figure 2.1	Organic and inorganic matters in a coal particle	7
Figure 2.2	Ash formation during coal combustion	8
Figure 2.3	Schematic of the chemical fractionation and the thermal behaviour of inorganic matter in biomass	12
Figure 2.4	Experimental procedure of the Chemical Fractional technique	13
Figure 2.5	Formation of Particle by Homogeneous Nucleation	17
Figure 2.6	Gibbs free energy for homogeneous nucleation	20
Figure 2.7	Interaction between coal and biomass during combustion	23
Figure 3.1	Schematic flow diagram of ash formation mechanisms and approach taken in modeling the ash formation pathway	24
Figure 3.2	Step-by-step procedure used for the determination of biomass speciation	29
Figure 3.3	Chemical compositions of the fuels studied	30
Figure 3.4	The burner and reactor tube of the lab-scale combustion simulator	35
Figure 3.5	Calculating Chemical Speciation using MINTEQA2	40
Figure 3.6	Speciation determination using LeachXS	42
Figure 4.1	pH dependent extractions of K and Na	45
Figure 4.2	pH dependent extractions of Ca and Mg	46
Figure 4.3	pH dependent extractions of Al and Si	47
Figure 4.4	pH dependent extractions of Cl and DOC	48
Figure 4.5	pH dependent extractions of SO_4 and PO_4	49
Figure 4.6	pH dependent extraction of oxalate	50
Figure 4.7	Leaching efficiency of pH extraction tests	52
Figure 4.8	Speciation of K in wood chips obtained from MINTEQA2 model	54
Figure 4.9	Speciation of Na in wood chips obtained from MINTEQA2 model	54

Figure 4.10	Speciation of Ca in wood chips obtained from MINTEQA2 model	55
Figure 4.11	General speciation for biomass with LeachXS	58
Figure 4.12	Speciation of K element in wood chips	59
Figure 4.13	Speciation of Na element in wood chips	59
Figure 4.14	Speciation of Ca element in wood chips	60
Figure 4.15	Speciation of Mg element in wood chips	60
Figure 4.16	Speciation of Si element in wood chips	61
Figure 4.17	Speciation of Al element in wood chips	62
Figure 4.18	Inorganics in wood chips using chemical fractionation method	69
Figure 4.19	Inorganic speciation of wood chips using pH extraction method	69
Figure 4.20	Inorganics in wood bark using chemical fractionation method	70
Figure 4.21	Inorganic speciation of wood bark using pH extraction method	70
Figure 4.22	Inorganics in straw using chemical fractionation method	71
Figure 4.23	Inorganic speciation of straw using pH extraction method	71
Figure 4.24	Release of inorganics from fuel during combustion as a function of time	72
Figure 4.25	Quantity and distribution of inorganic matter released from fuels during combustion	73
Figure 4.26	Comparison between K speciation and release data	75
Figure 4.27	Comparison between Na speciation and release data	75
Figure 4.28	Comparison between Ca speciation and release data	76
Figure 4.29	Comparison between Mg speciation and release data	76
Figure 4.30	Comparison between P speciation and release data	77
Figure 4.31	Comparison between S speciation and release data	77
Figure 4.32	Comparison between Cl speciation and release data	78
Figure 5.1	Schematic of ash formation model of coal/biomass	79

Figure 5.2	Elemental analysis of various fuels studied	81
Figure 5.3	High temperature distribution for K elements in wood chips	82
Figure 5.4	High temperature distribution for Na elements in wood chips	83
Figure 5.5	High temperature distribution for Ca elements in wood chips	83
Figure 5.6	High temperature distribution for Cl elements in wood chips	84
Figure 5.7	Homogeneous and heterogeneous condensation occurrence during fuel combustion	88
Figure 5.8	Average particle size distribution for coal ash	93
Figure 6.1	Schematic of a conceptual model showing the co-firing advisory tool functions	96
Figure B.1	Chemical fractionation experimental procedure	106
Figure C.1	Reproducibility of leaching data for wood samples	109
Figure D.1	Speciation for K element in wood bark	111
Figure D.2	Speciation for Na element in wood bark	112
Figure D.3	Speciation for Ca element in wood bark	112
Figure D.4	Speciation for Mg element in wood bark	113
Figure D.5	Speciation for Al element in wood bark	113
Figure D.6	Speciation for Si element in wood bark	114
Figure D.7	Speciation for K element in straw	114
Figure D.8	Speciation for Na element in straw	115
Figure D.9	Speciation for Ca element in straw	115
Figure D.10	Speciation for Mg element in straw	116
Figure D.11	Speciation for Al element in straw	116
Figure D.12	Speciation for Si element in straw	117
Figure E.1	High temperature distribution for K elements in wood bark	119
Figure E.2	High temperature distribution for Na elements in wood bark	119

Figure E.3	High temperature distribution for Ca elements in wood bark	120
Figure E.4	High temperature distribution for Cl elements in wood bark	120
Figure E.5	High temperature distribution for K elements in co-fired blend	121
Figure E.6	High temperature distribution for Na elements in co-fired blend	121
Figure E.7	High temperature distribution for Ca elements in co-fired blend	122
Figure E.8	High temperature distribution for Cl elements in co-fired blend	122

List of Tables

Table 2.1	Functions of the elements present in biomass	11
Table 3.1	Speciation of biomass based on literature review summary	27
Table 3.2	Summary of LCS features	36
Table 3.3	Solid and liquid phase partitioning	43
Table 4.1	Compilation of the formations of species predicted through MINTEQA2 model	56
Table 4.2	Wood chips speciation interpretation from LeachXS	63
Table 4.3	Wood bark speciation interpretation from LeachXS	64
Table 4.4	Straw speciation interpretation from LeachXS	66
Table 4.5	Comparison of elements leached using CF and pH extraction method	68
Table 5.1	Composition distribution of gaseous and solid phases derived from FACTSAGE at various temperature ranges	85
Table 5.2	Homogeneous and heterogeneous temperature occurrence for the main gas phases in biomass	92
Table A.1	Proximate, ultimate and elemental analysis of wood bark, wood chip, straw and Polish coal used in this research	105
Table D.1	Solubility constant values for the various compounds found in biomass	110
Table D.1	Input concentrations fed into LeachXS	111
Table E.1	Input concentration of fuels fed into FACTSAGE for equilibrium calculations	118
Table F.1	Gas-to-particle conversion calculations for KCl	123
Table F.2	Gas-to-particle conversion calculations for K_2SO_4	124
Table F.3	Gas-to-particle conversion calculations for NaCl	125
Table F.4	Gas-to-particle conversion calculations for Na_2SO_4	125

Nomenclature

d_p	Diameter of particle
D_i	Diffusion coefficient
G	Gibbs free energy
ΔH	Enthalpy
J_c	Rate of condensation
J_{hom}	Rate of homogeneous nucleation
K	Equilibrium constant
K_{sp}	Solubility product constant
M	Molecular weight
p_d	Vapour pressure of gas
p_i	Partial pressure of gas
r	Radius of particle
r_c	Critical radius of particle
R	Gas constant, 8.314J/kmol
S	Saturation ratio
ΔS	Entropy
SI	Saturation index
σ_p	Surface tension of particle
ρ	Density
γ	Activity coefficient
ν_ι	Volume of molecule

CHAPTER 1

Introduction and Objectives

Co-firing biomass with coal is a near term option to reduce greenhouse-gas emissions from existing coal-fired boilers for power generation. Biomass has been defined in the Handbook of Biomass Combustion and Co-firing as a 'variety of material that is directly or indirectly derived from photosynthesis reactions not too long ago, such as vegetal matter and its derivatives: wood fuel, wood-derived, fuel crops, agricultural and agro-industrial by-products and animal by-products' (Loo, 2002). The growing interest in the use of biofuels for energy purposes includes environmental benefits such as mitigation of greenhouse gas emissions, and emissions of SOx and NOx, reduction of acid rain and soil improvements. Large amounts of wood and other biomass residues remain unused so far and could possibly be made available for use as a source of energy.

Although co-combustion of biomass and coal represents a cheaper and low risk sustainable and renewable energy option, however technical issues associated with co-firing, which includes, fuel handling and storage challenges, decrease in overall efficiency, ash deposition issues, pollutant emissions, and carbon burnout still need to be looked into. However, the main focus in this work is on the fireside issues, as the focal problem during biomass combustion is the high alkali content of its ash. The high alkali content can significantly worsen ash fouling, slagging and also lead to corrosion, in worse case scenario (Bryers, 1996; Jenkins, et al., 1998 and Pronobis, 2005). Nevertheless on-going research is being carried out to broaden the application of modern bioenergy technologies, as most countries have set varying targets and implemented promotional policies to increase the usage of biomass in existing power station boilers**.**

1.1 Objective

Ash release from biomass can lead to problems in ash fouling and slagging and therefore this study is aimed at investigating the behaviour of ash during direct co-combustion in pulverised coal plants. The knowledge gained from the investigations can be used as a tool to improve the understanding of ash behaviour and gaseous emissions, paving a way towards efficient and effective utilisation of biomass. The scope of this research includes the study of ash-related issues during co-combustion of biomass with coal, with emphasis on development of a conceptual model for co-firing that will be able to predict ash properties in biomass and its behaviour during combustion. The model can be used to provide technical advice to organisations responsible for fuel planning, technical implementation of biomass feedstock as well as boiler operating staff.

In order to understand the release of ash it is of paramount importance to understand the actual chemical structure of coal and biomass. As the identification of the chemical structure is complex and has been under research for the last two decades, the investigation to develop a sound method is still on-going (Yan, 2000; Zevenhoven, 2001 and Gupta, 2005). The development of coal and biomass characterisation has previously been studied using Computer Controlled Scanning Electron Microscope (CCSEM) and Chemical Fractionation (CF). This information is critical in establishing the ash formation of both fuels during combustion. Although the ash formation models for coal has begun to achieve an advanced level using CCSEM and CF, ash formation study of biomass is still at an early stage and the importance of developing and ash formation model is necessary.

Therefore the main objective of this work will be to obtain an advanced characteristic method to determine the chemical speciation of a biomass and in conjunction with information already known for coal, arrive at a conceptual model for ash formation co-firing technology. This information will ultimately be useful in future work as an input for studying the behaviour of biomass relevant to ash deposition, emissions for various Air Pollution Control Devices and fly ash utilization.

1.2 Outline of thesis

The thesis commences with Chapter Two which is a literature review on the current status of co-firing technology and background knowledge available for coal and biomass and its behaviour during co-combustion. This chapter will address the current status of research in this field and the approach that will be taken by the author to formulate a model to predict ash formation during co-firing.

Chapter 3 introduces the experimental and modelling method that was developed during the course of this work to determine the chemical speciation of a biomass, whilst in Chapter 4 the speciation derived are validated with knowledge available from literature and experimental work carried out during this research.

The chemical speciation of coal and biomass that has been derived is then used as an input to study the behaviour of the main inorganic material during combustion. In Chapter 5, the mechanisms for ash formation during co-firing are described and the main compositions of the volatilised and condensed fractions during combustion are determined. The entire work done in this research can be compiled in the form of a model that interprets the ash formation of coal and biomass during co-firing. The description of this model has been explained in Chapter 6.

The final chapter (Chapter 7) ends with conclusions drawn from the present work followed by recommendations for future work to refine the modelling tool.

CHAPTER 2

Literature Review

The literature review provides insight into the background information and research that has been carried in relation to co-firing technology of pulverised coal and biomass in general; and in particular ash formation prediction models. The first section will briefly address co-firing technology, the benefits of co-firing and rising problems associated with firing biomass. The second part involves review of literature on the properties and behaviour of coal and biomass fuels, followed by methods to determine the chemical speciation of a biomass. The following parts go into details of the behaviour of ash forming materials in coal and biomass during combustion. This includes a process known as gas-to-particle formation which includes the vaporisation of the ash forming material in pf systems during combustion and the subsequent condensation of these materials on heat transfer surfaces of a boiler. The final section will look into summarising the available literature review and additional research required in creating an ash behaviour model for coal and biomass co-firing.

2.1 Co-combustion of Biomass with Coal

2.1.1 Co-combustion in pf boilers

Combustion in this work is defined as a process of total oxidation of a biomass at high flame temperature in pulverised fuel (pf) fired boilers. Co-combustion or co-firing of biomass with coal is one of the methods to achieve the objective of the Kyoto Protocol set by 15 EU nations to reduce Green House Gas (GHG) emissions into the atmosphere. Combusting biomass, a renewable and sustainable energy source with coal in coal-fired boilers, is a practical approach to partial replacement of fossil fuel for power generation. Biomass fuels are considered environmentally friendly as biomass consumes the same amount of carbon dioxide (CO_2) from the atmosphere during growth as is released during its combustion (Sami et al., 2001).

Furthermore firing biomass in conventional pf fired power plants is an economical option to maximise the use of existing coal-fired boilers.

It has been observed that when a good selection of biomass is made and boiler operations are carefully monitored, a reduction in emission of GHGs and other pollutants was obtained (Loo, 2002). One such example is when sulfur from coal reacts with alkali-chlorides from biomass in co-firing experiments, lower SOx emission and lower corrosion of the deposits was found (Robinson et al., 1998). Although co-firing has shown many benefits and there is a high motivation towards utilisation of biomass in the production of power, several issues still exist regarding how biomass materials will behave in boilers in terms of combustion and ash related matters (Gupta et al., 2002). The issues and challenges to be faced when using biomass will be discussed in Section 2.1.2.

2.1.2 Challenges in Co-firing of Biomass

Biomass has low bulk energy density, is generally moist and strongly hydrophilic, and is non-friable (Baxter, 2005). Biomass heating values generally are slightly over half that of coal, particle densities are about half that of coal, and bulk densities are about one fifth that of coal, which results in an overall fuel density roughly one tenth that of coal. In addition to that, biomass combustion has the potential to create ash deposition problems due to the high alkali contents in biomass compared to coal (Robinson et al., 2002). The difference in composition results in increased fouling, slagging and corrosion in pulverised coal-fired boilers, reducing the heat transfer in the furnace and convective surfaces of a boiler. Sub-optimal burner flow patterns, reduces burner stability and NOx performance, cause mechanical damage and result in the blockage of ash discharge ducts.

Traditional empirical indices used for coals are insufficient when predicting ash deposition for different biomass fuels. Coal based indices do not take into account the heterogenous nature of biomass and its mechanisms. Furthermore interaction between coal and biomass can also lead to inaccuracy when using the available indices for coal combustion (Bryers, 1996). The Energy Research Centre of Netherlands (ECN) has carried out numerous investigations on the impact of biomass

co-firing on fouling using a lab scale combustion simulator to simulate an actual pf combustion process. It was found that occurrence and speciation of the inorganics in biomass are different from coal, making tools such as fouling indices for coal likely to fail for biomass (Korbee, et al., 2002). It was also observed that fouling from biomass occurred mainly through alkali species that form a sticky deposit layer. Interaction also occurs with coal-derived minerals, thus changing its stickiness and viscosity. Therefore, the scope of this thesis is to look at developing a prediction model capable of determining the ash formation that occurs during co-firing of biomass.

2.2 Ash Formation during Coal Combustion

2.2.1 Coal Characteristics

Besides organic matter, between 5 wt% to 30 wt% of pulverised coal consists of inorganic matter. The volatile organic matter is vaporised with the gases when the heating process begins, which is followed by the burning of char. The incombustible inorganic matter in coal consists of discrete mineral grains and organically bound inorganic matter that form ash after combustion. There are more than 100 types of mineral grains that can be found in coal and some of the major ones are quartz, clay minerals like kaolinite, carbonates like calcites and sulfides such as pyrites. The minerals exist in several forms such as discrete mineral grains, flakes or different-shaped in combined form (Bryers, 1996). These minerals exist either within the coal matrix known as included minerals or outside the coal matrix and are called excluded minerals (Benson et al., 1996).

The organically associated inorganic matter is mainly alkali and alkaline matter bonded with the oxygen functional groups in coal. This material however is only a very small fraction of inorganics in high rank coals and are often ignored in the study of ash prediction models. Figure 2.1 illustrates the association of the organic and inorganic materials observed in a coal particle.

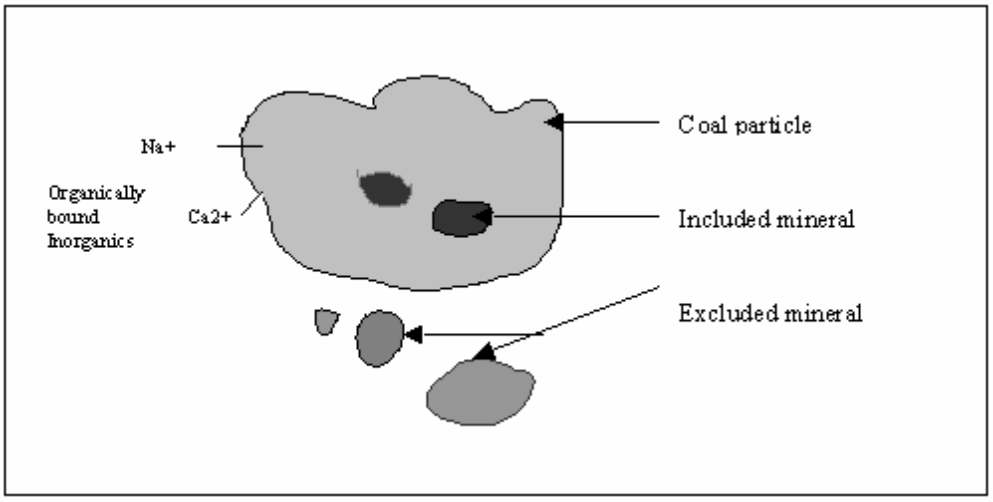

Figure 2.1: Organic and inorganic matters in a coal particle

2.2.2 Ash formation

Zevenhoven and co-workers in their paper have provided a thorough summary of the research that has been done in the field of ash formation of coal by several researchers including Sarofim, et al., 1977; McNallan, et al., 1980 and Benson, et al.,1996, especially in regards to the inorganic matter during combustion. This summary has been displayed in Figure 2.2.

Ash formation in coal combustion occurs mainly from fragmentation and coalescence of the mineral matter in the coal. However it is noted by researchers that a very small percentage (typically 1 wt%) of ash in coal is formed from vaporisation of the inorganic matter present in the coal (Yan et al., 2001). This reaction occurs mainly from vaporisation of fine mineral particles, vaporisation of refractory oxides and the vaporisation of organically bound matter during devolatilisation and char burnout (Buhre et al., 2003). The released material then nucleates homogeneously to form aerosols or condense with other available fly ash particles.

However, the main ash formation for coal occurs from the included and excluded mineral particles. As included minerals are close to each other in a char particle, during char burnout these grains become molten and enable coalescence and agglomeration to occur. Fragmentation occurs when the high heating rate in combustion chambers causes pressure build-up within minerals. The discharge of this

build-up causes the minerals to fragment. Included minerals seldom experience fragmentation as was seen in minerals such as silicates and clay minerals (Yan, et al., 2002).

On the other hand, excluded minerals mainly form ash through the fragmentation of the minerals. This releases several fragments of ash particles from one char particle, changing the particle size distribution (PSD). The fragmentation occurs based on the type of coal being used as fragmentation depends on char particle size, structure and ash loading. In terms of PSD of the overall ash, the larger ash particles (>2μm) are formed by mechanisms such as coalescence and shedding and the fine ash particles (<2μm) are formed from the vaporisation and condensation mechanisms (Wu et al., 1999).

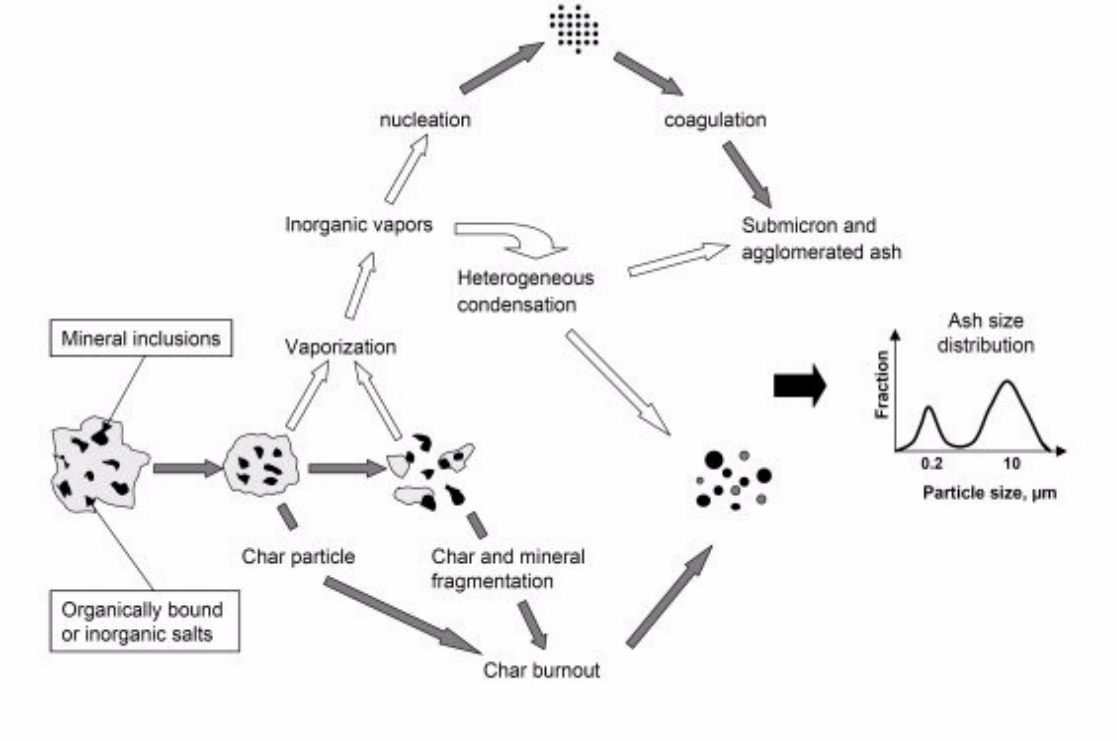

Figure 2.2: Ash formation during coal combustion (Zevenhoven, 2001)

2.2.3 Ash Formation Models

Understanding of the mechanisms of ash formation of coal has evolved with the progress of analytical tools and methods. The knowledge gained has brought about the development of several types of models that predicts the ash formation and ash

depositions of various types of coal during combustion. These models provide a comprehensive approach for predicting the behaviour of minerals in coal based upon various knowledge obtained from on going coal research. In these models, processes such as transformation and distributions of minerals in the coal is included for the ash formation model, whilst for the ash deposition models, transport of ash and heat transfer is taken into account. CRC for Coal in Sustainable Development, Newcastle, Australia in their Ash Effect Predictor (AEP) Model consider the influence of minerals that are included and excluded in coal, the coalescence behaviour of coals and the retention of ash particles to determine the characteristics and quantity ash deposition in boilers (Gupta, 2005).

The main input for this model is the conventional analysis of the coal being used and the Computer Controlled Scanning Electron Microscope (CCSEM) analysis. CCSEM is frequently used in characterisation of coal mineral matter together with EDX is able to characterise inorganics in terms of size and composition. Some of the typical conventional analysis includes:

- Proximate analysis (moisture, density, ash content)
- Ultimate analysis (C, H, O, N, S)
- Oxide analysis (Si, Al, Fe)

The CCSEM provides information about the minerals in the coal and the particle size distribution (PSD). CCSEM can also be used to predict the distribution of the included and excluded minerals based on the size and density of the coal particles. If it is not done with CCSEM, it also known that the Monte Carlo random distribution method can be used to determine this distribution (Yan, et al., 2001).

Studies on high rank coal have found that the fraction of ash formed through vaporisation is very small and therefore most models do not include this process (Wu et al., 1999). Three different sub-models are possible to study the coalescence behaviour, which are full coalescence, partial coalescence or no coalescence model. The first sub-model suggests that all the mineral particles in one char particle comes together to produce one ash particle whilst the third model advocates that each mineral grain in a char particle produces separate ash particles. However, based on experimental studies carried out by Li Yan concluded that based on the structure and

morphology of char particles, the partial coalescence model was found to be the closest model to the results obtained (Yan et al., 2002). Monroe in his thesis states that the extent of coalescence can be measured by the shell thickness of the char cenosphere, the size of the coal and mineral particles and the mineral volume fraction (Monroe,1989). In terms of fragmentation of minerals in coal, the Poisson distribution is used to determine the number of ash fragments envisaged during fragmentation of minerals (Yamashita et al., 1998).

2.3 Ash Formation during Biomass Combustion

2.3.1 Biomass Characterisation

The biomass term can be used to describe organic fuels that are formed through photosynthesis, including trees, agricultural crops and other living plant material. In comparison to fossil fuels such as coal or oil, biomass is relatively young fuel (Sami et al., 2001). Biomass can be categorized into four main groups, which are woody biomass like wood bark and waste wood, herbaceous biomass like straw and grass, agricultural by-products such as animal manure and fourthly, refuse-derived fuels and waste products (Williams et al., 2001). For biomass that comes under the plant category, its main structural composition mostly consists of cellulose, hemicellulose, lignin and the inorganic matter. Table 2.1 below briefly describes the main elemental structures in biomass and the function played by each of the elements to sustain the growth of the plant.

Table 2.1: Functions of the elements present in biomass (adapted from Zygarlicke, 2001)

Element	Chemical Symbol	Principal Form of Uptake	Function
Carbon	C	CO_2	Basic molecular component of carbohydrates, proteins, lipids, and nucleic acids.
Hydrogen	H	H_2O	Plays a central role in plant metabolism; important in ionic balance; main reducing agent; has a key role in energy relations of cells.
Oxygen	O	H_2O, O_2	Occurs in organic compounds of living organisms.
Nitrogen	N	NH_4^+, NO_3^-	Component of many organic compounds, ranging from proteins to nucleic acids.
Phosphorus	P	$H_2PO_4^-$, HPO_4^{2-}	Essential for all plant growth; plays central role in plants in energy transfer and protein metabolism.
Potassium	K	KCl, NaCl	Aids in osmotic and ionic regulation; functions as a cofactor or activator of many enzymes of carbohydrate and protein metabolism; the major ion inside every living plant and animal cell.
Calcium	Ca	Ca^{2+}	Is required for structural, osmotic, and signaling purposes.
Magnesium	Mg	Mg^{2+}	Component of chlorophyll; a cofactor for many enzymatic reactions.
Sulfur	S	SO_4^{2-}, SO_2	Involved in plant cell energetics.
Iron	Fe	Fe^{2+}, Fe^{3+}	Involved in N fixation, photosynthesis, and electron transfer; plant needs continuous supply to maintain proper growth.
Manganese	Mn	Mn^{2+}	Involved in photosynthesis; a component of enzymes arginase and phosphotransferase.
Boron	B	H_3BO_3	Essential for normal plant growth.
Zinc	Zn	Zn^{2+}	Essential component of several dehydrogenases, proteinases, and peptidases.
Copper	Cu	Cu^{2+} $Cu(H_2O)_6^{2+}$, $Cu(OH)_2$	Constituent of several enzymes; forms other compounds; relatively immobile element; important in plants' reproductive growth stage.
Molybdenum	Mo	MoO^{2-}	Required for assimilation of N in plants; an essential component of N_2 fixation enzymes.
Chlorine	Cl	KCl	Essential for photosynthesis; functions in osmoregulation of plants growing on saline soils.
Silica	Si	H_2SiO_3, $Si(OH)_4$	A structural component of some plant species; plays a role in disease resistance in crop plants.
Sodium	Na	NaCl	Cell wall structure component.
Aluminum	Al	Al^{3+}	Toxicity of Al decreases the uptake and distribution of other elements.
Selenium	Se	SeO_4^-	Forms seleno–amino acids, selenosysteine, and selenomethionine; translocated from roots to all parts of the plant including the seed; found in newly formed leaves of alfalfa, rather than older leaves.

The dry part of biomass is mainly formed from C, H and O, whilst a minor portion of it contains nitrogen, sulfur and phosphorus, which are vital for the plants metabolism and physiology (Jenkins et al., 1998). The combustion behaviour of biomass is found to be similar to combustion of low rank coals. In comparison to high-rank coals,

biomass fuels have lower fixed-carbon and higher volatile matter, thereby producing a lower heating value. Besides that, most biomass contains less sulfur and fuel bound nitrogen but a higher oxygen and nitrogen content than coal. Figure 2.3 illustrates a general layout of the contents of a biomass characterised by the work carried out by Baxter et al., 1996, Jenkins et al.,1998 and Zevenhoven et al., 2001. Besides organic matter, biomass consists of inorganic matters that are present in the following forms:

- Salts that are ionically bound
- Inorganics that are bound organically to the carbonaceous material
- Included minerals that are present in the fuel structure and adventitious minerals or foreign material from harvesting of biomass

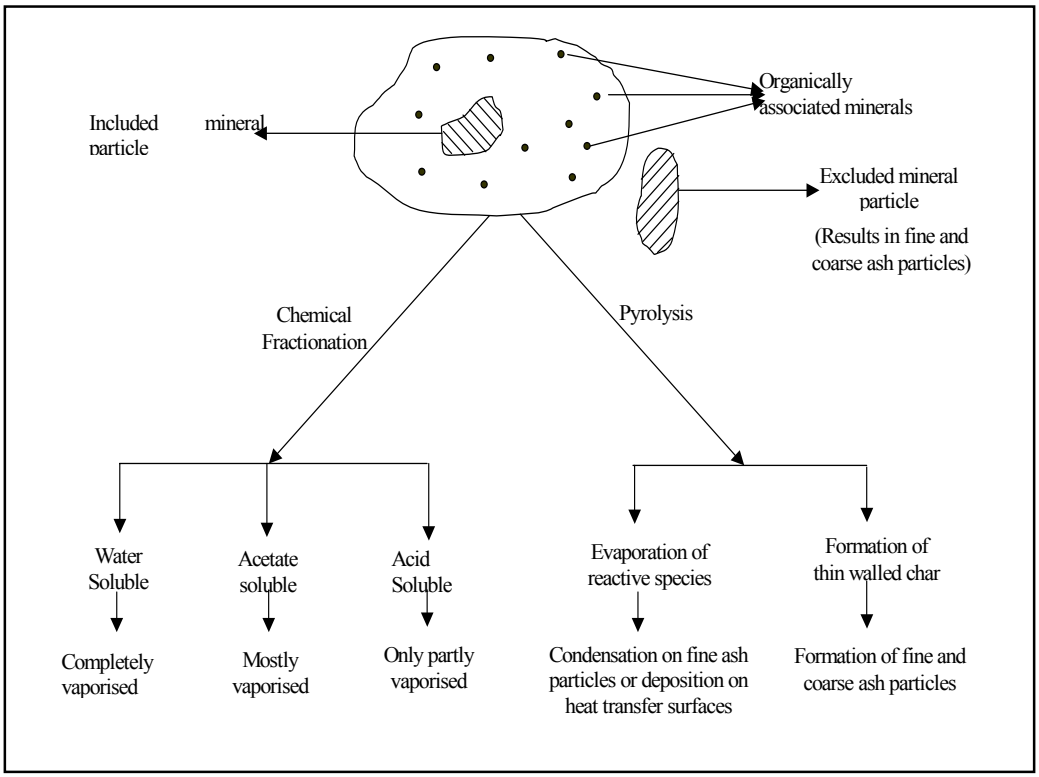

Figure 2.3: Schematic of the chemical fractionation and the thermal behaviour of inorganic matter in biomass (Gupta, et al., 2002)

By using the chemical fractionation (CF) method, which will be further discussed in Chapter 3, it is possible to have an idea of the manner in which the various ash forming matter is associated with the fuel. In this technique, increasingly strong leaching chemicals are used in order to extract the various matters based on their

solubility (Benson and Holm, 1985). This technique is further described in Figure 2.4. The first step involves the usage of water to dissolve elements that are water-soluble, which are primarily soluble salts (alkali sulfates, carbonates, chlorides). The remaining residue is subject to the second leaching step where ammonium acetate is added to extract elements bound organically to the inorganic matter. Finally the biomass is leached in HCl solution to extract alkaline earth carbonates, iron sulfates and other minerals. The remaining insoluble portion of the fuel consists of silicates, elements bound covalently to the organic phase of the biomass such as sulfur and also other acid insoluble minerals. (Zevenhoven, et al., 2001).

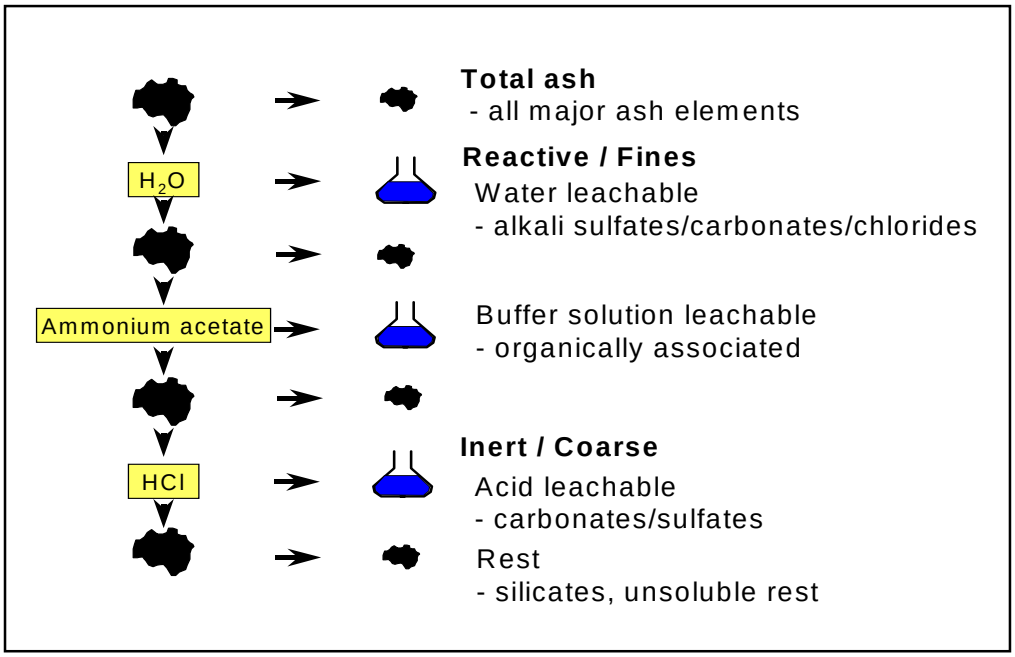

Figure 2.4: Experimental procedure of the Chemical Fractional technique (Zevenhoven, 2001)

In thermochemistry studies of coal and biomass Baxter makes the assumption that the ash forming elements leached out with water and ammonium acetate, which is the less aggressive solution, will represent the volatile species in biomass during combustion (Baxter, et al., 1996). These ash forming elements leached by water and ammonium acetate are combined to form the reactive/fines fraction. Those leached by hydrochloric acid which is the more aggressive solution will correspond with the less volatile matter, constituting the inert or coarse fraction. This assumption can be useful to predict the thermal behaviour of biomass to a certain extent. Korbee in his

work suggests that further refinement of chemical fractionation method is required for better classification of the chemical composition and the bonding of biomass inorganics (Korbee, et al., 2002). The present method is limited to classifying the inorganics rather broadly as the solubility is based on three different solutions and not a large range of pH.

2.3.2 Ash Forming Elements

Ash forming elements are elements that primarily cause formation of ash during combustion of biomass. Researches have identified the main elements that are responsible for ash forming issues and have studied the interaction between these main elements during and after combustion (Knudsen, et al., 2004). Some of the main elements that were looked into are K, Na, Ca, Mg, S and Cl.

Potassium

Potassium is a macronutrient for plant. It has a high mobility and is a facilitator for osmotic processes. In coal K is mostly in the form of clays, whilst in biomass it is mostly in the form of ionic material. More than 90% of potassium is found to be either water-soluble or ion exchangeable as observed during chemical fractionation tests (Baxter et al., 1998). K is volatile and combines with Si to form low melting silicates in fly ash particles.

Sodium

Na is a minor component (2%) in biomass. It behaves similiar to K , but at a very small fraction. Na is mainly attached as inorganic salts and is released as a gaseous species that undergoes gas phase reactions with Cl and S to form chlorides & sulfates. A significant gas-phase reaction forms Na_2SO_4, which has a low melting point and may further contribute to fouling (Knudsen et al., 2004). Excess Na will lead to the formation of NaOH and Na_2CO_3.

Calcium

Ca is a common constituent of cell wall and other organic component of cell structure, Through advanced analytical techniques, it is largely found as ion

exchangeable and acid soluble material. Ca tends to react mostly with Cl and SO4, but is less volatile compared to K. Combusted Ca oxalates transforms into oxides and carbonates.

Chlorine

Cl plays key role in transformations of inorganic materials by playing a shuttle role for inorganic materials. Principally, this anion serves as balancing charge. It reacts with alkali material to form volatile and stable alkali chlorides. KCl is the most stable at high temperatures (above 1000^{o}C species of Cl during gas phase, followed by KOH. Cl plays transports alkali from fuel to surfaces to form sulfates. At high temperature Cl reacts with metals to form corrosion problems, whilst at lower temperature corrosion occurs through formation of acid gases.

Sulfur

S present as free ions or bound organically mostly oxidizes and some the rest reacts with alkali and alkaline metals to form low melting compounds which leads to slagging & fouling at 800-900^{o}C. Most of the S oxidizes during combustion, whilst the rest reacts with K and Ca to form sulfates and condense on fly ash or deposit on walls.

2.3.3 Behaviour of Inorganic matter

The formation of ash likely to occur in different varieties of biomass fuels can be predicted from the composition of inorganic matter in the fuel. The manner of association and bonding of the inorganic matter with rest of the fuel can be used to roughly interpret the behaviour of a biomass during combustion. Alkali and alkaline earth metals, which are present largely in biomass, with other elements like Si, Cl, and S, can cause unfavourable or unwanted reactions that lead to problems like ash fouling and slagging. The high oxygen and organic volatile matter content of biomass makes it more reactive than coal. This is because devolatilisation will occur at lower temperatures, which creates the potential for releasing larger amounts of inorganic vapours during combustion.

Jenkins and co-workers discuss that the release of atomically dispersed inorganic material from a fuel particle which is influenced both by its volatility and the reactions of the organic portions of the fuel (Jenkins et al., 1998). The non-volatile material, on the other hand, is released by convective transport during rapid pyrolysis. Among the four groups of biomass, the woody ones are considered to be the most favourable fuel for co-firing due to its low ash & nitrogen content (Nussbaumer, 2003). For example the content of alkali metal such as K in wood fuels are approximately 0.5%, whilst in herbaceous biomass it is in the range of 1-3%. Furthermore, herbaceous biomass also contains more Si and Cl than wood samples.

Although biomass generally has lower ash content compared to coal, the composition of the ash in biomass is very different. Coal ash is mainly alumino-silicate with clay and quartz. On the other hand, quartz and inorganic salts of phosphates, sulphates and chlorides are the main composition of biomass ash (Loo, 2002). Korbee & co-workers, in their paper mention that biomass ash mainly contains elements from alkali metals (Na and K), and alkaline earth metals (Mg and Ca), in addition to smaller amounts of Si, P, S, Cl, Mn and Fe (Korbee et al., 2003). Another structure common in biomass are biominerals such as calcium oxalate or phytolith, which are rigid microstructure body that give structural stability to plants.

2.3.4 Ash formation Mechanisms

This section of the literature review looks into the mechanisms involved in ash formation of a biomass sample during combustion. The mechanisms involved are described below.

2.3.4.1 Vaporisation

Unlike coal, large fraction of the biomass ash is envisaged to go through the volatilisation process. During biomass combustion, significant quantities of alkali metals and chlorides are vaporized to form gases such as HCl (g), KCl (g), KOH (g) and NaCl (g) (Zheng, et al., 2007). When the flue gases are cooled, this material may condense and sometimes can be assumed to form the major part of the fine ash fraction (Zevenhoven et al., 2000). Besides the alkali chlorides and sulphates, the

trace elements also contribute to this mechanism. Buhre in his thesis mentions the vaporisation of refractory oxides such as silica also can occur at high temperatures (1700^{o}C) (Buhre, et al., 2005). So far no indications have been found that minerals contained in the biomass vaporise or oxidize, but research has seen that minerals generally go through a process of char and mineral fragmentation to form solid ash particles of larger size.

2.3.4.2 Gas-to-particle conversion

Gas to particle conversion occurs when compounds in the flue gas become supersaturated due to cooling as the gas moves from the radiant zone towards the heat exchangers (Freidlander, 2000). As the gas cools it moves towards equilibrium by condensing into liquid or solid form. According to Strand and colleagues, there are two competing routes for the condensing vapour (Strand et al., 2004). Firstly, the vapours may condense directly on the internal surface of the furnace forming slag. Otherwise, the vapors may undergo gas-to-particle conversion to form aerosols by either homogeneous nucleation or heterogeneous condensation on existing particles entrained in the flue gas. The droplets and aerosols begin to form larger particles through coagulation and agglomeration until finally accumulating as ash particles.

2.3.4.3 Homogeneous condensation

Homogeneous nucleation occurs when a gas nucleates to form a new phase, solid or liquid, without the aid of a surface (Jacobson, 1999). Figure 2.5 describes how the gas molecules converge to form a nucleus of the new condensed phase. This nucleus can then become a site for further condensation by other gas molecules.

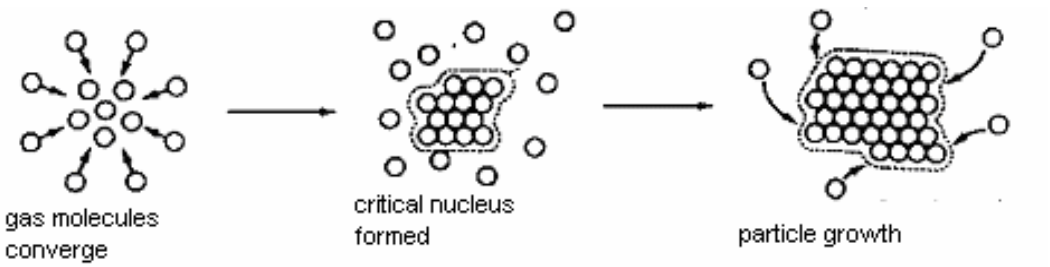

Figure 2.5: Formation of Particle by Homogeneous Nucleation (Jacobson, 1999)

Saturation ratio (S) calculation is generally used to predict the possible occurrence of homogeneous nucleation for a certain body of condensing gas. Homogeneous nucleation is expected to occur in systems when the saturation ratio of a vapor species is much higher than unity. The formula for saturation ratio is described here:

$$\text{Saturation ratio, S} = \frac{\text{partial pressure of condensing gas}}{\text{vapour pressure of condensing gas}} \qquad \text{Eq (2.1)}$$

where partial pressure is the pressure exerted by a certain gas in a mixture of gases (Dalton's Law) and vapour pressure is the pressure applied by a vapour that is in equilibrium with its liquid or solid phase.

Homogeneous nucleation can be homo-molecular or hetero-molecular. Homogeneous homo-molecular nucleation is due to the self-nucleation of a single species. An example is when one gas species such as KCl forms a nucleus of only KCl molecules. When two or more vapor species are present, neither of which is supersaturated, homogeneous hetero-molecular nucleation can take place as long as the participating vapor species are supersaturated with respect to a liquid solution droplet (Jacobson, 1999). This means a nucleus can be formed of two or more components as long as the saturation ratio of a mixture of the components is high enough for homogeneous nucleation to take place.

Analysis of the Gibbs free energy for homogeneous nucleation provides a greater understanding of this phenomenon (Seinfeld & Pandis, 1998). The change in Gibbs free energy during the nucleation of a cluster of molecules can be described by the following equation:

$$\Delta G = 4\pi r^2 \sigma - \frac{4}{3}\pi r^3 \rho \frac{RT}{m} \ln S \qquad \text{Eq 2.2}$$

where:

$\Delta G \equiv$ change in Gibbs free energy during nucleation

$r \equiv$ radius of nucleating cluster particle

σ ≡ surface tension of condensed cluster

ρ ≡ density of condensed cluster

R ≡ universal gas constant

T ≡ temperature of system

m ≡ molecular weight of condensing gas

S ≡ saturation ratio of condensing gas

The first term of the formula is described as a 'surface tension term' whilst the second a 'saturation ratio term'. Surface tension is a force per unit distance that acts to reduce the surface area of a body. The force arises because molecules in a body are equally attracted in all directions by other molecules, except at the surface, where the molecules adhere to other molecules adjacent to them, resulting in a net inward attraction. The surface tension decreases with decreasing radius of curvature. If molecules condense on a cluster the radius of curvature increases, hence increasing the surface tension of the particle, and therefore also increasing the energy required to expand the surface area of the cluster against the force of surface tension. The surface tension term symbolizes the energy required to expand the surface

The saturation ratio term on the other hand represents the energy available from latent heat release when a molecule condenses on the surface. A cluster can form if the latent heat energy released by condensation can overcome the surface tension required to increase the surface area of cluster. When the Gibbs free energy is increasing, the energy required to expand the surface is higher than that available from latent heat of condensation. The cluster is said to be unstable and will evaporate. When the Gibbs free energy is decreasing, the addition of a molecule adds more energy than is required to expand the surface and the cluster is said to become more stable and can increase in size as described in Figure 2.6. The radius of the cluster at which the energy required to increase the surface area equals the energy available from latent heat release is called the critical radius, r_c. Homogeneous nucleation will occur if a cluster contains enough molecules for the cluster radius to exceed the critical radius, r_c. Clusters of smaller radii will be unstable and tend to evaporate. Larger clusters however will act as sites for further condensation and will grow in size.

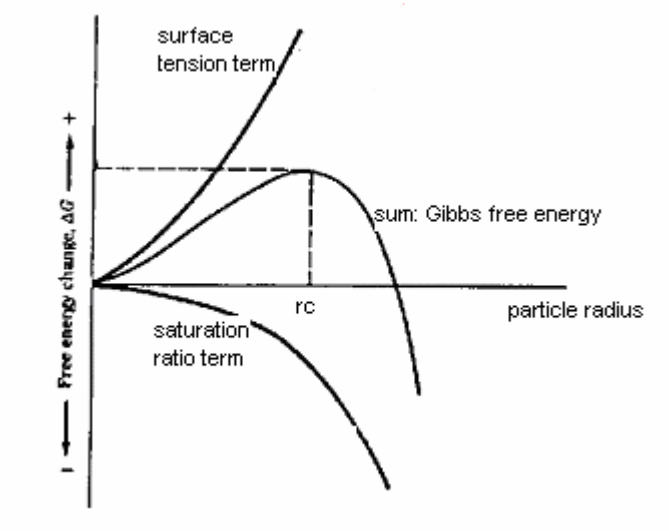

Figure 2.6: Gibbs free energy for homogeneous nucleation (adapted from Jacobson, 1999)

2.3.4.4 Heterogeneous Condensation

Condensation of vapor substances on an existing surface is known as heterogeneous condensation. Like homogeneous nucleation, there are also two types of heterogeneous condensation:

- Heterogeneous homomolecular: condensation of a vapor species onto a surface of the same species, eg KCl(g) condensing onto a KCl(l) droplet.
- Heterogeneous heteromolecular: condensation of a vapor species onto a surface of a foreign species, eg NaCl(g) condensing onto a particle of CaO(s).

Heterogeneous nucleation also only occurs when the body of gas is supersaturated, that is, when the saturation ratio is just above one; which means it is more thermodynamically possible than homogeneous nucleation. The free energy required for heterogeneous condensation is much lower than the amount required for homogeneous nucleation. (Seinfeld & Pandis, 1998). It is therefore generally recognized that heterogeneous condensation occurs more readily than homogeneous nucleation. In order for heterogeneous condensation to occur primary seed particles are required as a site for condensation. In biomass combustion these seed particles are commonly low volatility compounds such as oxides of calcium, zinc, silica and magnesium (Joller et al., 2005) or non-volatilized minerals that have experienced break-up and fragmentation.

2.3.4.5 Coagulation and Agglomeration

The final ash formation mechanism involves the collision and sticking of particles. Coagulation occurs when spherical aerosol particles collide and stick to form another, larger spherical particle. The mass during coagulation remains constant but a change is observed in the particle size distribution. Agglomeration is observed when colliding particles form an irregular shaped particle. Agglomeration produces larger particles of greater surface area than coagulation and takes place when particles collide, or when they come into contact on the surface of a deposit on the boiler walls. Particle collision and coagulation leads to a reduction in the total number of particles and an increase in the average size while also reducing the surface area for further condensation (Couch, 1994).

2.3.4.6 Interaction between coal and biomass

This section aims to look at available information in the literature on the effect inorganic matters in coal may have on the inorganics in biomass. It has been observed through experiments carried out by Biagini and colleagues that coal and biomass do not interact during the devolatilisation stage of combustion. They found that there was no interaction between both the fuels even though their volatile matter, devolatilisation rate and thermal reactivity were different (Biagini et al., 2002). However other researchers disagree with this idea as they have found some amount of interaction occurring between inorganics in coal with that of biomass during the condensation mechanism.

Equilibrium calculations have shown that mineral matter in coal such as kaolinite and clays 'capture' some of the gas phase alkali metals to condense with the minerals instead (Dayton et al., 1999 and Wei, et al., 2005). This means that reactions can occur between the Al and Si within the coal with that of the volatile elements (K, Na and Cl) in biomass. In a pilot investigation carried out to study the interaction between several fuels (three types of coal and five types of biomass), it was observed that sulphur from the coals did interact with K and Na from biomass (Robinson, et al., 2002). This shows that interaction does occur between volatile matter in biomass with Al, Si and S elements in coal.

2.5 Summary of Literature Review

It is known from the available literature review, that in order to create a model or tool that can predict the ash formation during co-firing of coal and biomass, several issues need to be looked into. Firstly, it is vital to have more detailed knowledge of the chemical speciation of the inorganics in a fuel to be able to predict its behaviour when it is combusted. Research in coal has provided deep insights into coal mineral matter, however, for biomass, an advanced analytical technique is required to predict its inorganic speciation. To date, no known method of analysing the detailed speciation of the alkali salts and the organically bound inorganics in biomass has been found. Therefore, this study will look into developing a method that combines the usage of an advanced analysis technique and a chemical equilibrium model to arrive at detailed prediction of biomass speciation.

Secondly, this research work will also make use of high temperature chemical modelling to predict the stable phases of the various gas and solid phases in a biomass when it is combusted in the radiant section of a boiler right down to its convective section. The results of the new fuel speciation method are taken as the input for this high temperature modelling. This will provide further knowledge about the composition and phases of ash released during combustion and the interaction between these ash-forming elements, with each other and also with coal particles.

Finally this thesis work will also look into the gas-to-particle formation of biomass when combusted, which will provide an insight into the vaporization and condensation of gases during combustion to form aerosol and coarse particles when it begins to cool. A summary of the ash formation mechanisms that will be looked into during co-firing and the interaction between the two fuels is described in Figure 2.7. With the combined knowledge of an advanced chemical speciation technique, stable phases of the inorganics at high temperature and the formation of ash particles; it will be possible to model the ash formation of various biomass fuels during combustion; thus providing an insight into the behaviour of a biomass when co-fired with coal.

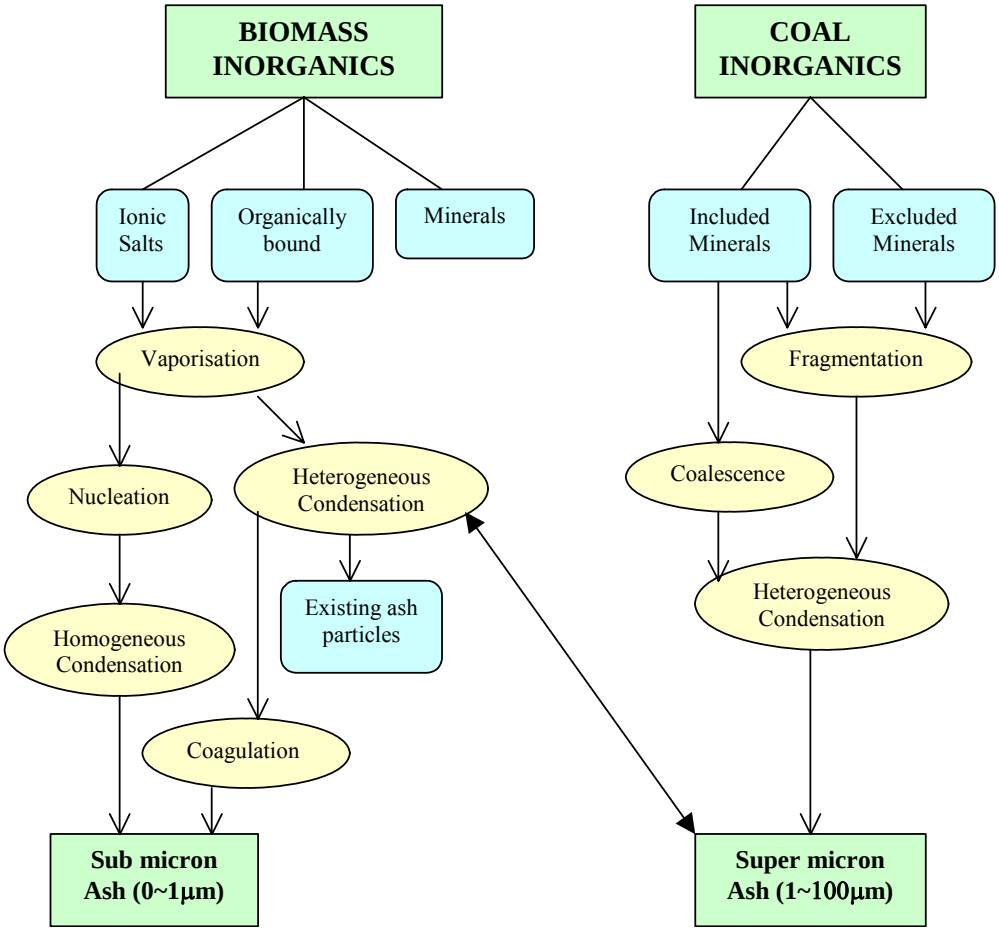

Figure 2.7: Interaction between coal and biomass during combustion

CHAPTER 3

Biomass Speciation Modeling

Based on background research, it is clear that a new and novel approach has to be taken to be able to develop a model that can predict ash formation during biomass combustion. Figure 3.1 summarises the pathway for ash formation of a biomass when combusted and the approach that will be taken to model these mechanisms using experimental methods and chemical equilibrium tools.

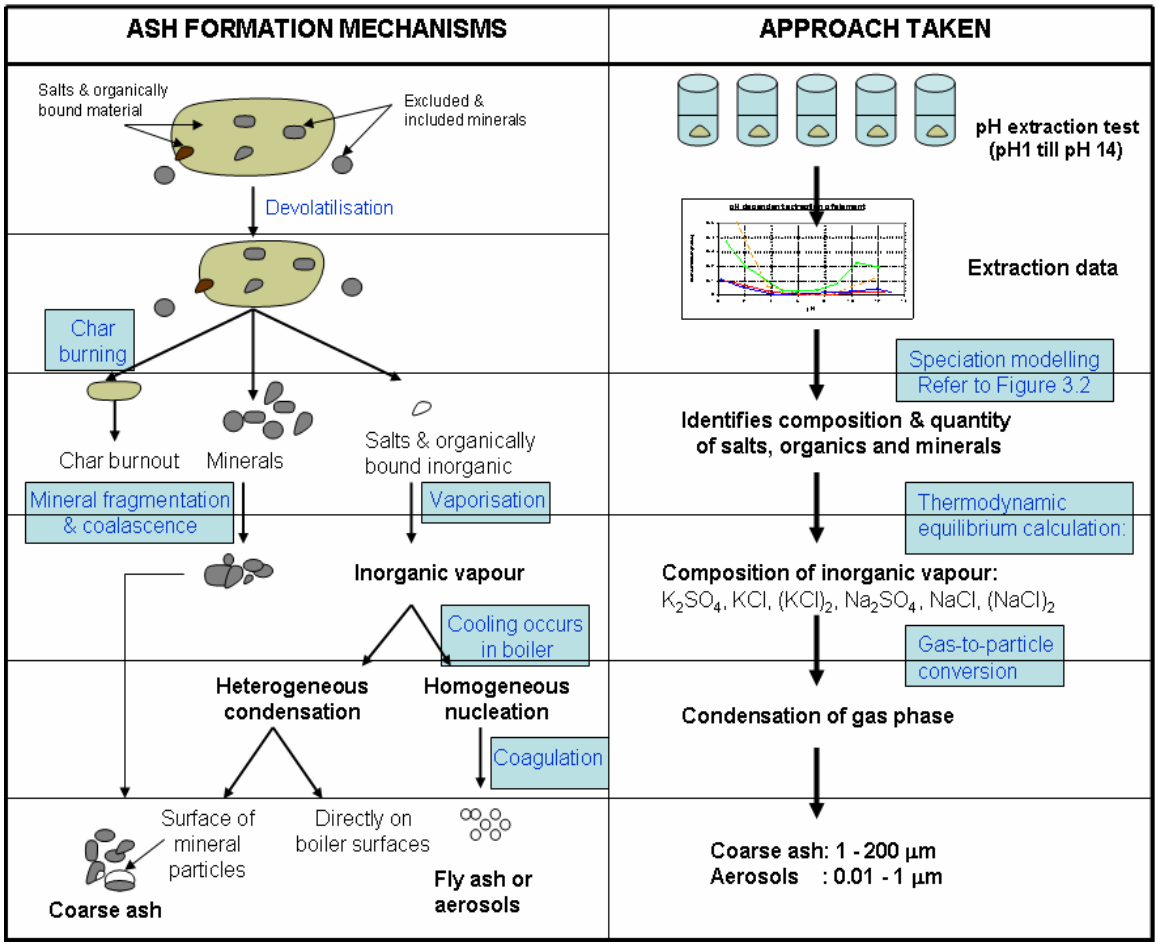

Figure 3.1: Schematic flow diagram of ash formation mechanisms and approach taken in modeling the ash formation pathway

3.1 Inorganic Matter in Biomass

An overview of the composition of inorganic matter in biomass and its functionality has been discussed in the section 2.3.1 of the literature review. This chapter will discuss the approach that was taken in deriving the chemical speciation of biomass. To date, the sole method available to identify the ash-forming matter in biomass is a solubility method known as Chemical Fractionation (CF) (Werkelin, 2005). This method has been used by researchers to determine how the inorganic matter present in a biomass is incorporated within the fuel. Scanning Electron Microscope (SEM) method has also been used to a lesser extent, as its usage is limited to identifying the mineral matter in biomass and not the other inorganics such as salts and organically bound material, which are of interest for ash formation modelling. The SEM method involves the automated analysis of coal samples embedded in resin/wax blend, followed by computer aided interpretation of the SEM-EDX data. EDX analysis enables the study of Na, Mg, Al, Si, P, S, Cl, K, Ca, Ti, Cr, Fe and the Computer Controlled Scanning Electron Microscope (CCSEM) is then used to classify the elements into its minerals.

CF method, on the other hand involves the usage of increasingly aggressive solvents to leach a biomass sample in a series of leaching solutions to produce four different samples for characterization. Firstly, the leaching involves using water to dissolve elements of the water-soluble form. These are primarily soluble salts such as alkali sulfates, carbonates and chlorides. The remaining residue is leached in an alkaline solution of ammonium acetate, to remove elements that are organically bound. The third solution is HCl solution that is used to remove element-bearing minerals salts (e.g. alkaline earth carbonates, iron sulfates). The remaining insoluble portion of the fuel consists of silicates and other acid insoluble minerals (Baxter, et al., 1996). Detailed experimental methods are described in Appendix B.

From this analysis, biomass inorganics have then been grouped into two main categories, which are the “reactives” (includes both the ionically bound salts and organically associated inorganics) and secondly the “non-reactives” (includes mineral matter and the remaining insoluble inorganics). The thermal behaviour and reactivity of the ash producing matter can be predicted based on this association or

bonding of the inorganics. Ionically bound salts and organically associated inorganics materials have weaker bonds and therefore are more volatile, and thus concluded to be 'reactive' and vaporize during combustion. They tend to form finer particles, whilst inorganics that exist as mineral matter, are 'non-reactive' or inert at high temperature during combustion. Although the information derived from this advanced analytical method can be used to predict the behaviour of the inorganics during combustion to a certain extent, this method still has a large margin for improvement.

One of the drawbacks of the CF method is that the classifications of the inorganics are based only on three solutions, which are acid, alkaline and neutral. Aside from that, the pH of the three solutions are not controlled or measured. This means that although the original pH of the solution is known, the actual difference after the addition of biomass is not measured. This makes the study of the solubility of the biomass inorganics rather broad or rough and therefore a different approach is required to improve the determination of the chemical speciation. In this thesis, the introduction and development of an advanced analytical method has been carried out to enable the determination of biomass speciation. The detailed description of this method is addressed in Section 3.2.

Literature, research was carried out to assemble all the possible elements and speciation present in plants (Marschener 1995; Loo, 2002; Zygarlicke, 2001). This was done to understand the fundamental composition of biomass in detail, so that it can be used to verify the results obtained from the characterisation techniques at a later stage of this research. The findings made from the chemical speciation of biomass in the literature review have been summarised in three groups that are based upon the bonding of the inorganics to the fuel. These categories are ionic salts, organically bound inorganics and minerals and its composition is as listed in Table 3.1.

Table 3.1: Speciation of biomass based on literature review summary

Element	Ionic salts	Organically associated Inorganics	Minerals
Na	Sodium nitrate Sodium chloride		
K	Potassium nitrate Potassium chloride		
Ca	Calcium nitrate Calcium chloride Calcium phosphate	Calcium pectate	Calcium oxalate Calcite
Mg	Magnesium nitrate Magnesium chloride Magnesium phosphate	Chlorophyll Magnesium pectate	
Si	Amorphous silica		Phytolite Quartz
S	Sulfur tetraoxide -2ion	Sulfolipids	
N		Amino acids, protein Sulfolipids	
P	Phosphate -3ion	Nucleic acids	Phytates Phytic acid
Cl	Chloride ion		
Al			Kaolinite
Mn		Organic structures of proteins & carbohydrates	
Fe		Chelates Organic sulfates	Phytoferritin Iron oxide

Note: Speciation is compiled and summarised from literature (Marschener, 1995; Baxter, et al., 1996 and Loo, 2002)

3.2 Determination of Biomass Speciation

The current work looks into finding a better method to determine the speciation of biomass, as detailed speciation will be useful for further interpretation of its identification and behaviour. CF method gives the solubility of the elements in three regimes, which are acid, alkaline and neutral, providing a coarse interpretation of the

elements that are soluble in these solutions. It is known that the solubility of a material in different pH solutions can be useful to understand the characterisation of an unknown material, or in this case, the inorganics in the solution. As pH is a dominant factor in this characterisation process, it is important that the pH is well defined and measured as expected in any wet analytical techniques.

However, as mentioned previously, in the CF method the pH is neither controlled nor measured. The final pH of the solution is based on the biomass dissolved in it. This means that when two different biomass fuels are analysed for a common unknown inorganic, it would be very likely that the CF method would interpret different speciation for the same unknown inorganic as the speciation will depend on the final pH of the biomass in the three solutions. Therefore, for this research work it was thought that carrying out the solubility of leaching of the inorganics at a larger, frequent and controlled pH values would provide better resolution of the solubility behaviour of the biomass, thereby giving additional information such as pH solubility, eH, ion complexation and other chemical properties.

Previously work has been carried out in geochemical speciation modelling to find out the chemical processes that determine the release of contaminants from waste materials (Sloot van der and Zomeren van, 2005). Leaching is the process by which inorganic or organic contaminants are released from the solid phase into the water phase under the influence of mineral dissolution, desorption, complexation processes as affected by pH and dissolved organic matter. The rate and extent of constituents release are a function of its chemical and physical properties and the characteristics (eg, pH and oxidation-reduction potential) of the environment in which the material is placed. Sloot van der and colleagues, (2003) developed a database/expert system for environmental risk assessment in soil to model the chemical behaviour and release of substances in different scenarios. The data evaluated with this system are derived from the leaching behaviour obtained from pH dependence test, as this test provides the geochemical fingerprint of the material under study. The model uses this data and provides insights into the chemical speciation of the fuel including the possible presence of minerals.

Similarly, in this research it was proposed that for determining the speciation of biomass, the extracted concentration of each element that is leached at various pH solutions; or simply known as pH extraction analysis will provide the solubility data of the elements. The extraction data also provides the leaching pattern of all the elements present and by using equilibrium chemistry it is possible to interpret the likely speciation that was originally present in the biomass. Figure 3.2 shows the steps taken in this research work in the attempt to interpret the speciation of the biomass. Details of the experimental methods and equilibrium calculations are discussed in the following sections of this chapter.

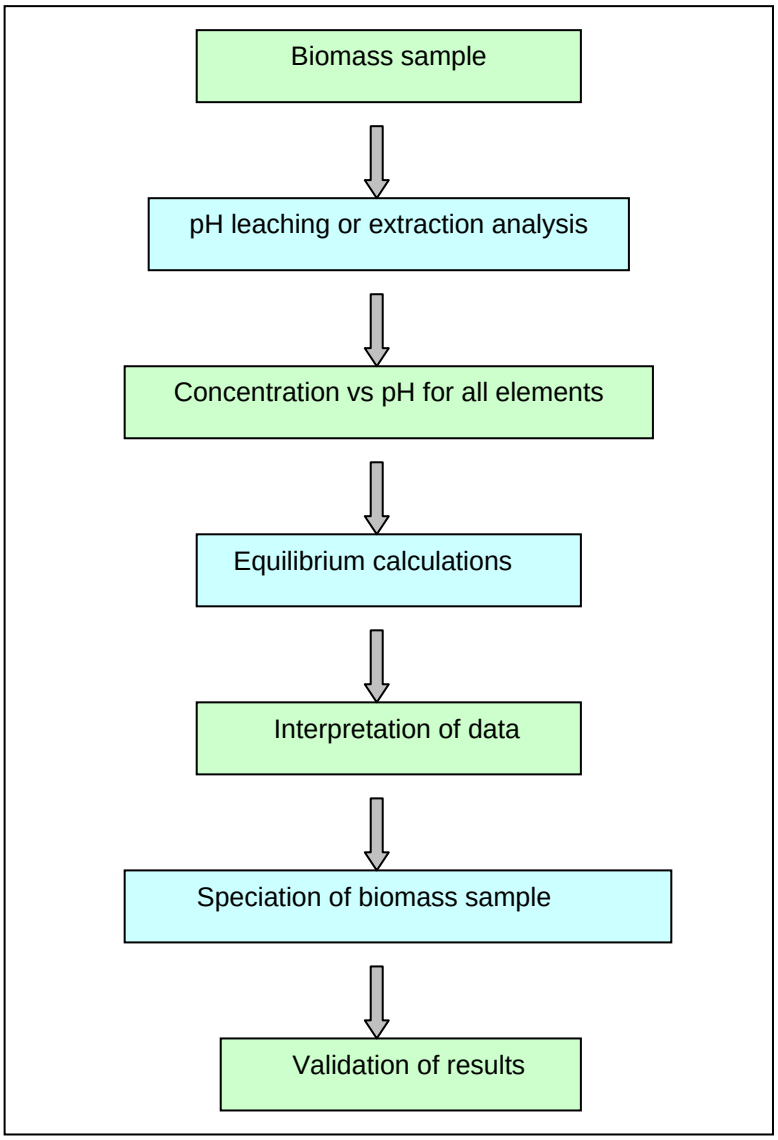

Figure 3.2: Step-by-step procedure used for the determination of biomass speciation

3.3 Experimental Procedures

3.3.1 Coal/Biomass Selection

As mentioned in the literature review section, biomass can be categorised as woody material, herbaceous material, agricultural by-product and refuse or waste matter. A wide range of fuels has been used in the present work, which are representative of current and near-future co-firing activities. The selected fuels include bark (spruce), wood chips (spruce), straw (wheat) and a type of Polish coal (PO58). These samples have been introduced under a European Commission framework project to investigate ash related problems in co-firing of biomass in coal fired plants. The fuel characteristics are described in Table A.1 (Appendix A). Before carrying out the combustion tests, the fuels were milled and sieved on a Retsch SM 100 shaker until 99% were smaller than 500 μm. This ensures complete extraction in the subsequent leaching procedure (Korbee and Cieplik, 2006). The samples were dried at 105°C prior to the experiment and then analysed for its chemical composition. The results are presented in Figure 3.3. The results are the average of six different analyses carried out on every sample.

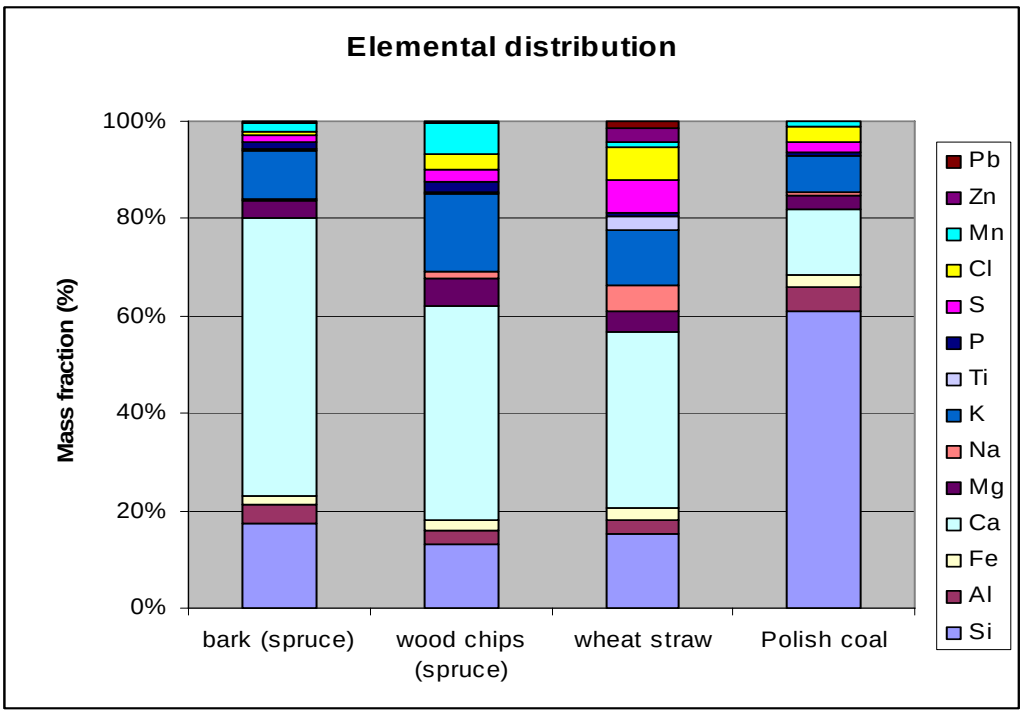

Figure 3.3: Chemical compositions of the fuels studied

3.3.2 pH dependent leaching

pH leaching or extraction experiments provide information on the influence of pH on the release of the inorganic constituents from the biomass; thereby allowing the recognition of the factors that control the release of these elements. The method can be used as a mutual comparison with other samples and therefore is a good basis for international comparison. The leaching method is based on a European Committee for Standardization (CEN) test entitled Leaching behaviour tests – influence of pH on leaching with continuous pH-control, (CEN292, 2005). The method was developed to obtain information on the short and long term leaching behaviour and characteristic properties of waste material. The leaching curve of the elements (metals, oxyanions, major and minor elements and dissolved organic carbon) obtained from this test can be seen as a material characteristic or the "geochemical fingerprint". In the leaching experiments, equilibrium condition is established at different pH values as a result of reaction between pre-selected amount of acid or base and test portions of the material studied. This CEN test method has been adopted in the current research work to study the extraction model of the inorganics in a biomass at various pH solutions.

The leaching experiments for the fuel samples were carried out at eight different pH solutions to determine the leached concentration of the different components in a biomass at equilibrium conditions. The data obtained is then used for prediction study of the speciation of the inorganic matter in biomass. The eight final pH-values required, cover the range of pH 2 to pH 12 in order to provide the solubility behaviour of the inorganics throughout a wide pH range. The amount of acid (HNO_3) added to obtain pH<7 or base (NaOH) added to obtain pH>7 is derived from the results of the predetermined maximum consumption of acid and base. The tests are carried out at a fixed contact time at the end of which equilibrium condition is assumed reached for all components. During this time period, the leaching process goes through the initial period of acid/base addition, equilibrium period at constant pH and finally the verification period of the equilibrium condition. This test method verifies that these three stages are achievable within a contact period of 48 hours.

This time limit was found to be sufficient for the biomass studied in the current work and the details will be addressed later in the chapter.

The test parameters include Liquid to Solid (L/S) ratio of 10 L/kg, which quantifies to 15g per 150 mg of demineralised water. The sample has to be crushed to a size less than 2mm to enable good leachability (Dijkstra, 2006). Further details about this experimental method can be derived from the CEN 292 test method (Appendix C.1). Based on the expected speciation of biomass inorganic matter from the summary in shown Table 3.1, only the relevant elements of concern to the fireside issues (ash formation) were studied. The concentration of elements in the biomass are determined using the ICP method and include cations such as K^{+}, Na^{+}, Ca^{2+}, Mg^{2+} Al^{3+}, Si^{4+}, Fe^{2+} and Mn^{2+} whilst the anions that were studied are NO_3^{-}, PO_4^{-}, CO_3^{2-}, $C_2O_4^{2-}$, SO_4^{2-}, Cl^{-} and dissolved organic carbons (DOC). Appropriate analysis techniques are suggested in sections 3.3.3-3.3.6. Analytical data from the tests on the influence of pH on leaching may be used as input data for geochemical speciation codes to analyse the speciation of the ash forming constituents in biomass. The function and operational method of the geochemical model used in this study is discussed in a later section.

3.3.3 ICP analysis

Inductively coupled plasma-optical emission spectroscopy (ICP-OES) is a technique for analysing the concentration of metallic elements in solid and liquid samples. This analysis uses optical emission principles of exited atoms to determine the elemental concentration. When using ICP-OES, solid samples are dissolved (digested) in an appropriate solvent (typically acid) to produce a solution for analysis. The resulting sample solution is often diluted in water to obtain a final specimen suitable for analysis.

3.3.4 Ion Chromatography

Calcium oxalate (CaC_2O_4) is the most widely distributed “biomineral” observed in woody biomass. Werkelin, 2005 in his attempt to study the chemical forms of ash forming matter in fuels applied the ion chromatography method successfully to

determine the concentration of all anions in the leaching solution. Therefore the same method was adopted in the current work to analyse the oxalates, as ICP method was found to be unsuitable for this compound. The standard method for oxalates requires separation in a Dionex AS17 column with eluent KOH solution (variable concentration between 3 to 50 mMol). 25μL of the leached biomass solution of various pH values are injected into the column to determine the leached concentration of oxalate in the solutions.

3.3.5 HFO extraction

The iron and aluminium oxides and hydroxides or "HFO" were used to calculate the active surfaces available for adsorption reactions. The amorphous aluminium surfaces were considered to be important, and in the modelling the FeOOH was substituted as the HFO species. The portion of amorphous iron (hydr)oxides was estimated by an ascorbate extraction (Kotska and Luther III, 1994), whilst the amount of amorphous aluminum (hydr)oxides was estimated by an oxalate extraction (Blakemore, et al., 1987). The site densities of amorphous aluminium and iron hydr(oxides) for adsorption were assumed to be $600 m^2/g$ (Dzombak and Morel, 1990), the same as that of FeOOH, whilst the crystalline iron hydr(oxide) was assumed to have a site density of $100 m^2/g$ (Hiemstra et al., 1989). All concentrations were converted to kg/kg FeOOH, taking into account the site densities of the different reactants (Dijkstra et al.,2006).

3.3.6 SHA Extraction

The solid humic acid (and fulvic acid) or also known as "SHA" content are assumed to account for the reactive solid phase organic material and are combined in the LeachXS model as the active organic component. Humic acid is the fraction of humic substances that is not soluble in water under acidic conditions (pH < 2) but is soluble at higher pH values, whilst fulvic acid is the fraction of humic substance that is soluble in water under all pH conditions. Concentrations of humic substances in the solid and the solution phase (humic and fulvic acids) were estimated quantitatively by a batch procedure (Zomeren van, submitted 2006) derived from the method currently recommended by the International Humic Substances Society

(Swift, 1996; Thurman and Malcolm, 1981). For the prediction of biomass speciation, the SHA quantity is useful in calculating the amount of organically bound materials in the biomass. In terms of predicting the quantity of the dissolved organic carbon (DOC) in biomass, it was seen that SHA does not directly relate to DOC. This is because only part of DOC is made up of "reactive" carbon towards metal complexation and therefore this quantity is assumed to be 20%.

3.3.7 Kinetic Experiments

The time estimated to allow equilibrium to be achieved is 48 hours for the leaching tests. Therefore additional tests were carried out at a longer period of time determine the extent to which this assumption is valid. The sample chosen is wood chips and the time frames measured for the extractions tests are 6 hours, 48 hours, 120 hours and 168 hours. The particle size of the sample was not changed as it was found to be fine enough (<500nm) for the leaching analysis. The test results were obtained at four different pH solutions, which are approximately pH 4, pH 5.5, pH 9 and pH 12. It was found from this test that 48 hours was a sufficient time for the leaching process to achieve equilibrium.

3.3.8 Lab Scale Combustion Simulator

In order to determine the composition and quantity of ash released during combustion of coal and biomass, the Lab-scale Combustion Simulator (LCS) was used. It is vital to know the composition and quantity of ash to be able to study the ash behaviour of fuels during combustion in a small scale. The ash release behaviour data will also be used for the purpose of comparing and possibly linking the speciation of fuels obtained with the ash release data.

The LCS is an advanced drop tube furnace that is used to study the behaviour of single or multiple solid fuels under typical pulverised fuel fired furnace conditions. This equipment was designed for simulation of ash formation and deposition of various coal and biomass samples during combustion. A schematic of the LCS is given in Figure 3.4. The facility comprises a drop tube reactor together with a primary/secondary gas burner to simulate a flame/flue gas environment in which the conversion behaviour of fuel particles can be studied as a function of time. In this

study, the LCS was used for the purpose of analysing the release of inorganic matter from the various fuels.

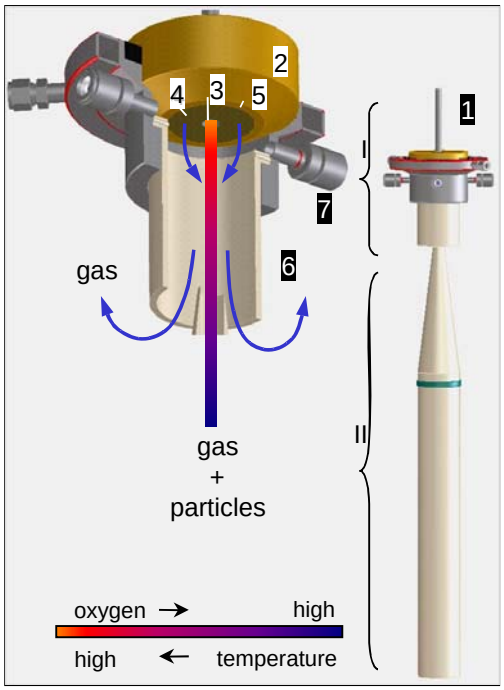

Legend

I	Devolatilisation zone
II	Combustion zone
1	Solid fuel feed
2	Multi-stage flat flame gas burner
3	Inner burner
4	Outer burner
5	Shield gas ring
6	Reactor tube
7	Optical access

Figure 3.4: The burner and reactor tube of the lab-scale combustion simulator

The LCS comprises of a drop tube reactor with an integrated, premixed and multi-stage flat flame gas burner. The staged gas burner accommodates high initial heating rates and temperatures and provides the possibility to simulate air staging as in low-NO_x burners and also the presence of specific combustion products. The flat flame gas burner consists of two concentric sub-burners viz. a primary inner burner and a secondary outer burner. Fuel particles are fed through the inner burner and are rapidly heated (>10^5 °C/s) to the high temperature level of up to 1400-1600 °C. The fuel is brought into a cylinder and a piston presses the powder against a rapidly rotating commercial rotating ram brush feeder and the particles are dispersed by the brush and transported into the reactor pneumatically.

Usually the particle feed rate is low (1-5 g/h) in order to control the gaseous environment of each particle by means of the imposed gas burner conditions. For low-NO_x operation, this implies that heating and devolatilization of the fuel particles

takes place in an oxygen-deficient zone provided by the primary, inner burner, whereas subsequent char combustion takes place in a zone with excess oxygen. A cooled probe was used for sampling char and ash at four locations along the reactor vertical axis. The particle residence time is taken to be that of a particle with an aerodynamic diameter of 50 μm. Residence time calculations is based on the gas velocity, assuming laminar flow and taking into account the reactor geometry, axial gas temperature profile and the particle terminal velocity, showed. A cascade impactor is used to obtain eleven fractions in the size range ~0.3 μm to 50 μm . SEM coupled with EDX system was used to analyse each stage of the impactor. An EDX measurement was performed by scanning the whole of a deposit of particles formed underneath an orifice in the corresponding impactor jet stage. In this way a ZAF-corrected analysis of 1-3 deposits per stage was obtained for the following elements: Si, Al, Fe, Ca, Mg, Na, K, P, S, Cl, Mn and O.

Table 3.2: Summary of LCS features

Particle feed rate	1-5 g/h
Particle residence time	10-3000 ms
Particle heating rate	$>10^5$ °C/s
Gas supply primary burner	CH_4, O_2, N_2, H_2, CO, CO_2, H_2S
Gas supply secondary burner	CH_4, O_2, N_2, H_2, CO
Operating pressure	0.1 Mpa
Reaction tube inner diameter	0.076 m
Reaction tube length	1.0 m
Max. electrical heating temperature	1700 °C

In the European Commission framework project mentioned in the beginning of Section 3.3, the LCS is to obtain experimental data of the release behaviour of the inorganics during combustion (Korbee and Cieplik, 2006). The inorganics released is estimated as the difference between the amounts of inorganic matter originally in the fuel and the amount of inorganic matter left in the solid residue after combustion. The final release of inorganic matter includes both gaseous species and aerosols and basically refers to inorganic matter that is in the form of particle and has detached from the parent fuel, with a size smaller than 1 μm. Using this calculations and performing mass balance provides the release behaviour of the fuels at various

residence time. The data obtained will be later used to create a link between biomass speciation and ash release behaviour.

3.4 Speciation model development

In order to determine the speciation of a biomass from the leachability data, two different thermochemical models were used. Two separate thermochemical models that operate differently were used in order to make a comparison of both techniques before adopting the better model for this particular function. The models are known as MINTEQA2 and Orchestra. MINTEQA2 quantitative tool for predicting the equilibrium behaviour of metals in a variety of chemical environments and is a valuable tool for environmental risk assessment. Orchestra is the model that does the speciation calculation within a system known as LeachXS that is used for characterisation and environmental assessment of data derived leaching tests. The background information and description of both these models are addressed in this section whilst the comparison and importance for both methods will be addressed in Chapter 4.

3.4.1 MINTEQA2Thermochemical Model

MINTEQA2 is a geochemical speciation model developed in order to study the movement of pollutants into ground water, in particular the transport and speciation of metals. The concentration output obtained from the pH based leaching analysis is used as an input into MINTEQA2 for the model to calculate the distribution of the species among dissolved, adsorbed, solid, and gas phases using the low temperature "equilibrium constant method" (Allison et al., 1991). The chemical equilibrium of each component is calculated using its solubility constants (under standard conditions) for dilute aqueous systems.

In the present work, MINTEQA2 was used to retrieve information of a biomass that has been leached in solutions of different pH. When a biomass is leached into these solutions, the extracted concentrations of the various elements are fed as input for MINTEQA2. With the information of the concentration of the various elements, the model uses equilibrium knowledge of the various species available in the database to predict the possible speciation of biomass before it had undergone the leaching

process. This way it will be possible to gain better knowledge about the speciation of the leached (and unleached) inorganics in the biomass. The equilibrium knowledge that is used for the calculation is the equilibrium constant or the solubility product constant (K_{sp}). As an example, in a reaction that is hypothetically described in Eq 3.1, the equilibrium constant formula is as shown in Eq 3.2

$$aA + bB + ... = cC + dD + ... \qquad \text{Eq 3.1}$$

The equilibrium constant is given by:

$$K = \frac{[C]c * [D]d * ...}{[A]a * [B]b * ...} \qquad \text{Eq 3.2}$$

where:

[A] = activity or partial pressure of species A, B, C, etc.

a = stoichiometric coefficient of species A in reaction

n = stoichiometric coefficient of a species in reaction (a, b, c, ...)

R = gas constant = 8.314 J/(Kmol)

In MINTEQA2, the equilibrium constant used is the solubility product constant (Ksp). This is defined as the equilibrium constant for the equilibrium that exists between a solid ionic solute and its ions in a saturated aqueous solution. Since the density of any pure solid or liquid does not vary with the extent of a reaction, the concentration of both compounds can be regarded as a constant and can be absorbed into the equilibrium constant (Dios, not dated). The equilibrium between a solid and the corresponding ions in solution is given by:

$$AB(s) \rightarrow A^{+}(aq) + B^{-}(aq)$$

$$K_{sp} = [A^{+}][B^{-}] \qquad \text{Eq 3.3}$$

Figure 3.5 illustrates the schematic flow of the calculations carried out in MINTEQA2 to determine chemical speciation of a material. The calculations begin with an initial guess for the activity coefficient of each element which is used to calculate the concentration of all the available species based on mass action expression, written as component activity. The total mass of each component is calculated from the concentration of all the species that contain that particular element. This total mass is then compared with the known input concentration of each element. This is done until a close value is found between the input concentration and the calculated concentration.

MINTEQA2 also calculates the saturation index of the materials, thereby making it possible to predict if a species may precipitate. Zero represents full equilibrium, negative values represent under-saturation and positive values represent over-saturation. In the output, the concentrations of the main elements put into MINTEQA2 are found to be in the following forms:

Type 1: Components as species in solution
Type 2: Species predefined with a fixed activity
Type 3: Precipitate

For example, in terms of the expected outputs for the leached K element in a biomass, MINTEQA2 will process the likelihood of a component; say potassium existing as a species (free ion) in the solution (K^+), as a species (KCl), or as a precipitate (KCl mineral). This way a large portion of the inorganics associated with K-element is predicted which is useful in knowing its distribution as ionic salts, organically associated inorganics and precipitates.

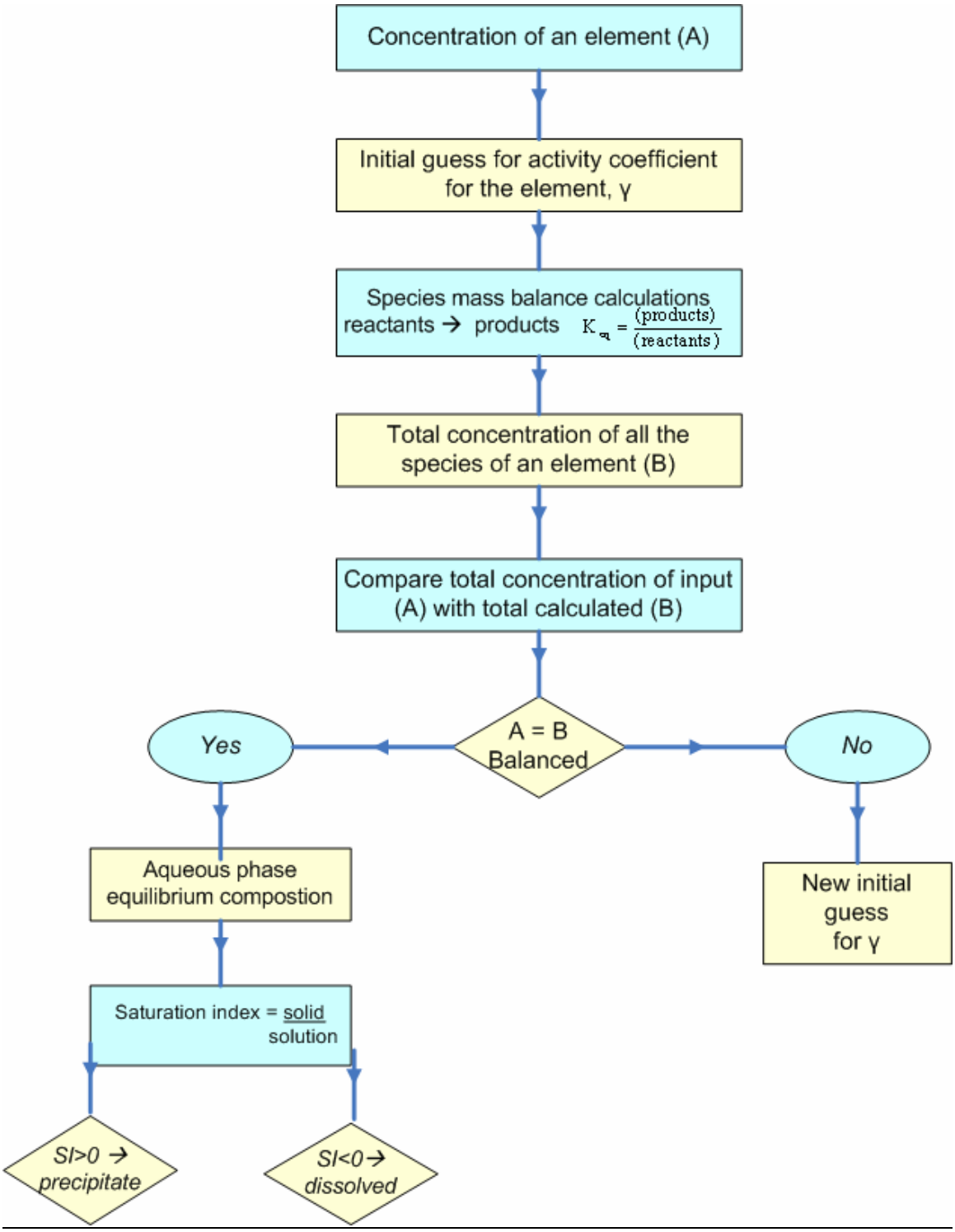

Figure 3.5: Calculating Chemical Speciation using MINTEQA2

3.4.2 LeachXS Thermochemical Model

LeachXS is another available geochemical speciation system that can be used for determining the main chemical processes that verify the behaviour of contaminants from waste materials (Van der Sloot, 2005). LeachXS utilizes the ORCHESTRA model to carry out chemical speciation calculations and solubility predictions. ORCHESTRA contains the information to calculate the saturation indices of the minerals that has been fed into its model, whilst taking into account the organically bound speciation. Two main differences seen in this model when compared to MinteqA2 are:

1) ORCHESTRA includes calculations of adsorption or binding of metals to organic matter, using the Nica-Donnan model (Kinniburgh et al, 1999). Nica-Donnan model is usually used for humic acids which are degraded production from plant material, as the organic binder. Therefore in this work the humic acids were substituted with organic ligands of biomass, as humic acids are not likely to be present in biomass samples analysed in this work.

2) Possibilities to add new adsorption models including iron and aluminium hydroxides (Dzombak & Morel, 1990) and clay ion exchange model.

The following points highlight the steps taken in order to determine the chemical speciation of a fuel, whilst Figure 3.4 explains the work flow of LeachXS:

1) A pH based extraction or leaching test was carried out to identify the leachibility of the biomass in different pH conditions.
2) The database was firstly updated with thermodynamic properties of the various speciations that are likely to exist in biomass. These speciations are as summarised in Table 3.1.

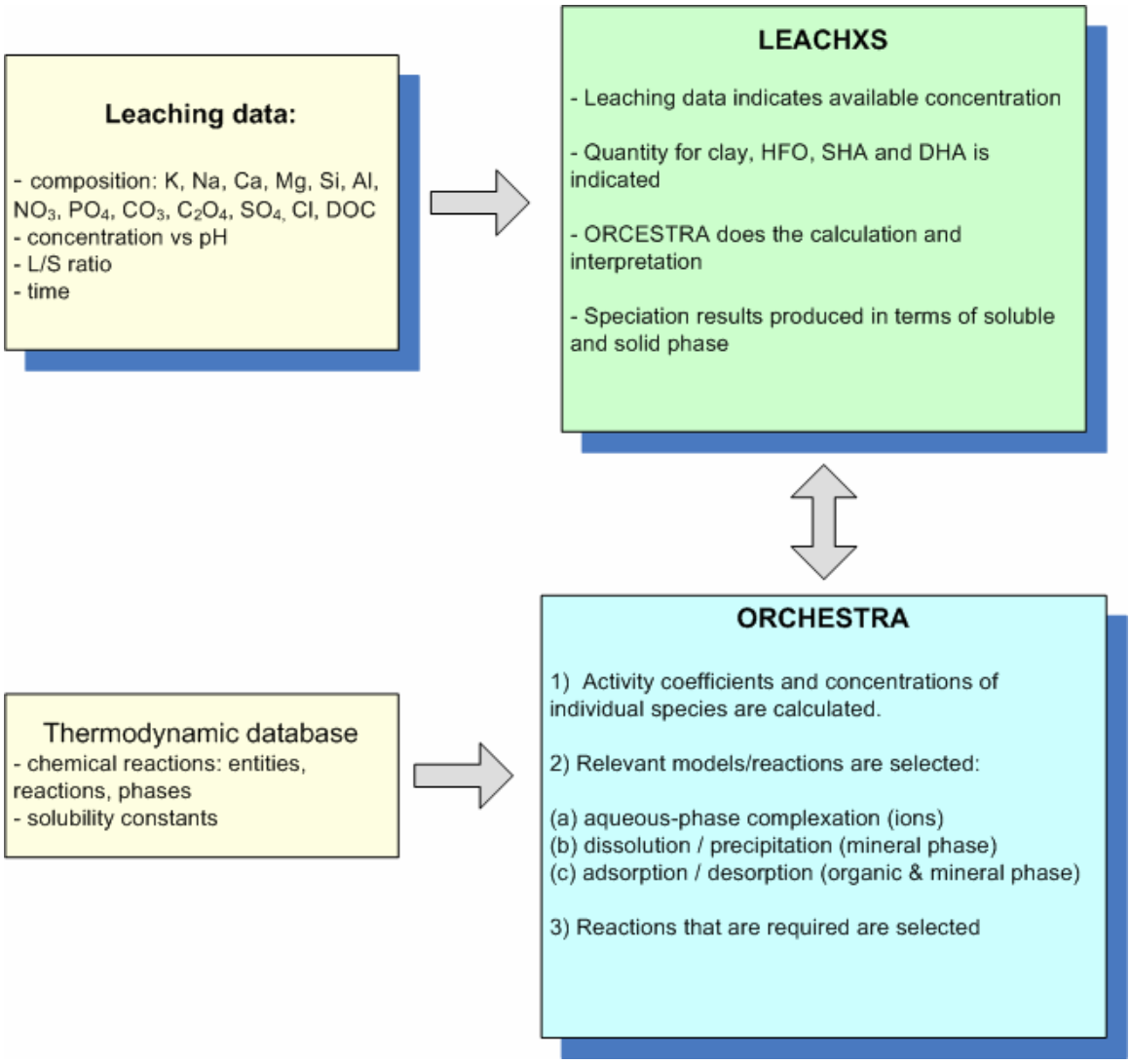

Figure 3.6: Speciation determination using LeachXS (adopted from LeachXS User Manual, Sloot van der, et al., 2005)

3) Data obtained from extraction were used to identify relevant mineral phases using the support of saturation indices calculations. This section of the model works in a similar way to MINTEQA2.

4) The quantity of total organic carbon was included to obtain the speciation of the organically bound material.

5) The saturation index units can be used to select relevant minerals for a subsequent chemical speciation prediction run. The saturation index is calculated for more than 650 minerals in the thermodynamic database and the selection of the most likely

phases was made based on the closeness of the saturation index to zero or also known as equilibrium.

6) The model calculates speciation from pH 1 to 13 with a 0.2 interval.

7) Initial calculations show the dominating minerals that could be present in the biomass and consequently the possible minerals based on background knowledge of the biomass are selected.

8) After making the appropriate selection, the final output is generated in two main ways, one for the chemical speciation in the solution and the other for the solid phase distribution. Table 3.3 shows the available speciation types, which have been divided into the soluble material and the solid phase material.

Table 3.3: Solid and liquid phase partitioning

Solubility prediction	**Solid phase prediction**
Free ions and salts	Clay bound
Dissolved organic carbon (DOC)	Al or Fe-oxide bound
	Particle or solid organic matter bound (POM)
	Mineral precipitate
	Incorporated in solid solution

CHAPTER 4

Speciation Results and Validation

4.1 pH extraction analysis

The elements that were studied for this analysis are K, Na, Ca, Mg, Al, Si, Cl, DOC, PO_4 and SO_4. C_2O_4 extraction was also analysed using GC method. The pH extraction curves show the concentrations determined in the leachate as a function of pH (Figures 4.1 to 4.6) for several biomass, namely wood chips, wood bark, straw and Polish coal. This way it is possible to observe the leaching pattern of the various biomasses and also to compare them with coal.

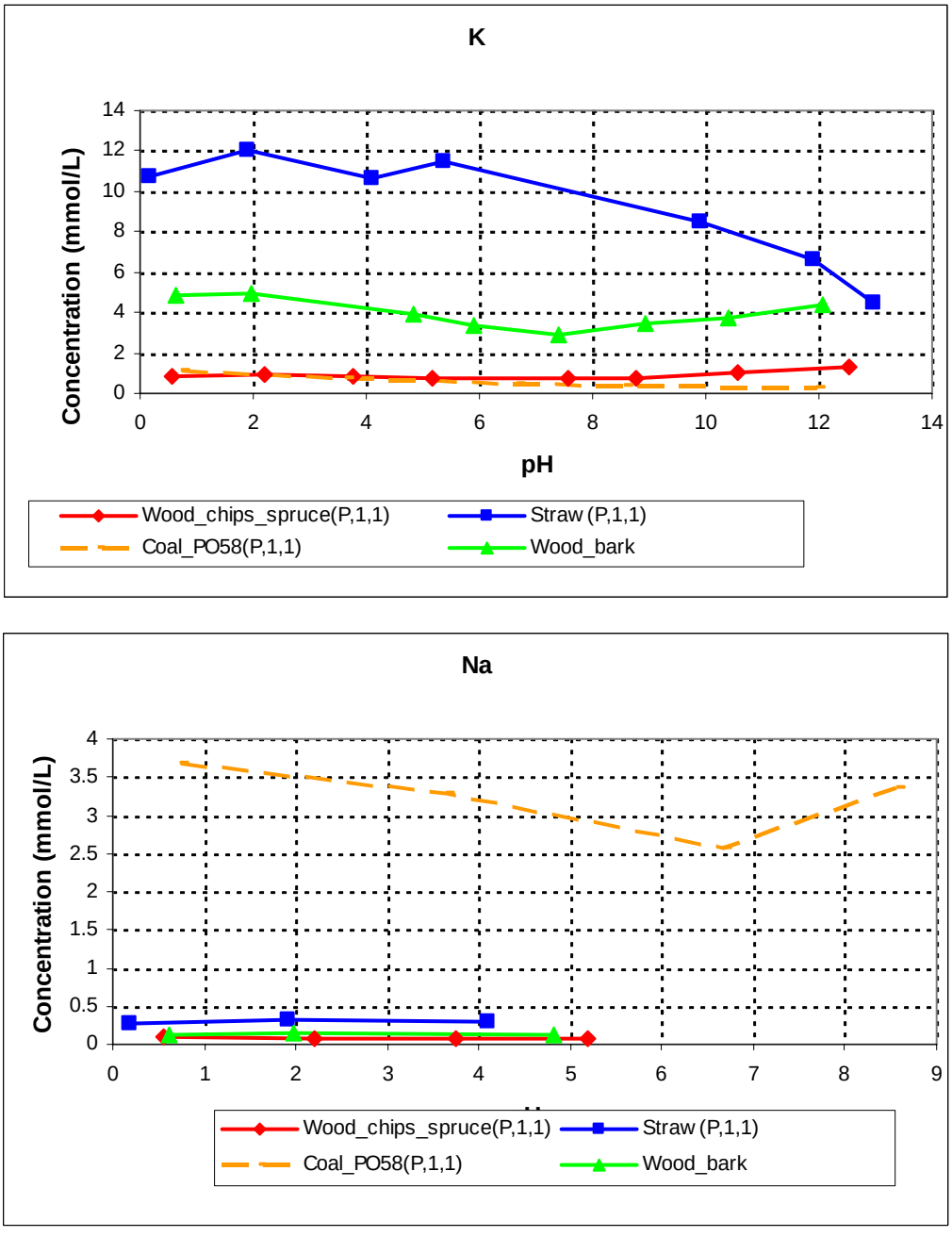

Figure 4.1: pH dependent extractions of K and Na

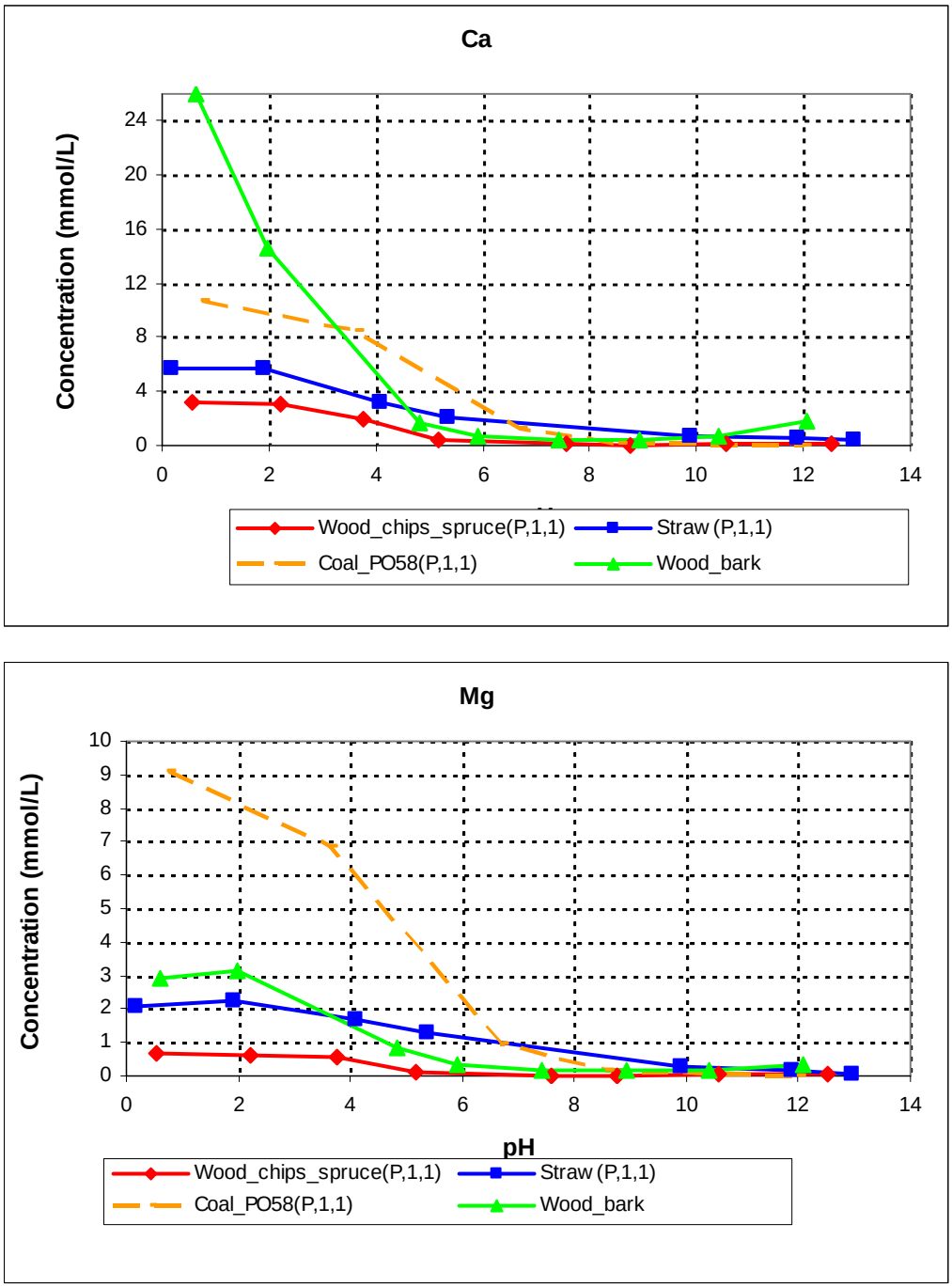

Figure 4.2: pH dependent extractions of Ca and Mg

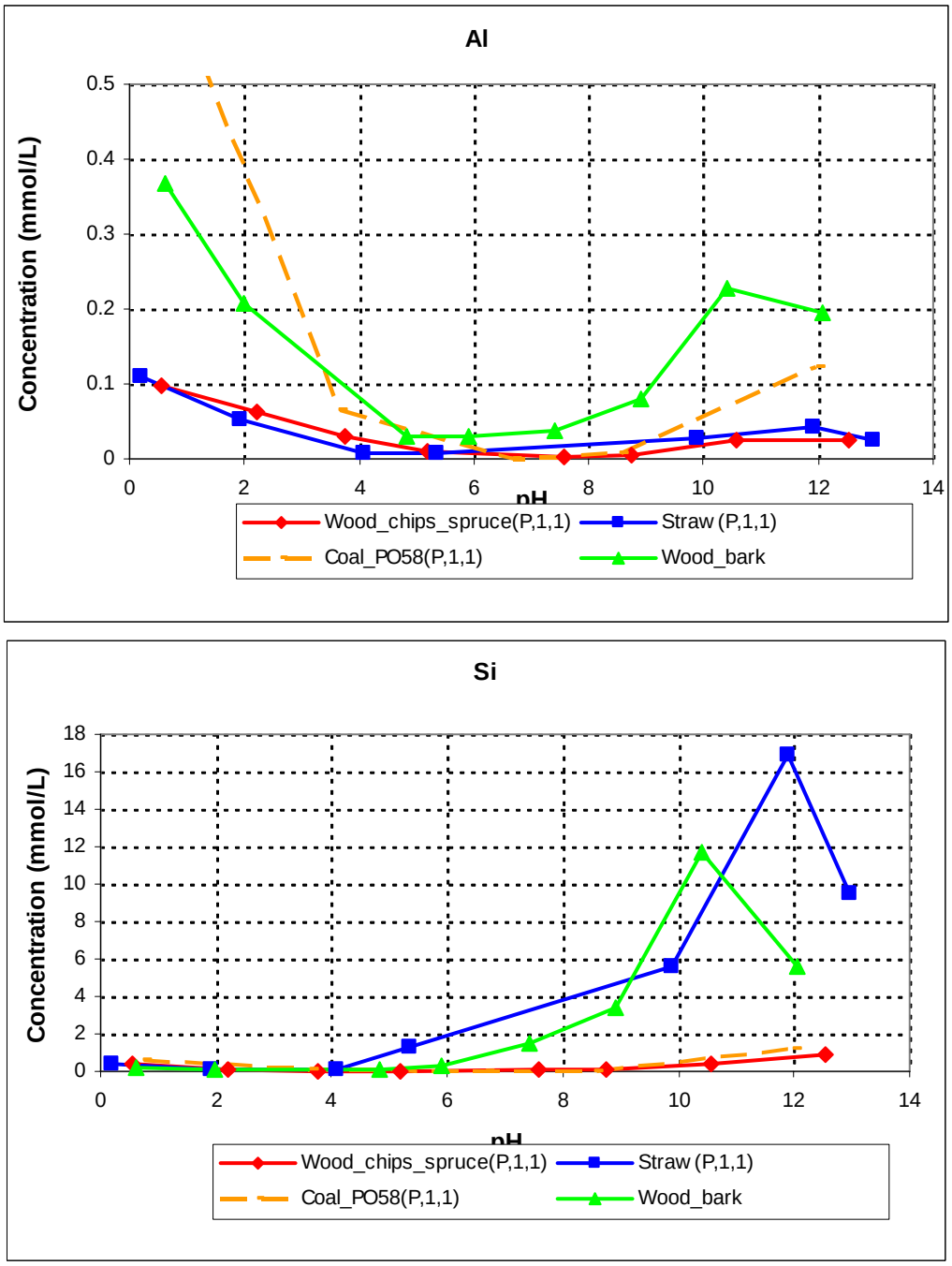

Figure 4.3: pH dependent extractions of Al and Si

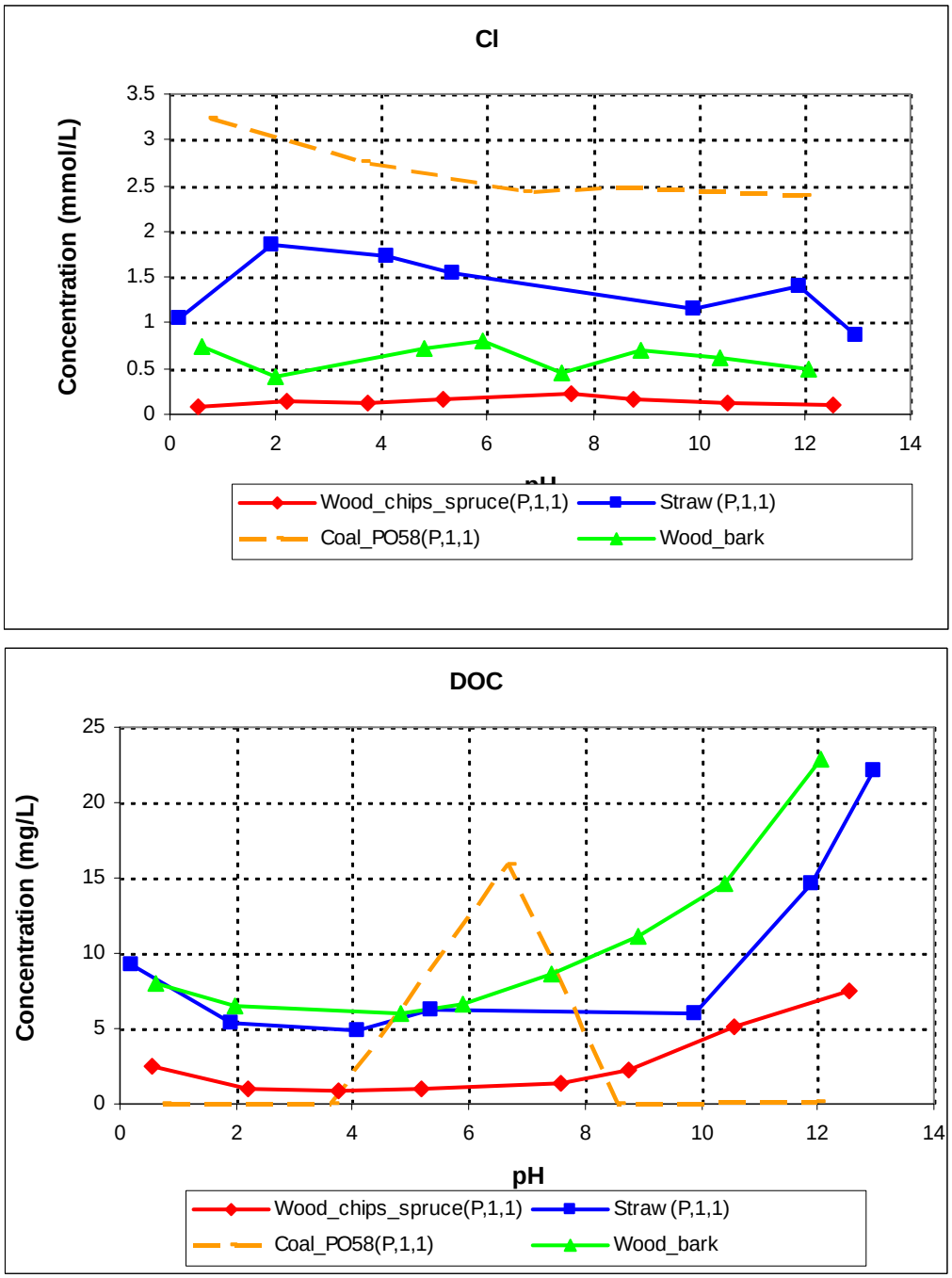

Figure 4.4: pH dependent extractions of Cl and DOC

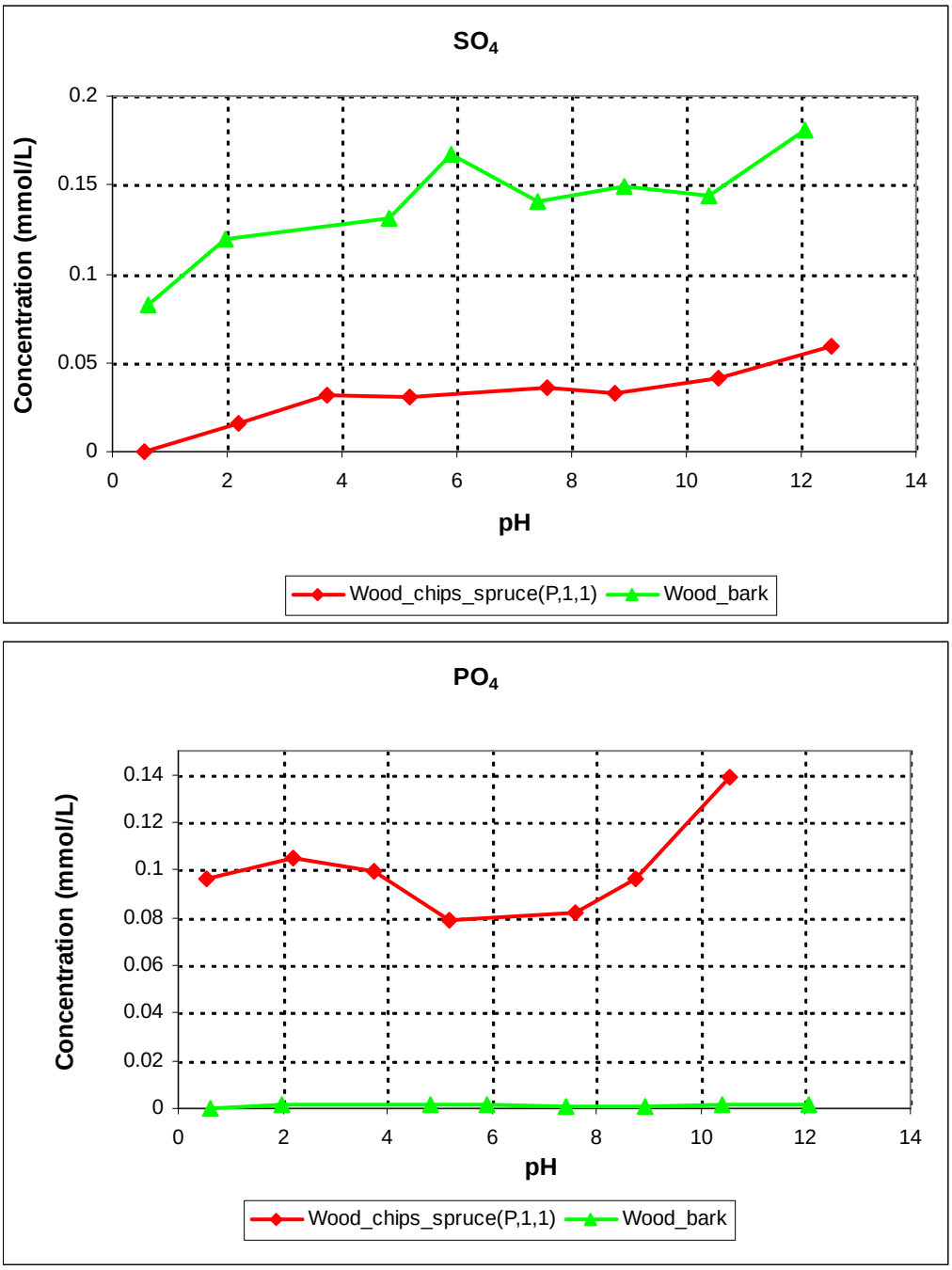

Figure 4.5: pH dependent extractions of SO_4 and PO_4

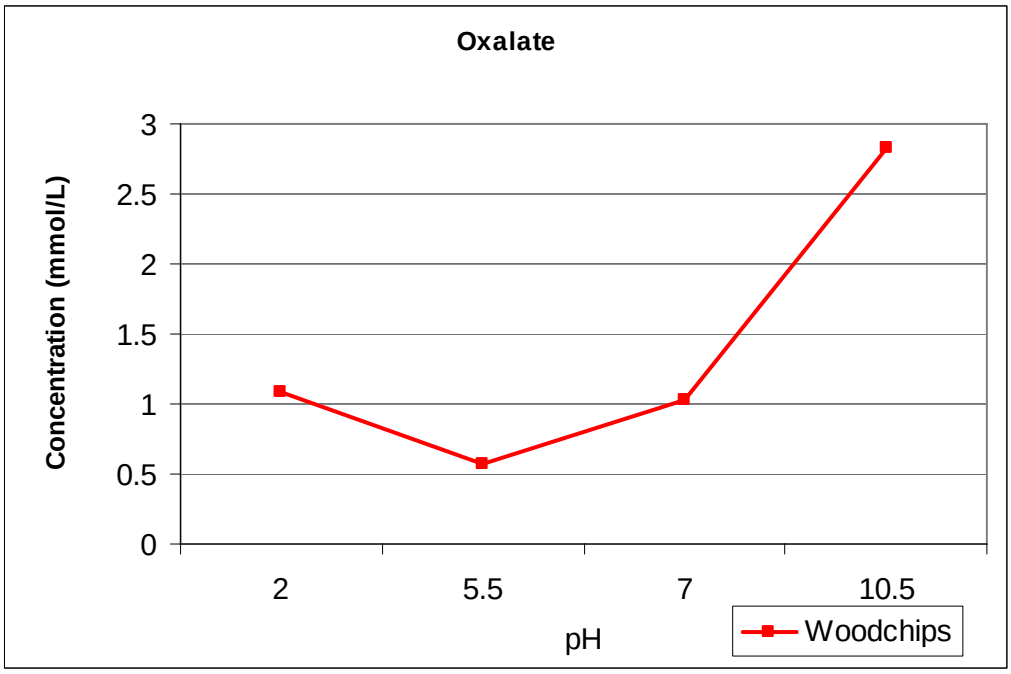

Figure 4.6: pH dependent extraction of oxalate

It was observed for the K and Na that the extracted concentrations of these elements are constant at all pH, except for the leached quantity of K in straw. For Ca and Mg it was seen that the peak of the leached concentration was obtained at the most acidic region and this amount reduced as the leaching curve moved towards the alkaline region. In the case of the Al, a parabolic curve was observed in its leaching curve, whereby the minimum was seen at neutral pH and the highest peak observed at the most alkaline area of all samples. For Si it was found that the leaching concentration increased as the pH value increased, however a maximum in leachability is seen between pH 10 and 12, after which the concentration starts reducing. This shows that all the elements have an optimum pH range, during which the elements are easily leached into the solution, though the trend and optimum range also depends on the fuel studied.

For the anions such as SO_4, PO_4 and Cl, it was generally observed that a constant leaching curve was obtained at all pH. For DOC it was seen that for the biomass samples, the leaching concentration increased as the pH increases, where as for coal, a hyperbolic curve pattern was observed with the maximum leached at neutral pH. The leaching pattern of oxalate was observed to be similar to that of the DOC's, as oxalates are a subset of DOC's. A higher quantity of oxalates was leached in

comparison to calcium for wood chips in the higher alkaline region. This indicates that there may be other speciation of oxalates apart from Ca-oxalate in wood chips.

The similiarity in the leaching pattern for the elements of different fuels indicates that a geochemical fingerprint can be derived for each of the elements. It can also be seen from the graphs that an optimum pH value exists for some of the elements, namely Ca, Mg, Al, Si, DOC and oxalates, unlike for elements such as K, Na and PO_4 which usually have a constant leaching data at all pH. Optimum leached data here means that at a particular pH, most of the available amount of an element is leached out. This maximum leaching concentration represents the quantity of that particular element in the fuel and therefore is used as the available amount to predict the speciation of each of the elements using the geochemical speciation models. It was also found that the data from leaching tests are reproducible and accurate for various fuels (Appendix C.2)

In order to study the leaching efficiency of all elements during the pH extraction tests, an analysis was done to see if all the elements were fully leached out or if there was a certain amount remaining as residue. This test was carried out at neutral pH to compare percentage leached in solution against the overall total (leached and residual) of the elements. The results obtained have been summarised in Figure 4.7. As it can be seen that for the elements that are leached out equally at all pH such as K, Na and PO_4, the leaching efficiency is satisfactory (more than 70%). The leaching efficiency for elements such as Ca, Mg, Al, Si have a lower efficiency as neutral pH is not the optimum range for its leaching, therefore causing the elements to still remain in the residue. However, judging by the efficiency of K, Na and PO_4 it can be summarised that the pH extraction method gives satisfactory leachability when an element is leached in its optimum pH solution.

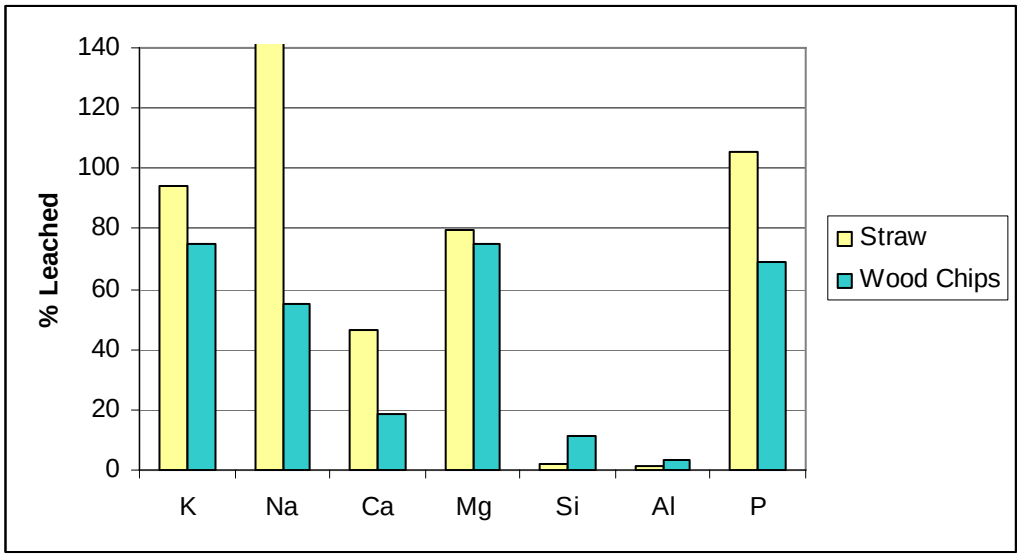

Figure 4.7: Leaching efficiency of pH extraction tests

(Note: Fluctuations in Na is due to the usage of NaOH as the base solution)

4.2 MINTEQA2 Modeling Results

The calculations carried out within MINTEQA2 are summarised in the flow chart in Figure 3.5. Although MINTEQA2 has an extensive database, due to the variety of inorganic salts and organically bound matter in the speciation of biomass, the database was supplemented with additional components and their related reactions and constants. This addition requires several thermochemistry data which were derived from chemical databases such as HSC Chemistry 5.11 and NIST; among which are the solubility product constant (Ksp). Solubility product values that could not be obtained from databases were calculated using equilibrium relations from known standard state properties. The solubility of the products was determined from the thermodynamic equations:

$$\ln K_{sp} = \Delta Gr / (-RT)$$

$$\ln K_{sp} = \Delta Hr / (-RT) + \Delta S/R \qquad \text{Eq 4.1}$$

Whilst this exercise determined the Ksp values for most of the salts and minerals (as shown in Appendix D.1), it was however difficult to obtain the required data for the organically bound inorganics due to the complexity of the organic composition.

When pH-leaching results were put into MINTEQA2 at the various pH, the model calculated the most likely species to form at room temperature conditions. The outputs can be classified into three different types. Type I outputs are the input components found as free ions in the solution such as K^+, Cl^- and Ca^{2+}. They form a large part of the output. Ionic salts such as KCl have been interpreted to be part of Type I outputs as the test is in a very dilute system, and therefore some of the ionic salts are recognised as free ions. Types 2 and 3 are the organically associated inorganics and minerals respectively. It has to be noted that MINTEQA2 assumes that the state of equilibrium during the calculations and this assumption may not describe the actual leachability data obtained from the pH leaching test. The analysis with MINTEQA2 was carried out with all the biomass samples and the results obtained are summarized in Table 4.1. It also has to be noted that NaOH and HNO_3 were used as the acid and base during the experiments, therefore the usage of Na and NO_3 data were discarded in the related ranges.

Graphs 4.8 and 4.9 show that most of the K and Na elements exist as free ions throughout the pH range while Ca-free ions (refer Graph 4.10) are only seen in the lower acidic range (pH<5). Aside from free ions, Ca-oxalates are found to form in the acidic conditions, whilst calcium phosphates tend to form in alkaline conditions. Work done in CF previously reports that most of the K, Na and Cl in woody fuels are leaching out in the first step of water leaching, whilst Ca was leached out in the second and third step of leaching (Werkelin, 2005). This explains the free K, Na and Cl found in MINTEQA2. As for Ca the model does not include calculations for organically bound material therefore it may be possible that some of the free Ca^{2+} ions found in MINTEQA2, are not actually free ions, but organically bound species such as Ca-pectate.

The overall speciation for a biomass sample (wood chips) has been summarised in Table 3.4. Type I includes the speciation of the free ions and salts for all the elements whilst it was observed that none of the Type II or the organics is derived for any of the elements. This shows that this model is not suitable for biomass as it does not take into account organically associated inorganics. Type III is the speciation of inorganics that have a saturation index that is close to or higher than 1, thus existing

as precipitated material or minerals. However, as the overall speciation does not include the organically bound material, it was found that it is necessary to look into models that include this possibility for better speciation predictions.

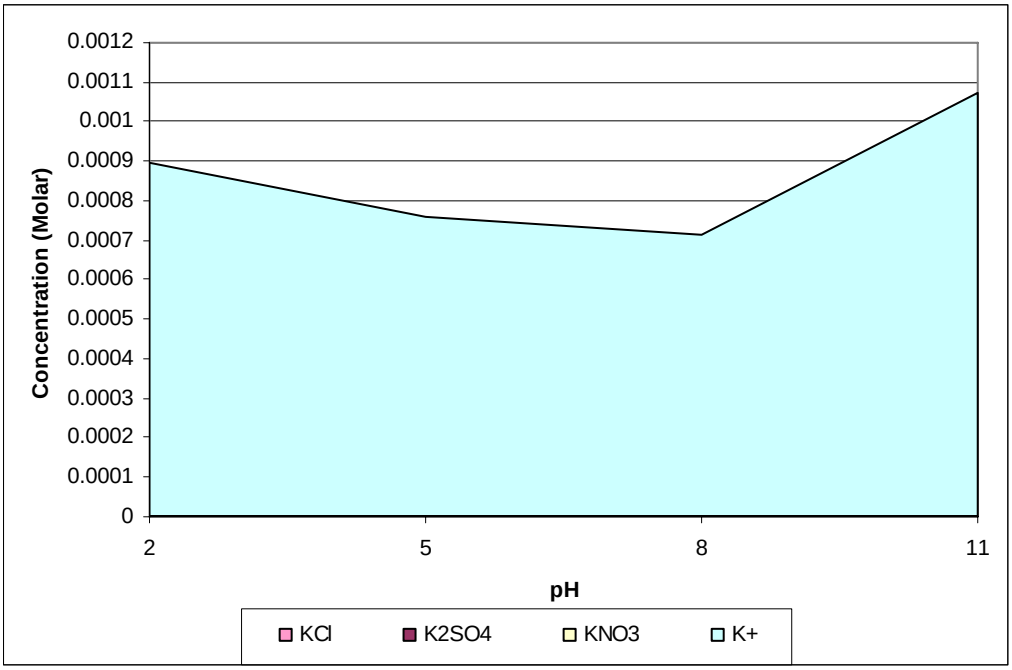

Figure 4.8: Speciation of K in wood chips obtained from MINTEQA2 model

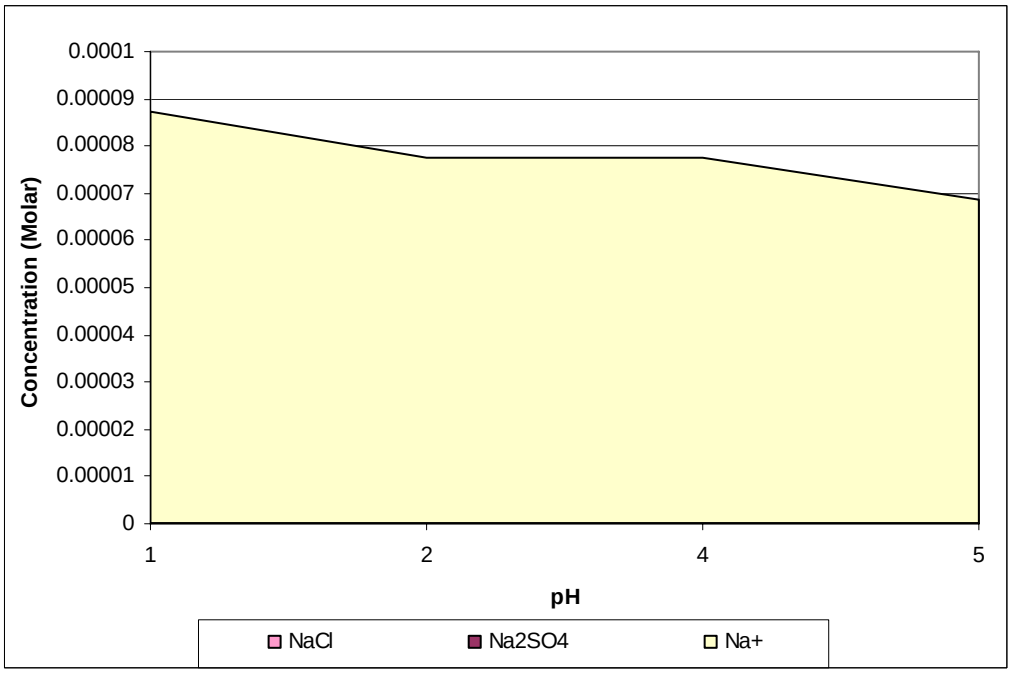

Figure 4.9: Speciation of Na in wood chips obtained from MINTEQA2 model

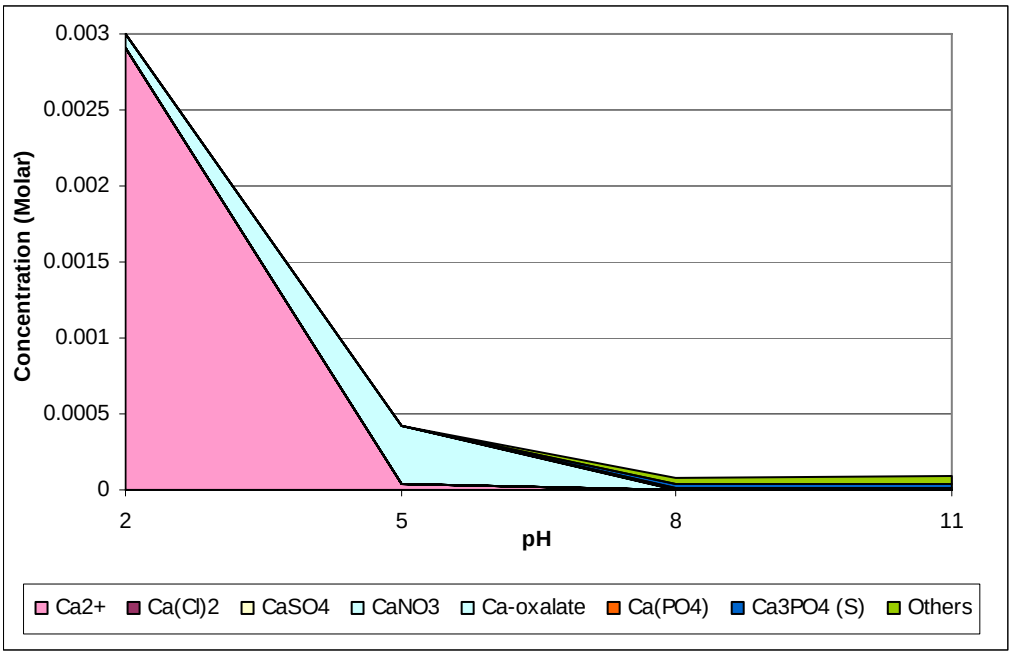

Figure 4.10: Speciation of Ca in wood chips obtained from MINTEQA2 model

Table 4.1: Compilation of the formations of species predicted through MINTEQA2 model

pH	Type I (Free ions and salts)	Type III (Minerals)
2	NaCl, KCl K_2SO_4, $CaSO_4$, $MgSO_4$ $Ca(PO_4)_2$	Calcium oxalate Quartz Silicates
5	NaCl, KCl K_2SO_4, $CaSO_4$, $MgSO_4$ $Ca(PO_4)_2$	Calcium oxalate Kaolinite Quartz Silicates
7	NaCl, KCl K_2SO_4, $CaSO_4$, $MgSO_4$ $Ca(PO_4)_2$ KNO_3	Calcium phosphate Kaolinite Quartz
11	NaCl, KCl K_2SO_4, $CaSO_4$, $MgSO_4$ $Ca(PO_4)_2$ KNO_3	Calcium phosphate Quartz

4.3 LeachXS Results

The samples that were extracted from pH leaching experiments and sequentially evaluated using LeachXS include wood chips, wood bark and straw. This section describes the step-by-step method in obtaining the speciation for the three biomass samples. The cations that were studied for this analysis are K^+, Na^+, Ca^{2+}, Mg^{2+}, Si^{4+} and Al^{3+}, whilst the anions studied are Cl^-, DOC, $C_2O_4^{2-}$, NO_3^-, $PO4^-$ and SO_4^{2-}. The results indicate the quantity of elements that are considered to be free ions, DOC-

bound and also its solid phase. Figure 4.11 has been used to simplify how the speciation of a biomass is interpreted using LeachXS.

The measured curve shown is the extraction curve obtained from leaching data of a certain element. The area under the leaching curve represents the soluble species, which are the free ions and the ionic salts. The highest soluble concentration of an element is determined from the maximum of the extraction curve and is taken as the available concentration for speciation calculation. This value is indicated by the dotted red lines at the top end of the curve. Predictions are made with the dissolved element concentration using the solubility data for every reactant. The remaining area between the highest coordinate and the extraction curve represents the section where other possible speciation exists such as the minerals and solid organic matter, which are obtained through equilibrium calculations. The maximum leached concentrations for every element is summarised in Appendix D.2 and is used as the input into LeachXS.

The speciation of the fuels have been categorised into six main groups, which are:

1) Free: free ions or dissolved salts (excluding complexation)
2) Dissolved organics (DOC bound): elements bound to dissolved organics
3) Solid organics (POM bound): elements bound to solid organics
4) HFO: elements bound to iron oxide
5) Clay: elements bound to clay
6) Minerals: elements that exist in mineral form

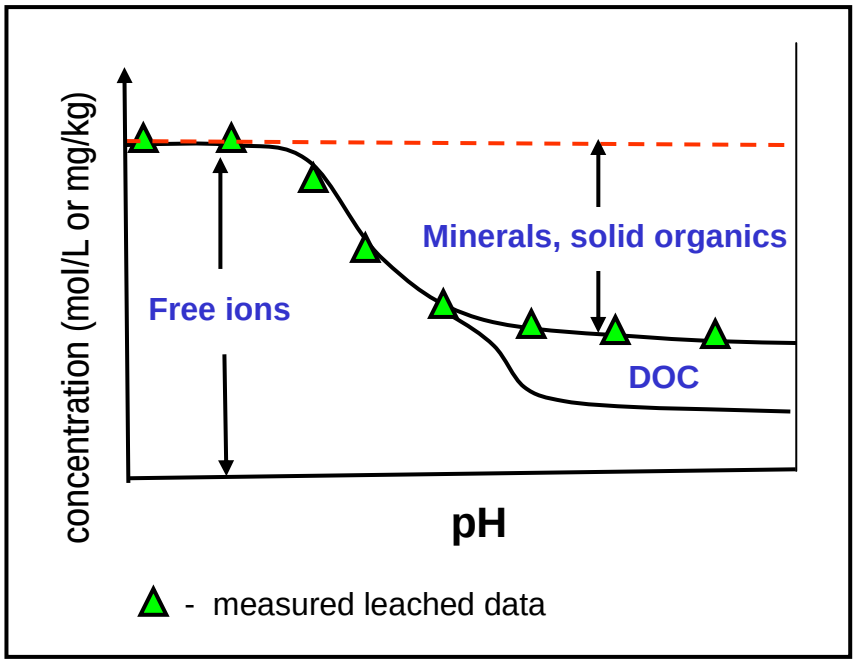

Figure 4.11: General speciation for biomass with LeachXS

When wood chips were analysed, it was seen that the K-element speciation consists mainly of free ions or dissolved salts as shown in Figure 4.12. At high alkaline region, DOC-bound and solid organic bound speciation was also seen. The same observation was seen for the Na element that is shown in Figure 4.13, but at lower concentrations.

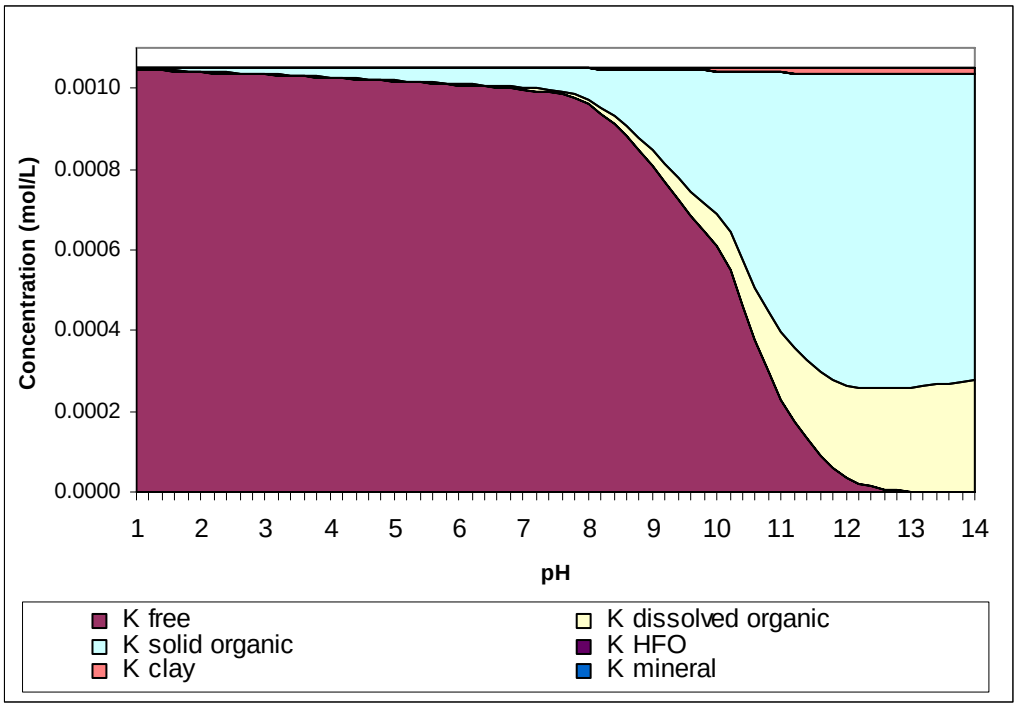

Figure 4.12: Speciation of K element in wood chips

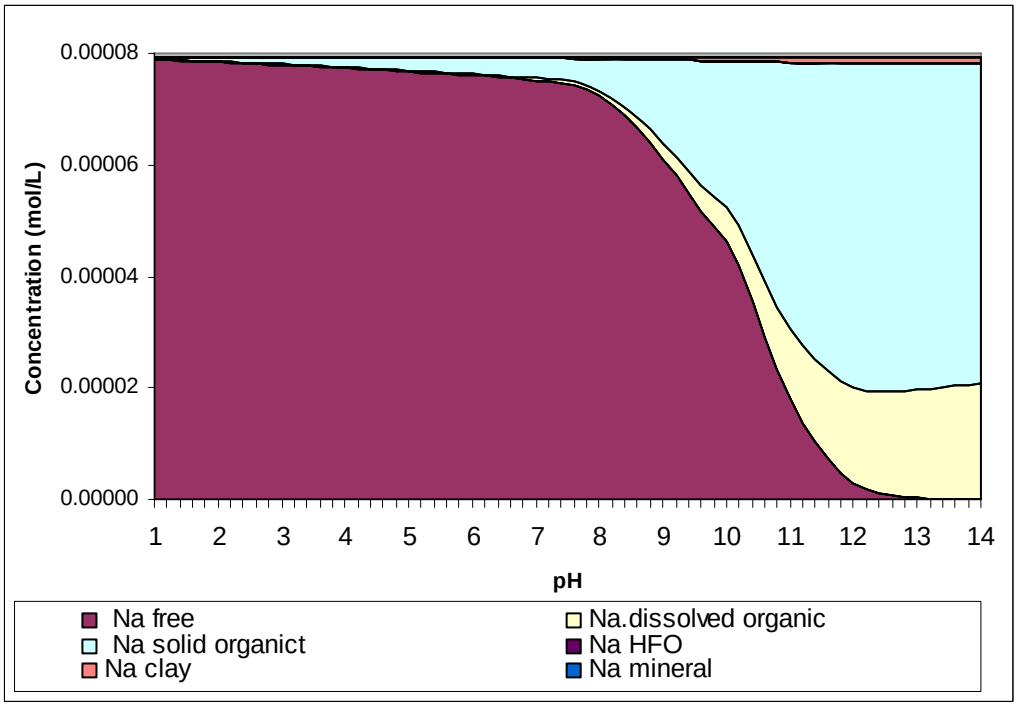

Figure 4.13: Speciation of Na element in wood chips

For Ca the main outputs are as shown in Figure 4.14, whereby in the acidic region, dissolved Ca material was observed and in the alkaline region solid organic bound material was mainly seen. Calcite minerals were observed in the speciation of the Ca.

Similar pattern of behaviour was observed for Mg speciation in Figure 4.15, except that no minerals were seen in its speciation.

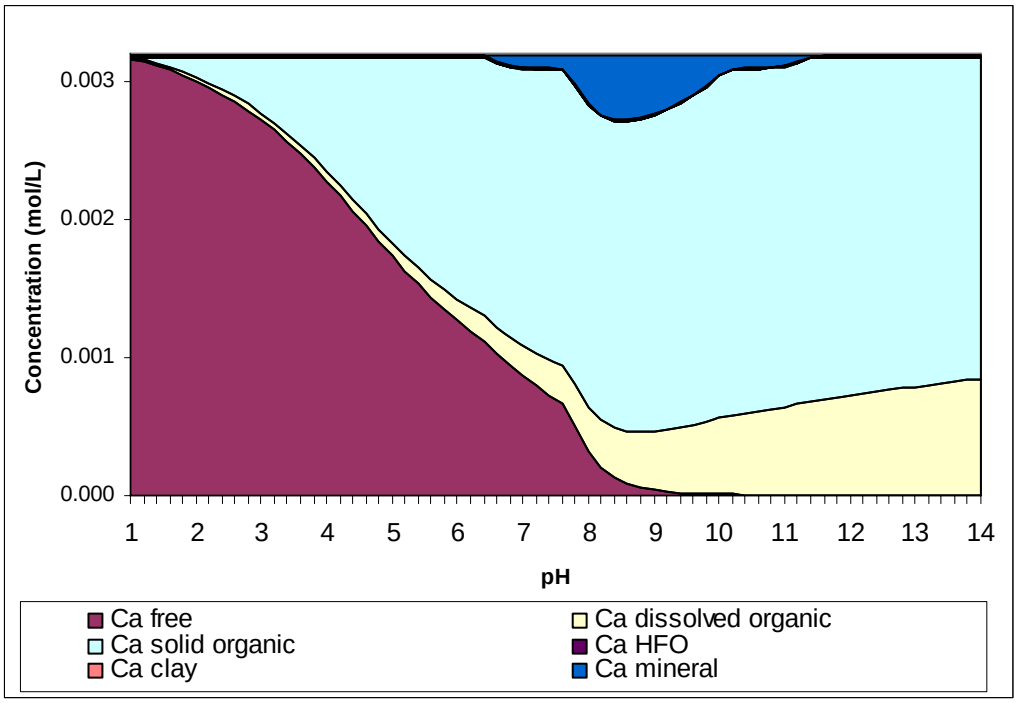

Figure 4.14: Speciation for Ca element in wood chips

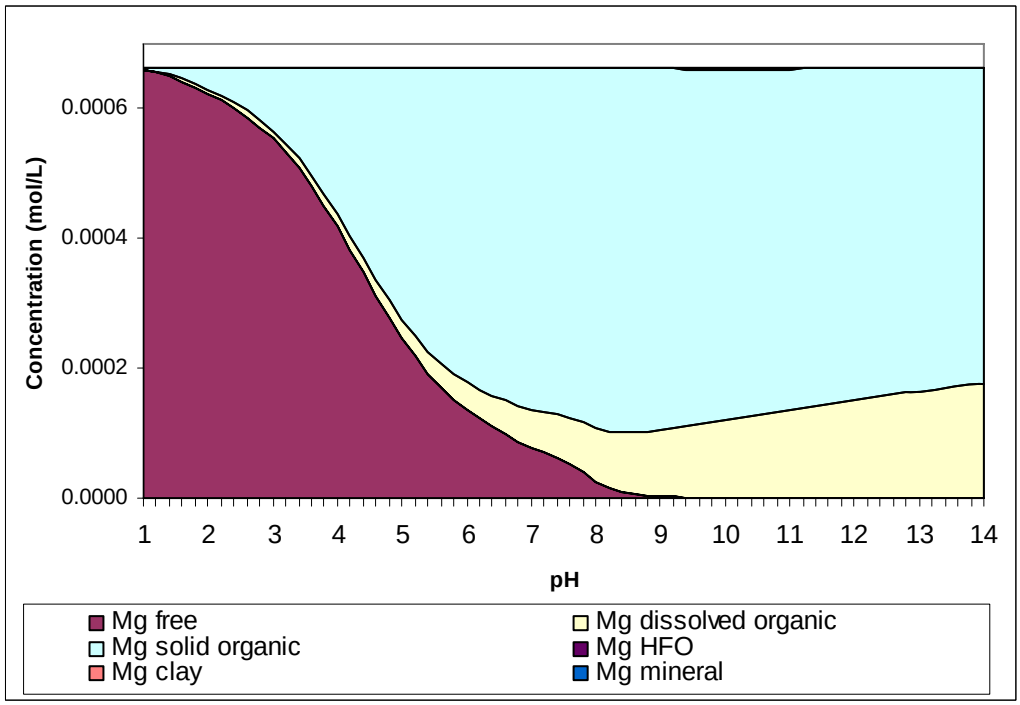

Figure 4.15: Speciation for Mg element in wood chips

For the Si element, Figure 4.16 shows that the speciation mainly consists of free or dissolved silica in the high pH region and minerals such as quartz in the low pH region. For Al, dissolved species were only found in the very high acidic or alkali region, whilst at moderately acid conditions solid organics were seen. At moderate alkaline sections Al mineral speciation were observed.

For the anions, namely CO_3^{2-}, PO_4^{-}, NO_3^{-}, SO_4^{2-} and Cl^{-}, it was seen that its speciation mainly consist of free ions or salts, except for PO_4 which consists of up to 25% minerals and HFO bound material. The results obtained from the LeachXS can be qualified and quantified as displayed in Table 4.2, which gives an overview of the likely chemical speciation of woodchips. As the concentration of a certain speciation is different at various pH, the concentration that is taken is the one that is at the highest concentration. For example in K the speciation of the dissolved organics is seen at several pH but the highest concentration was measured at high alkaline pH (pH 13.8), therefore the concentration of the K-dissolved organic speciation is measured at that particular pH. Table 4.3 and 4.4 summarise the speciation observed for wood bark and straw respectively.

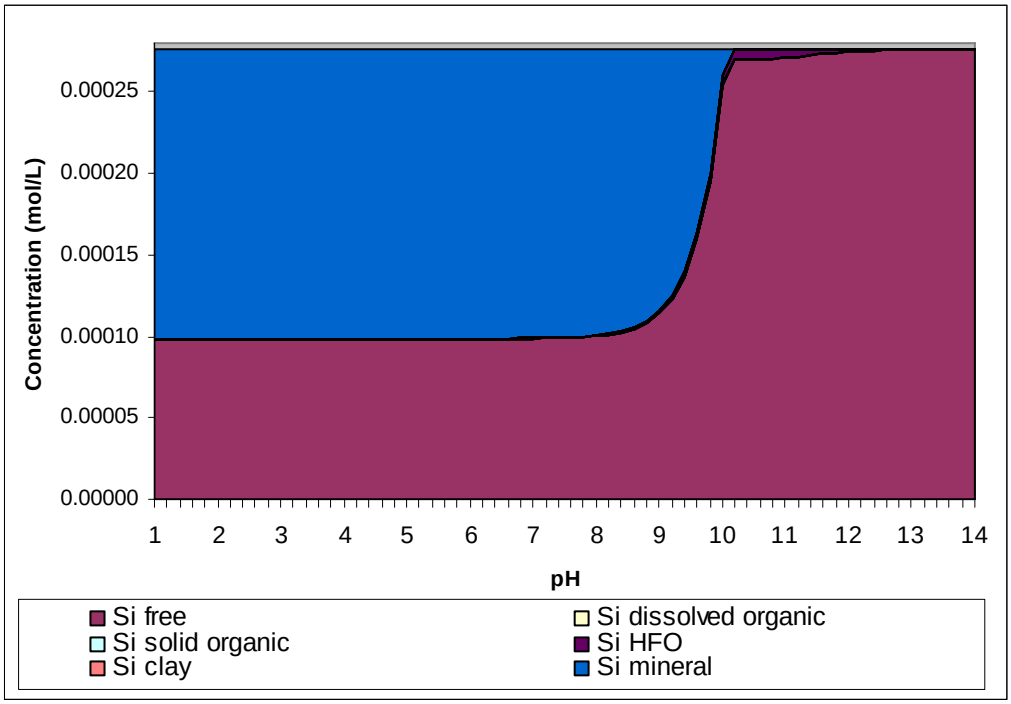

Figure 4.16: Speciation for Si element in wood chips

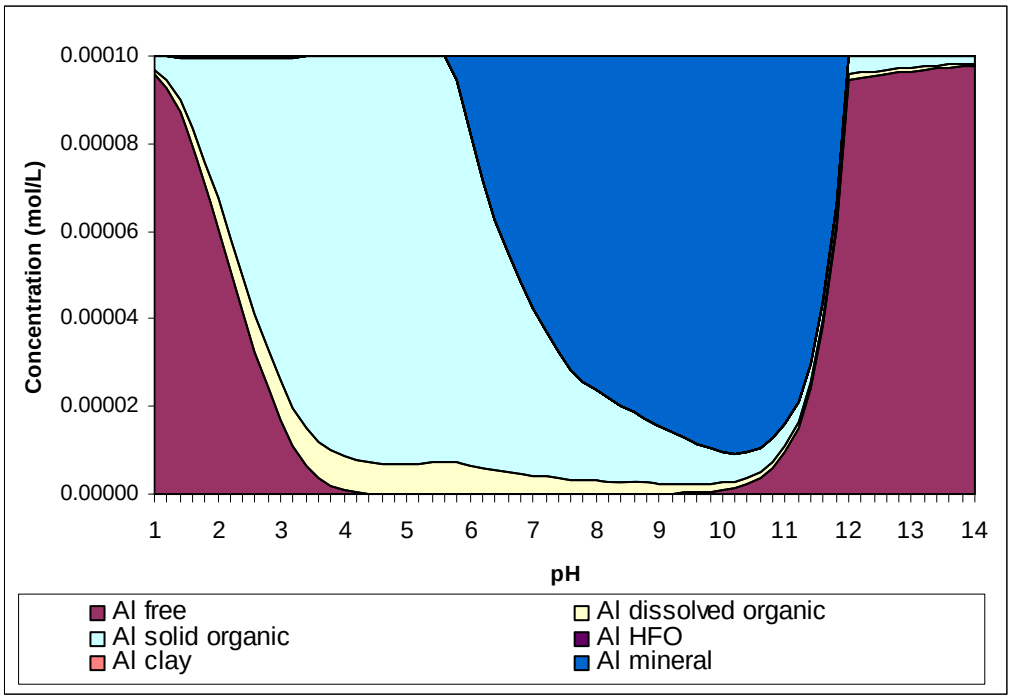

Figure 4.17: Speciation for Al element in wood chips

Table 4.2: Wood chips speciation interpretation from LeachXS

Element	Speciation in solution	Percentage (%)	Solid speciation	Percentage (%)
K	Free ions/salts	49.8	POM bound	36.9
	DOC-bound	13.0	Clay	0.6
Na	Free ions/salts	49.4	POM bound	36.9
	DOC-bound	13.0	Clay	0.6
Ca	Free ions/salts	45.3	POM bound	35.7
	DOC-bound	12.1	Mineral	6.6
Mg	Free ions/salts	47.0	POM bound	40.0
	DOC-bound	12.6	HFO	0.3
Si	Free ions/salts	60.1	Mineral	38.6
			HFO	1.3
Al	Free ions/salts	33.3	POM bound	31.8
	DOC-bound	2.5	Mineral	31.0
PO_4	Free ions/salts	98.0	HFO	2.0
NO_3	Free ions/salts	100.0		
CO_3	Free ions/salts	95.7	Minerals	4.0
SO_4	Free ions/salts	100.0		
Cl	Free ions/salts	100.0		

Table 4.3: Wood bark speciation interpretation from LeachXS (derived from Appendix D.3)

Element	Speciation in solution	Percentage (%)	Solid speciation	Percentage (%)
K	Free ions/salts DOC-bound	58.0 30.0	POM bound	12.0
Na	Free ions/salts DOC-bound	57.0 30.0	POM bound	13.0
Ca	Free ions/salts DOC-bound	44.9 19.6	POM bound Mineral (Calcite, Ca-oxalate)	8.4 27.1
Mg	Free ions/salts DOC-bound	34.7 14.1	POM bound HFO	16.5 34.5
Si	Free ions/salts	50.7	Mineral HFO	49.2 0.1
Al	Free ions/salts DOC-bound	34.4 8.2	POM bound Mineral	23.1 34.2
PO_4	Free ions/salts DOC-bound	31.7 31.8	Minerals HFO	34.0 2.5
NO_3	Free ions/salts	100.0		
CO_3	Free ions/salts	50.0	Minerals	50.0
SO_4	Free ions/salts	100.0		
Cl	Free ions/salts	100.0		

It was observed from the speciation summary of wood bark in Table 4.3 that this biomass has a speciation similar to wood chips for Si and Al elements and different speciation for the other elements. For K and Na, wood bark shows a higher percentage of speciation in solution and a lower tendency to be present as solid organics, whilst for Ca and Mg wood bark is seen to have a higher speciation of minerals such as calcite and HFO bound matter. However, when compared with literature research and SEM analysis, it is seen that the main mineral in wood bark is calcite. This difference is observed as the equilibrium constant value for calcite is lower than calcium oxalate, therefore more likely to be formed using equilibrium

models. In reality it is expected that both calcium oxalate and calcite will be seen in wood bark speciation.

For the anions, the speciation of nitrates, sulfates and chloride were similar for both biomass fuels, which are mostly associated as salts, where as for phosphates and carbonates, wood bark showed a higher association to minerals. In regards to comparison of speciation of straw that is summarized in Table 4.4, it can be seen that straw contains a higher percentage of K, Na, Ca and Mg in dissolved organic phase rather than solid form. Si and Al speciation was similar to the other biomass. For anions however, it was seen that apart from phosphates, all anions were found to be associated as free ions or salts. Phosphates that were not associated as free ions or salts were seen to exist as minerals and HFO bound species.

Table 4.4: Straw speciation interpretation from LeachXS (derived from Appendix D.3)

Element	Speciation in solution	Percentage (%)	Solid speciation	Percentage (%)
K	Free ions/salts DOC-bound	47.3 46.2	POM bound	6.5
Na	Free ions/salts DOC-bound	47.3 46.2	POM bound	6.5
Ca	Free ions/salts DOC-bound	45.4 44.5	POM bound	10.0
Mg	Free ions/salts DOC-bound	45.0 44.0	POM bound	11.0
Si	Free ions/salts	50.5	Mineral	49.4
Al	Free ions/salts DOC-bound	39.6 40.0	POM bound	20.3
PO_4	Free ions/salts	42.9	Minerals HFO	41.9 15.1
NO_3	Free ions/salts	100.0		
CO_3	Free ions/salts DOC-bound	99.5 0.4		
SO_4	Free ions/salts	100.0		
Cl	Free ions/salts	100.0		

Gathering results obtained from both the available speciation models, it is seen that the ORCHESTRA model within LeachXS is the better option to determine biomass speciation. LeachXS has the Nica-Donnan model that makes it possible to have interpretation of the organically bound inorganics, in addition to interpreting the mineral composition. The adsorption model also makes it possible to deduce the binding of Al and Fe hydroxides and the clay speciation to the rest of the biomass. Through MINTEQA2 it was seen that a large quantity of free ions existed for most elements but it has been seen through LeachXS that in reality some of these free ions are bound as either organics or adsorbed as hydroxides or clay. With LeachXS, it

was also possible to derive the ratio of the organics that can be found as either dissolved or as solid particle, as seen in the speciation results (see Tables 4.2-4.4).

4.4 Comparison between pH Extraction and CF Method

In this section, the results obtained from both the pH extraction and CF method will be compared in order to clearly substantiate the benefits of pH extraction technique to produce a more detailed speciation of biomass. The results obtained for the CF are based on the work carried out for the BioAsh project (Frandsen, et al., 2006). CF method is done sequentially, where the same biomass sample is leached firstly in water, then ammonium acetate and finally acid (usually HCl). However pH extraction is a batch test, meaning that the biomass is analysed separately at various pH. Therefore the amounts leached are difficult to compare for both methods. In the CF method, the biomass is immersed in three different solutions, whereby the final pH is not monitored or controlled. On the other hand, for pH extraction tests, the biomass is immersed in solutions that have its pH values controlled throughout the test, thereby giving more reproducible and consistent results. This is because the extraction method is less dependent of specific biomass organic part, which can influence equilibrium pH in solution and can vary from one biomass sample to another. These demonstrated characteristics later become an input to determine the speciation present in the biomass.

An example to show the differences in output from both these methods are shown for a wood bark sample. As both methods have one common pH, which is at neutral, the wood bark sample was analysed using both methods to compare the results obtained. Table 4.5 presents the results obtained for the quantity of biomass leached using both methods. The second column of the table shows the quantity leached in water when CF method was used, whilst the third and fourth columns represent the quantity leached in the pH extraction test at pH solutions of 7 and 5 respectively. It is seen that when biomass was immersed in water (pH 7) using the both the methods, the results are different. This difference is seen for all elements because the biomass sample has a natural pH of around 4, meaning that the bark sample is slightly acidic. Therefore when the pH of the water is not controlled as done in the CF method, the

pH of the water will move towards the acidic region. This means that in reality, the leached amount should be compared to a biomass that has been leached at a slightly acidic pH (eg pH 5) using the pH extraction method. When this is done it is seen that the amount leached using water (CF technique) is almost similar to pH 5 results of the pH extraction technique. In this way it can be seen that the leaching results are comparable. However, with the pH extraction method a more detailed leaching data is obtained, thereby allowing a more accurate interpretation of the speciation.

Table 4.5: Comparison of elements leached using CF and pH extraction method

Bark (mg/kg)	Water (CF method)	pH 7 (Extraction method)	pH 5 (Extraction method)
Ca	393	157	319
K	1595	1206	1355
Na	53	35	35
Mg	137	42	84
Si	57	436	80
Al	28	10	8

Figures 4.18, 4.20 and 4.22 briefly summarises the results obtained from experimental data using CF. These figures describe the percentages leached out from the various biomass fuels at different leaching stages, starting from water, followed by NH_4Ac (ion-exchanger), HCl and the amount left as residue. On the other hand, Figures 4.19, 4.21 and 4.23 describe the overall speciation of biomass when the pH extraction technique is used.

It is seen that the sections that were interpreted as Residue in the CF tests, have been identified in a more detailed manner with the pH extraction method, as can be observed for elements such as Na, Si and Al. As the leaching data gives a more detailed analysis, it is possible to understand the leachability of the elements at extreme and diverse ranges and therefore making it possible to identify speciation that was simply classified as Residue before. It was also observed that a higher percentage of organics were seen for several elements using the pH extraction method. The main reasons to explain this would be:

- Residuals as interpreted by CF are recognized as organics using pH extraction method
- Organics as described in the new method consists of dissolved organic carbons and solid or complex organics. CF method on the other hand, only includes dissolved organics therefore it possibly interprets the solid as either minerals or residue
- The higher resolution of leaching, enables the more complex organics to be leached out during pH extraction

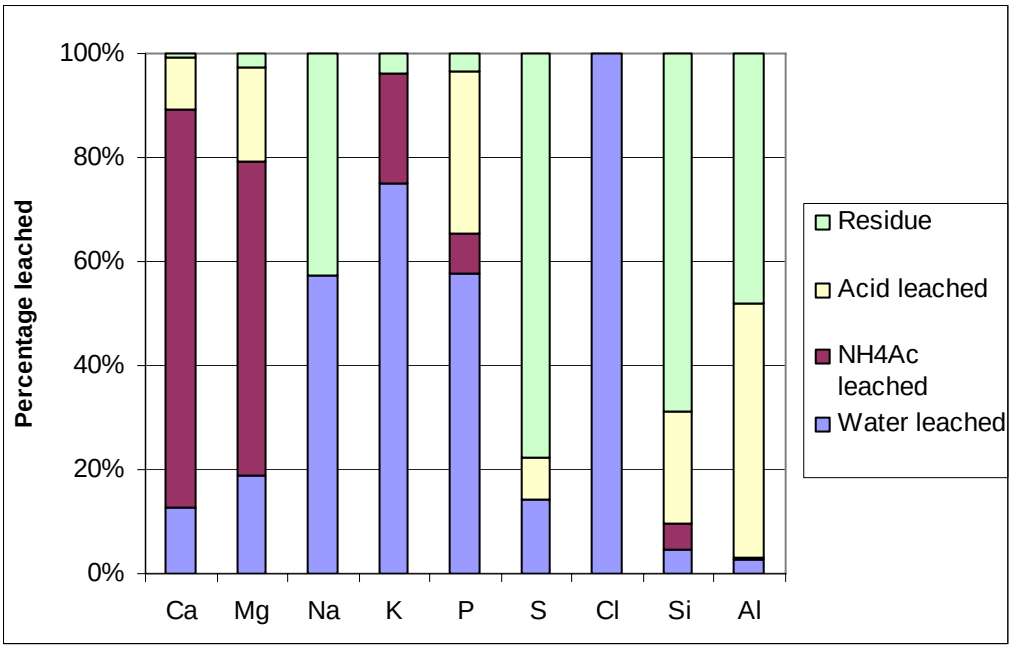

Figure 4.18: Inorganics in wood chips using chemical fractionation method

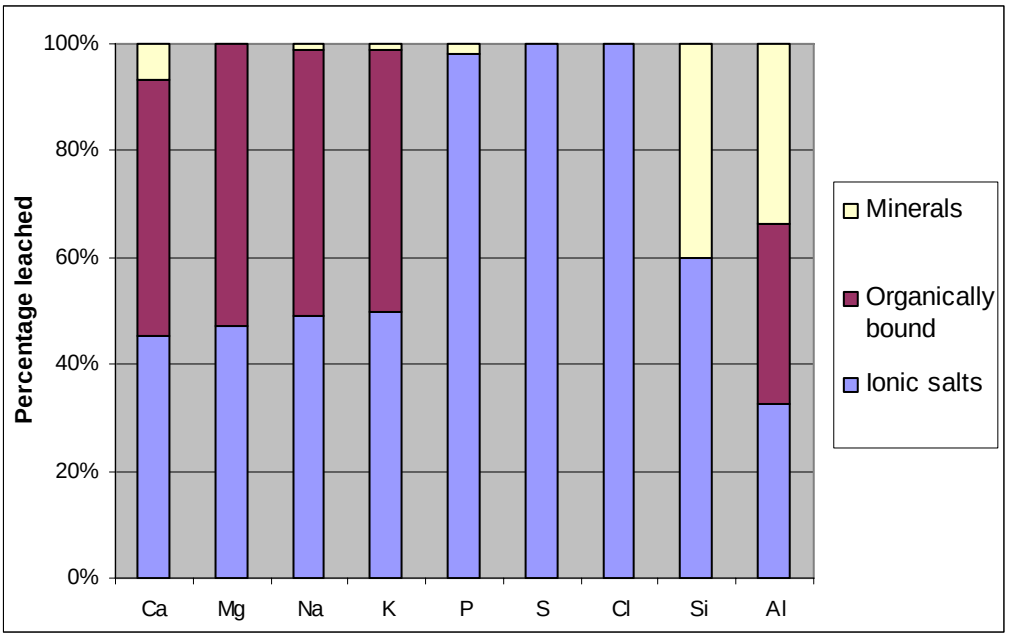

Figure 4.19: Inorganic speciation of wood chips using pH extraction method

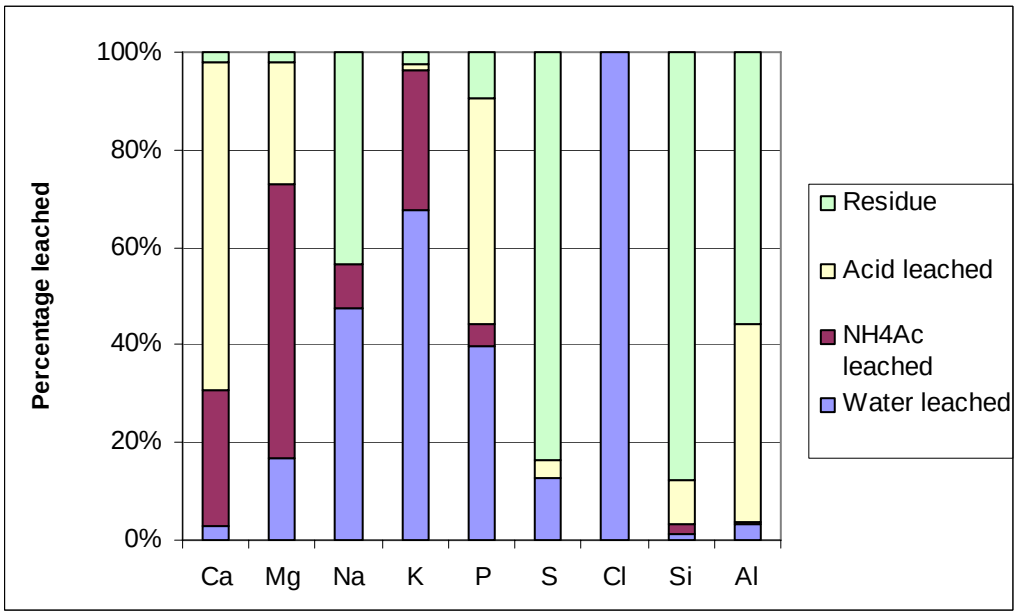

Figure 4.20: Inorganics in wood bark using chemical fractionation method

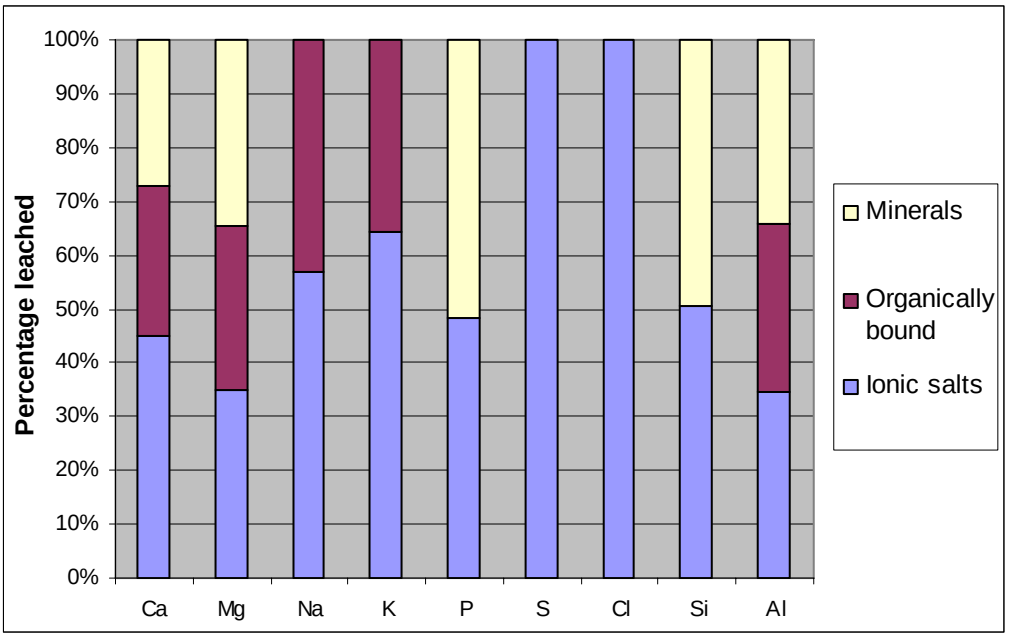

Figure 4.21: Inorganic speciation of wood bark using pH extraction method

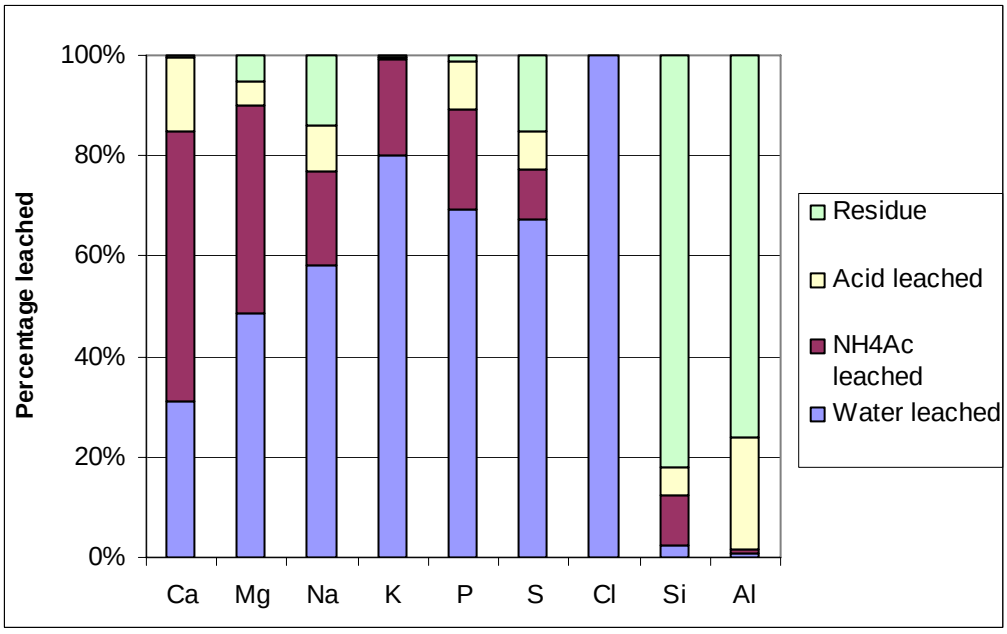

Figure 4.22: Inorganics in straw using chemical fractionation method

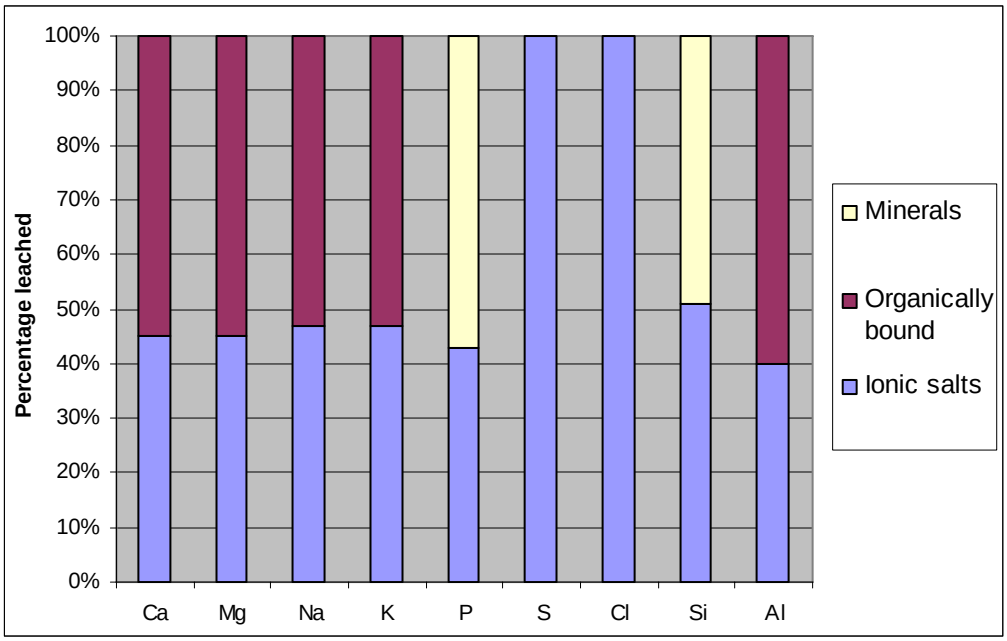

Figure 4.23: Inorganic speciation of straw using pH extraction method

4.5 Ash release results

The results obtained for the ash release against residence time from the LCS experiments (described in Section 3.3.8) are summarised in this section. This data can be used to compare the release behaviour of the inorganics in the fuel during combustion, as shown in Figure 4.24. It can be seen that the release of the inorganics in the various fuels does not happen instantaneously. However, by the time the residence time has reached 1300ms, the combustible matter has combusted for the entire biomass sample.

Figure 4.24: Release of inorganics from fuel during combustion as a function of time

The maximum (based on complete combustion) amount of ash released has been described in Figure 4.25, whereby it is seen straw releases the highest amount of inorganic elements at 1300ms, followed by coal, wood bark and wood chips. Straw released 40% of its inorganic elements after the 100ms residence time, where by the inorganics mainly consisted of K, Cl and S. The original straw before combustion mainly comprises of Si, K and Cl, however the Si are partially found in the mineral speciation (Table 4.4), whilst the K and Cl mainly comprised of salts and dissolved organics. This means that the released elements are mostly those that were bound both to the salts or organics, and not to the minerals. Wood bark and wood chips

released mainly Ca and K during combustion although in the original fuel the quantity of Si and Al were also high. This again, relates to the explanation that parts of Si and Al are bound either to minerals or solid organic matter (Tables 4.2 and 4.3), thus not easily released during combustion. In coal, most of the inorganics released are S and Cl, which are released in the form of SO_2 and HCl.

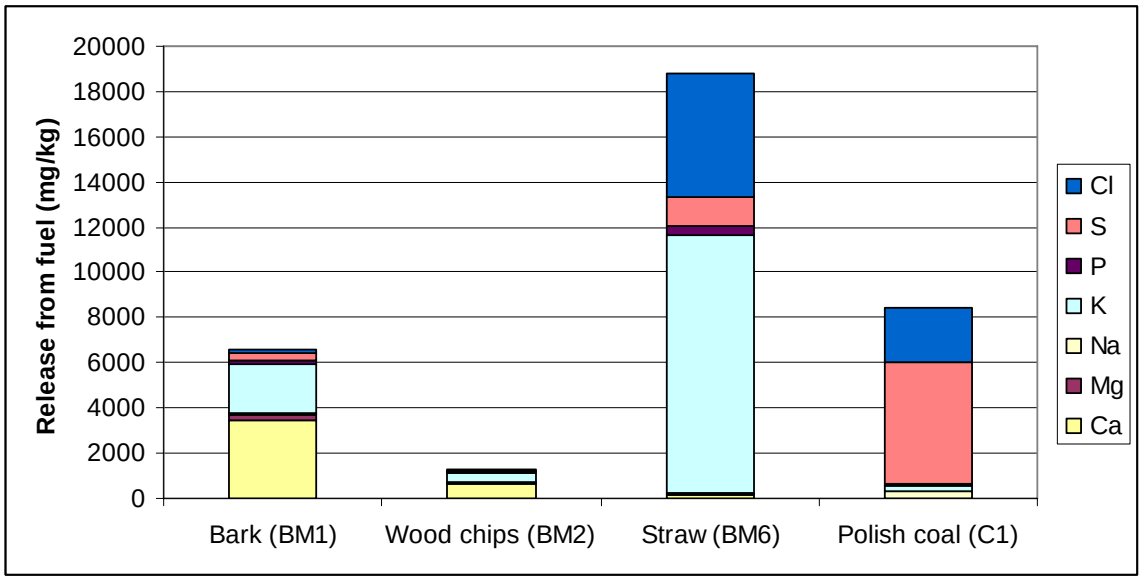

Figure 4.25: Quantity and distribution of inorganic matter released from fuels during combustion

Since the rate and quantity of inorganics released is believed to depend on the actual speciation of the fuel, the release test data can be used for the purpose of developing correlations or links with the results obtained for biomass speciation. The links are made with the released inorganics shown in Figure 4.25, namely Ca, Mg, Na, K, P, S and Cl and the speciation of the fuels summarised in Tables 4.2 - 4.4. The speciation in biomass that was used for linking to the release data are the speciation that are mostly likely to vaporize during combustion, namely the free ions or salts and the organically associated inorganics. The combinations used to derive these links are:

1) Free ions/salts only
2) Organically bound inorganics (sum of dissolved and solid organics)
3) Sum of free ions/salts and organically bound inorganics
4) Sum of the free ions/salts and dissolved organics

The outputs obtained from the exercise of relating the speciation results with the released inorganics are presented in Figures 4.26-4.32. It was seen in most cases that the best match was seen for the woody samples - wood chips and wood bark with various combinations. Best match here refers to a good correlation between inorganics released during combustion with that of the actual speciation present in the fuel before combustion. It was difficult to establish any relationship between the release data of the inorganics with the speciation of straw. For element K and the anions studied, a match was observed for the total released inorganics with that of the sum of salts and organically bound material in wood chips and wood bark. This indicates that the release of these inorganics during combustion is directly related to the volatilized salts and organically bound material in the fuel. For Ca and Mg on the other hand, a good link was seen between the total inorganics released in wood chips and wood bark with that of the organically bound speciation in these fuels.

For both the woody fuels, the dominant element released are K and Ca, thereby indicating the main release of inorganics in these fuels are the volatile ionic salts and organically bound inorganics. Further studies need to be carried out for straw to find a correlation between its speciation and ash release. The contribution of fragmentation of minerals within biomass has also to be looked into to determine the significance of fragmentation in the release of inorganics.

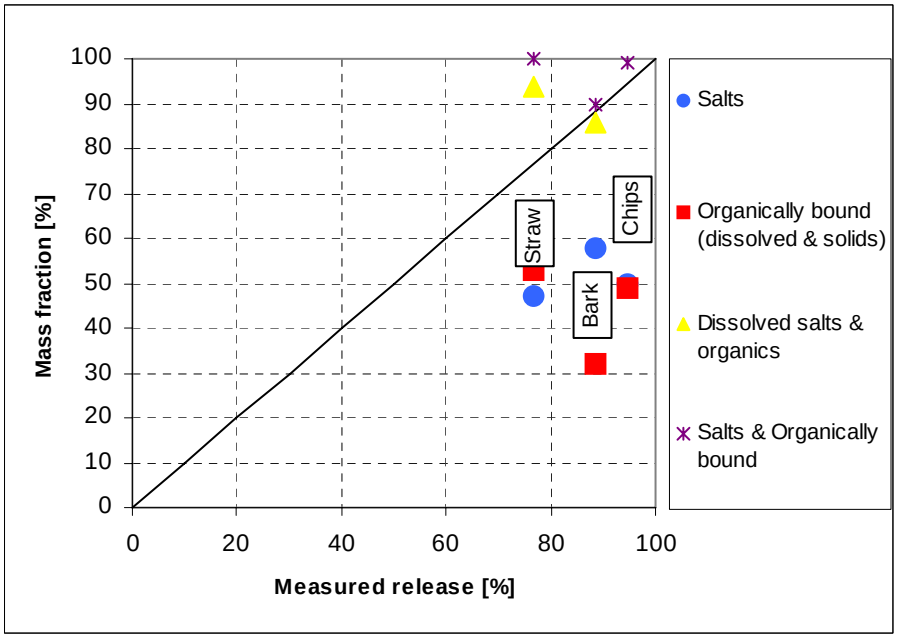

Figure 4.26: Comparison between K speciation and release data

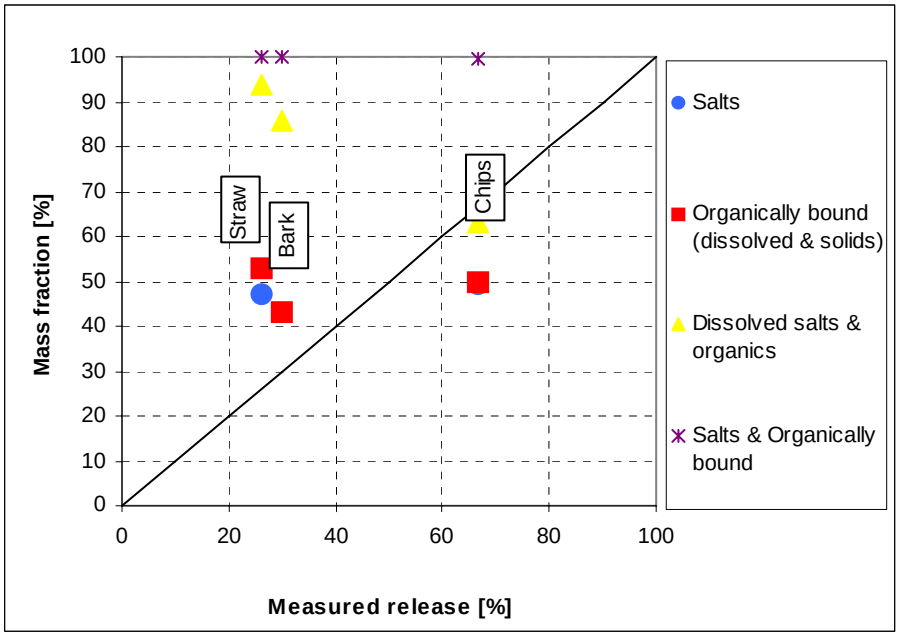

Figure 4.27: Comparison between Na speciation and release data

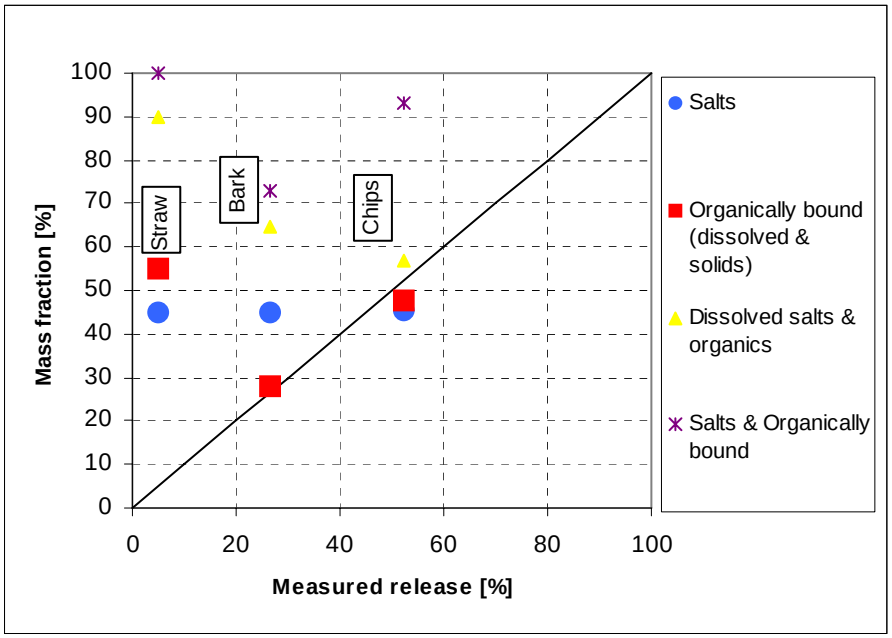

Figure 4.28: Comparison between Ca speciation and release data

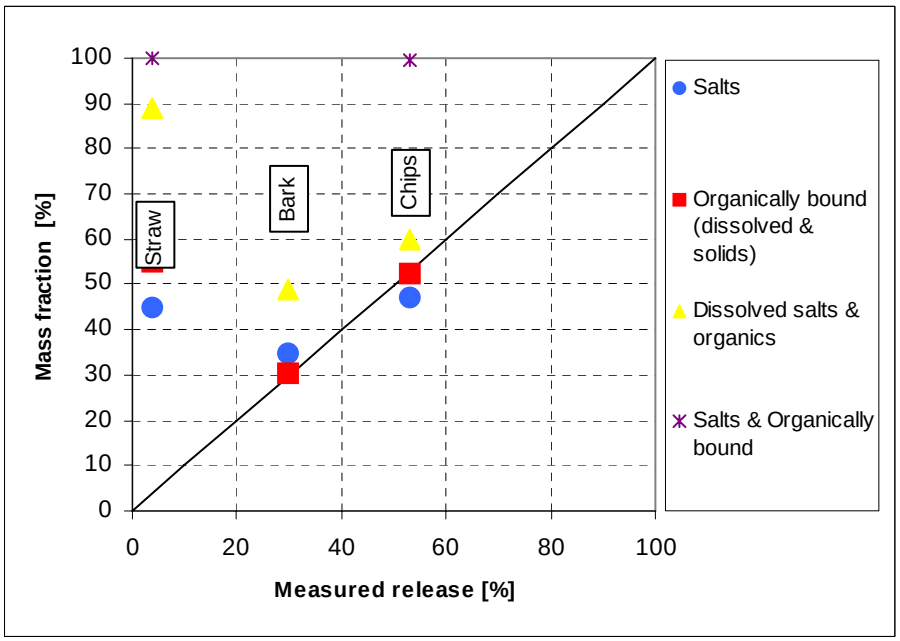

Figure 4.29: Comparison between Mg speciation and release data

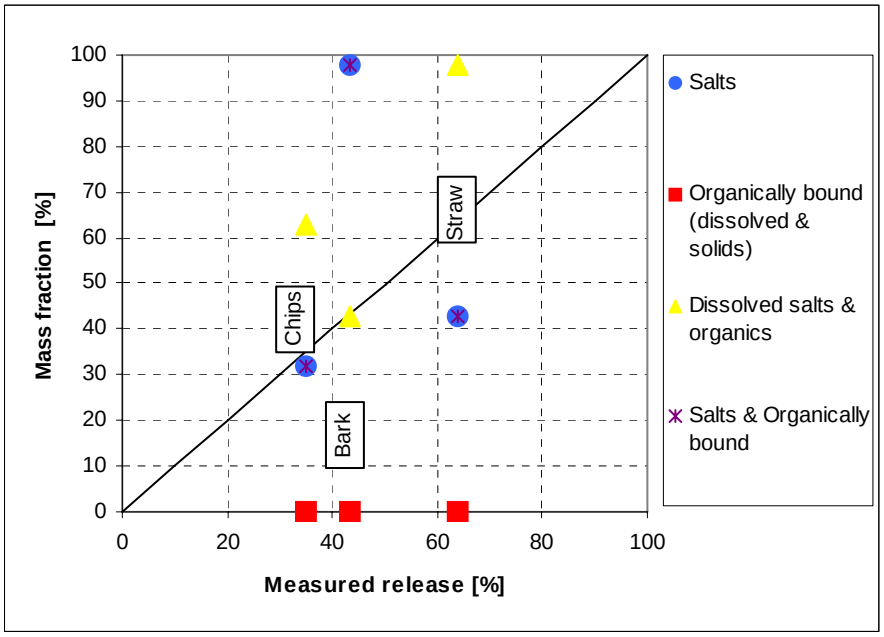

Figure 4.30: Comparison between P speciation and release data

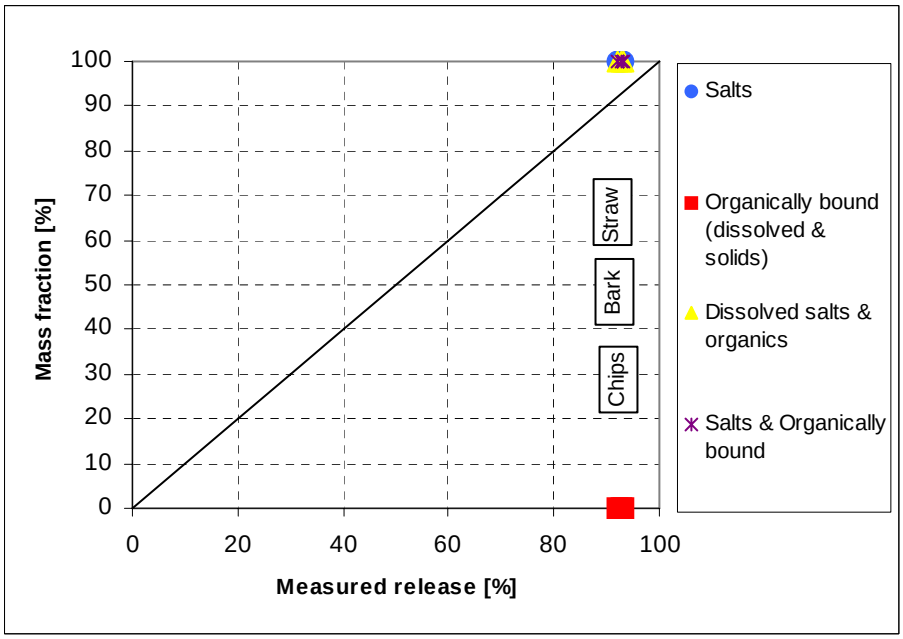

Figure 4.31: Comparison between S speciation and release data

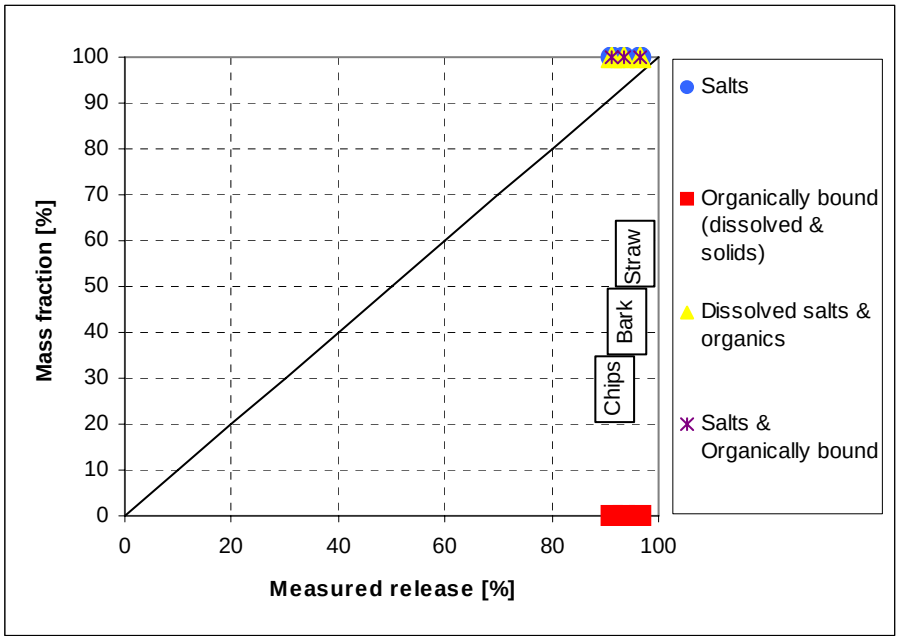

Figure 4.32: Comparison between Cl speciation and release data

CHAPTER 5

Ash Formation Modeling

In order to be able to develop an ash formation model it is firstly vital to understand the release behaviour of the elements in the fuel when combustion takes place. The method adopted in this work was to analyse the composition of the stable chemical phase in biomass when it goes through thermal conversion. Biomass forms inorganic gas species and particulate matter when combusted in boilers. By using thermodynamic equilibrium calculations, it is possible to simulate a combustion system in pf boilers and predict the stability of various solids and gaseous compounds when fired.

Also known as Global Equilibrium Analysis, thermodynamic equilibrium calculations has been used by several researchers to study the release of elements into the gas phase through volatilisation (Blander et al., 2001 and Skrifvars & Backman, 2001). The composition of this gas phase is then used as an input for the gas-to-particle calculations, to determine the condensed phases in the system after combustion. This chapter looks into the development of a model suitable to study ash formation in biomass and co-fired blends and the approach taken is shown in the schematic diagram in Figure 5.1.

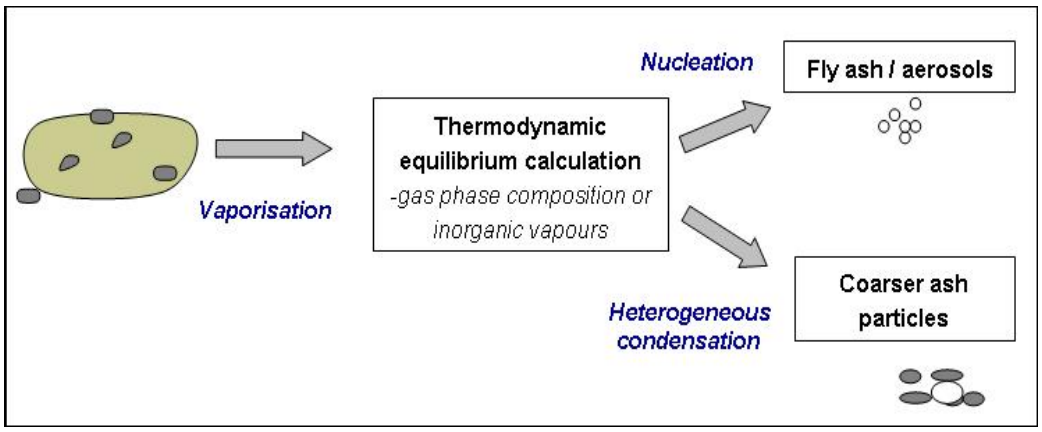

Figure 5.1: Schematic of ash formation model of coal/biomass

5.1 High Temperature Thermochemistry

FACTSAGE is the combination of two linked models in the area of computational thermochemistry: FACT-Win and ChemSage that consists of a series of information, database, calculation and manipulation modules that enables the users to access and operate pure substances and solution databases in relation to a variety of thermochemical calculations. These calculations are based upon concept of Gibbs free energy minimisation (Bale et al., 2002). During combustion of coal and biomass, the fuel is heated to a temperature between 1200 to 1500^{o}C. The elements released by the combustion process in the radiant section, then goes through a convective section where cooling begins to take place. The usage of an equilibrium thermochemistry model to calculate the gas composition or distribution at these temperatures can be helpful in predicting the main inorganic vapours expected at this temperature range. FACTSAGE model calculates the concentrations of chemical species when specified elements or compounds react (or partially react), to reach a state of chemical equilibrium for a given system at defined temperature and pressure conditions (Jak and Saulov, 2005).

The input supplied for the model is the elemental analysis of the fuel and the model than determines the most thermodynamically stable species that is likely to be present at a certain temperature. FACTSAGE then calculates the formation of the gaseous compounds, liquid phases (salt & liquid melt), solid solution phases and pure condensed phases. Zevenhoven, et al., 2005 in their research did not use all the elements in the fuel as an input into the equilibrium model, but only relevant elements that were categorised as ‘reactives’ through CF tests. This is because it is usually the ‘reactives’ that are vaporised and go through condensation.

5.1.1 Application of FACTSAGE

The cases examined with FACTSAGE are wood chips, wood bark and a blend sample of 80% coal and 20% biomass. The ultimate analysis of the samples is shown in Figure 5.2. The main inputs considered are C, H, O, S, Cl, S, P, Al, Ca, Fe, K, Mg, Mn, Na, Pb, Si, Ti, Zn and N, in general whilst the main ones are K, Na, Ca, Cl and S (Appendix E.1). FACTSAGE processes the expected reactions at a particular

temperature based on Gibbs free energy minimisation. For this study the temperature range considered was from 500°C to 1500°C with a step of 50°C. This range is chosen to simulate the changing composition of the biomass ash during combustion at high temperature, to the formation of solid ash in the convective section of the boiler. 20% excess air was considered as a typical combustion condition. The expected speciation distribution for each of these elements was also studied from literature for comparison purposes.

The full system contains more than 300 gaseous, liquid, and solid phases, including salt melt and silicate melt. For the current work, only the pure gases and solid phase result were analysed. The samples analysed are pure biomass (wood chips, wood bark, straw), coal (Polish coal) and a blend of coal (80%) and biomass (20%). The blend test will be able to give greater insights into the interaction between coal and biomass during combustion in a pf boiler.

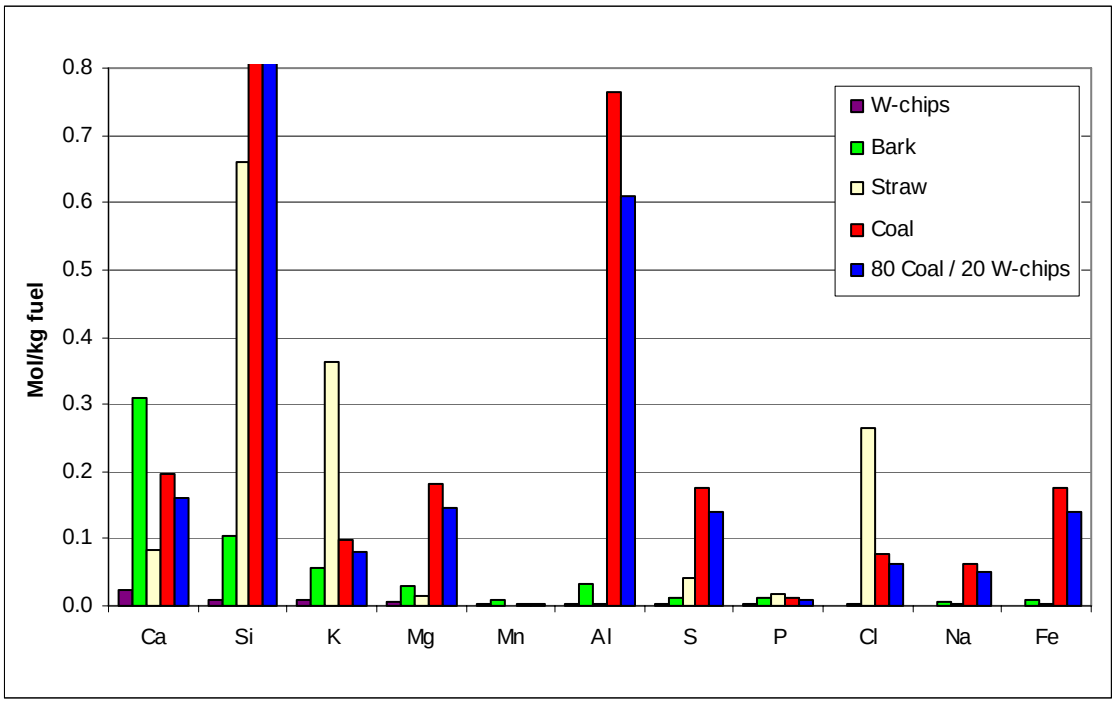

Figure 5.2: Elemental analysis of various fuels studied

The model performs the prediction of the distribution of the gases in the biomass samples in the analysed temperature range. Figures 5.3, 5.4 and 5.5 show the equilibrium composition of elements in the gaseous and solid phase during

combustion of woodchips for elements K, Na, Ca and Cl respectively. For the other biomass fuels, the results have been tabulated in Table 5.1 and detailed analysis can be found in Appendix E.2.

From Figure 5.3 can be seen that the gas distribution for K is in the form of KOH, KCl and K_2SO_4. Some quantity of the KCl dimer was also observed. However below 800^{o}C, most of the constituents at equilibrium exist as of solids. Similar observations were seen for the Na-element whereby at temperatures higher than 800^{o}C, the expected gases are NaOH, NaCl and a small amount of Na_2SO_4 in agreement with several researchers (Christensen, et al., 1998, Joller, et al., 2005 and Jimenez and Ballester, 2007). On the other hand, for elements Ca and Mg, hardly any gases are found during combustion as shown in Figure 5.5. The equilibrium data analysed from FACTSAGE illustrates that the solids obtained are mainly silicates and phosphates.

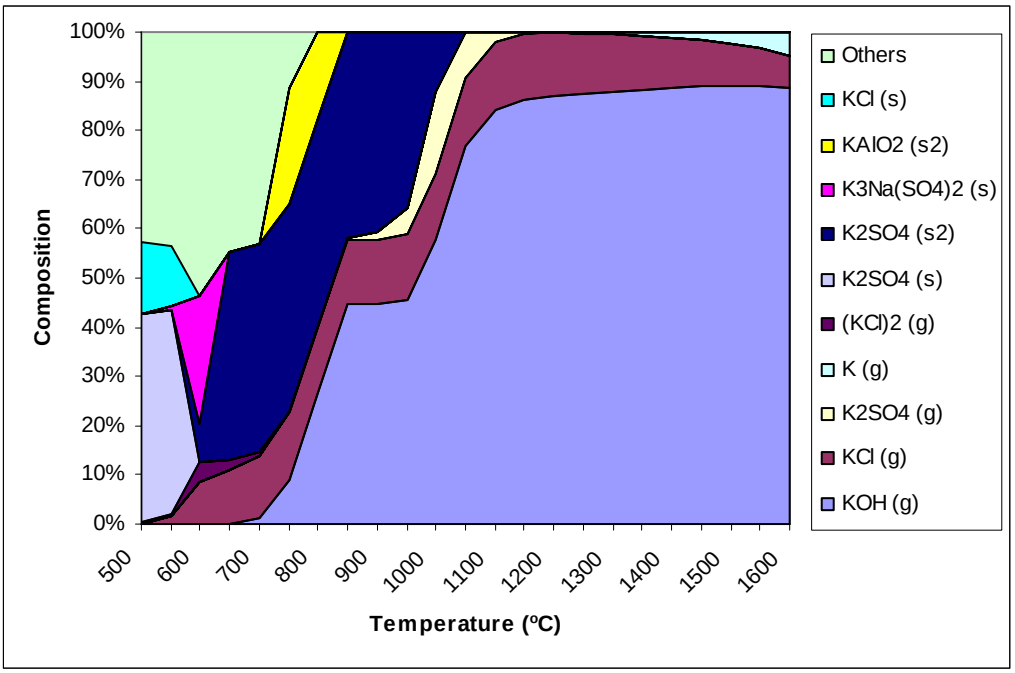

Figure 5.3: High temperature distribution for K elements in wood chips

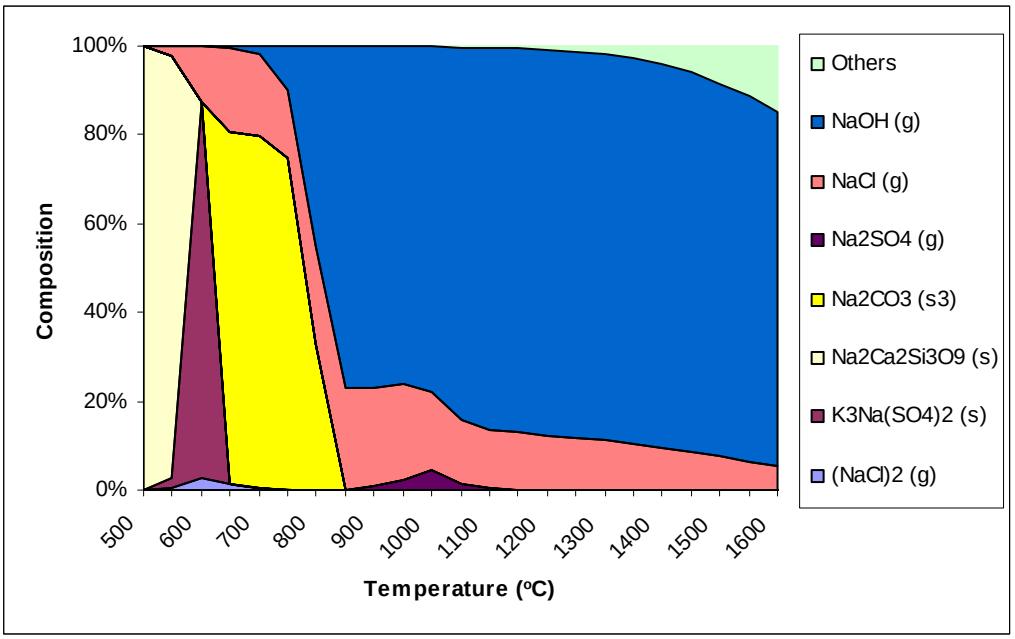

Figure 5.4: High temperature distribution for Na elements in wood chips

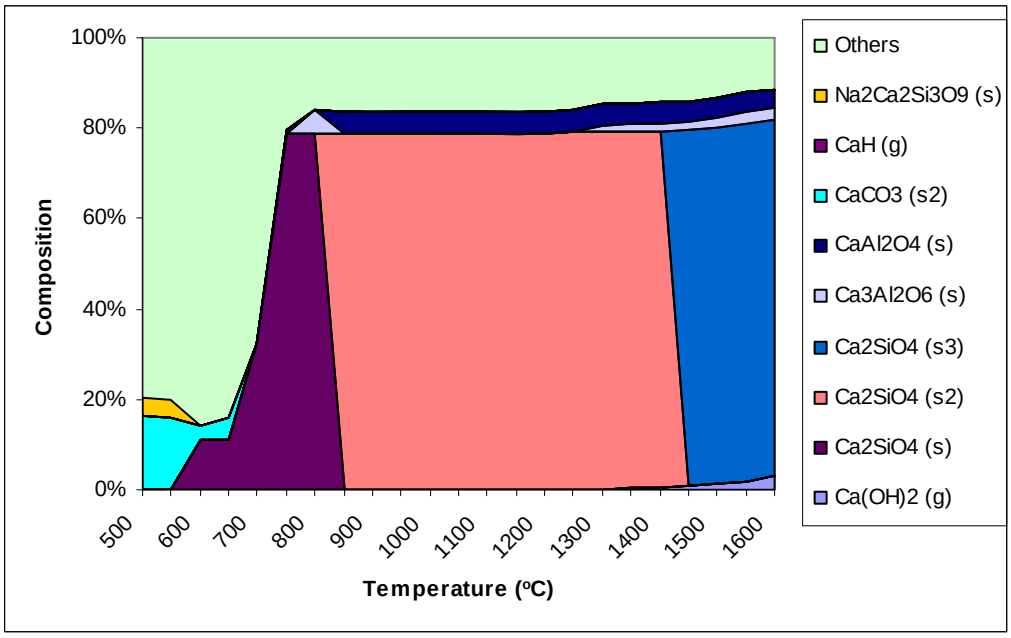

Figure 5.5: High temperature distribution for Ca elements in wood chips

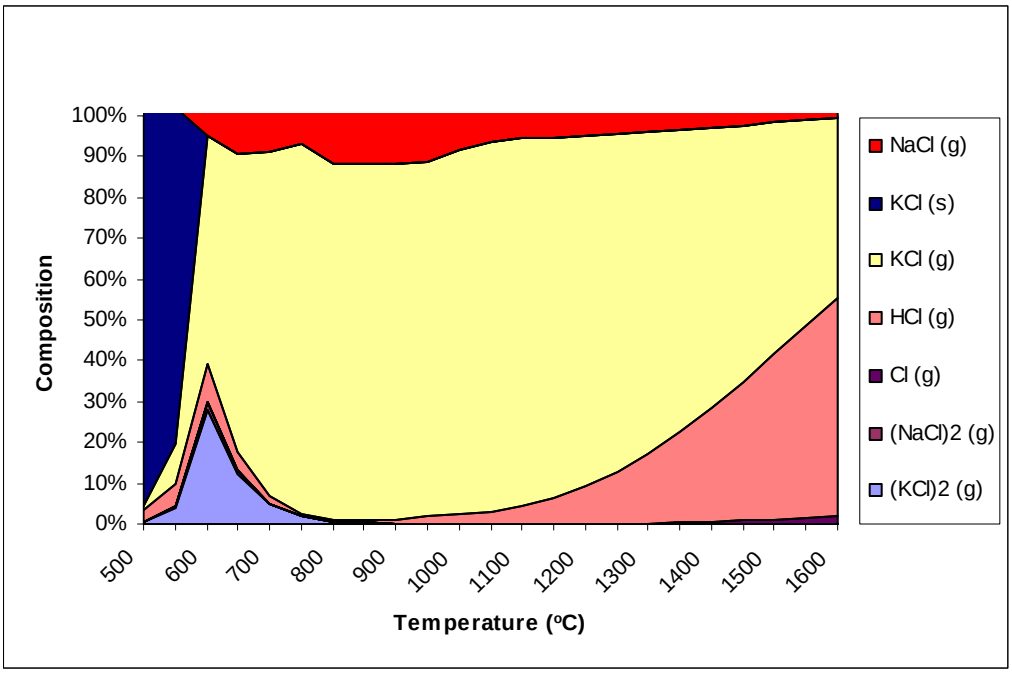

Figure 5.6: High temperature distribution for Cl elements in wood chips

Among the anions that were looked into are chlorine, sulphates, phosphates, nitrates and carbonates. Figure 5.6 displays the analysis for chlorine, whereby it is seen that at equilibrium mainly gases such as KCl, NaCl, HCl and $(KCl)_2$ are seen. For sulphates, mainly SO_2 gas and K_2SO_4 solids were found to be stable in this temperature range, where as for phosphates only solids were present at equilibrium. For the remaining samples, the main composition distribution at the specified temperature range can be seen from Figures E1-E8 in the Appendix.

Table 5.1: Composition distribution of gaseous and solid phases derived from FACTSAGE at various temperature ranges

Temperature range	**>1000 °C**		**1000-600°C**		**<600°C**
Wood chips	KOH KCl	65% 15%	KOH KCl K_2SO_4	45% 10% 20%	Solid phase
	NaOH NaCl	70% 15%	NaOH NaCl	40% 15%	
Wood bark	KOH K_2SO_4 KCl	85% 10% 5%	KOH K_2SO_4 KCl	50% 43% 7%	Solid phase
	NaOH Na_2SO_4 NaCl	90% 5% 5%	NaOH NaCl	90% 10%	
Coal (80%) and wood chips (20%)	KCl	10%	Solid phase		Solid phase
	NaCl NaOH	35% 5%			

The knowledge obtained from the distribution of the gas and solid phase for each biomass will be used for the following reasons:

1) Determine the expected gas composition from biomass fuel when combusted
2) Compare the gases released when biomass is fired with coal
3) Using the gas concentration as a basis for further calculation of the vaporisation and condensation

In the case of co-firing of coal and biomass blend, it was observed that the increase of Si and Al from coal decreased the amount of volatile K, thus reducing KCl formations. This was also found in the work done by Wei et al, 2005 and Zheng et al,

2007. To be able to see the pattern of the behaviour of fuels during combustion, several relations and ratios of the main elements in the feed have previously been made by researchers who have carried out experimental and equilibrium studies on co-firing cases (Knudsen, et al., 2004 and Jimenez & Ballester, 2005). Some of these relations were seen in this work and comparisons to work that were done previously are mentioned here:

- For co-fired sample at 80% coal and 20% biomass, the main stable species in gas phase are similar but found to be in the range of high temperatures (above 1000^{o}C). This is because the addition of coal increases the ratio of Si and Al from coal and reduces the quantity of K from the biomass. This means the ratio of K/Si reduces, thus reducing the gas phase, whilst increasing the proportions of aluminasilicates.
- Another relationship found was that of the ratio of K over S and Cl. It was seen that the lower the ratio of K/(2S +Cl), the less the formation of KOH as all the K present reacts with S and Cl. This was observed for the wood chip sample that has a lower K/(2S +Cl) ratio and thus a lower KOH concentration than wood bark.

These ratio calculations can help interpret the composition distribution obtained from using FACTSAGE. The summary of the distribution made from FACTSAGE will be used as an input for performing further calculations on ash formation.

5.2 Gas-to-Particle Conversion Modeling

The background knowledge of gas-to-particle conversion of the vapour phase of biomass during combustion was discussed in section 2.3.4 of the literature review chapter. Inorganic vapours released during combustion, nucleate to form new submicron particles when it goes through cooling process. The cooling process decreases the vapour pressure of the species, causing supersaturation. If adequate surface of particles is not available for reaction; the supersaturation continues to increase, resulting in homogeneous nucleation (Christensen, et al., 1998). McNallan and co-authors summarise that the occurrence of homogeneous nucleation depends

on the cooling rate of the combustion and the number and size of existing sites available for condensation (Mc Nallan et al., 1980).

On the other hand, if surface areas of particles are already present, then it is more likely that heterogeneous condensation will occur. Fly ash produced from homogeneous nucleation is of sub-micron size, whilst inorganics that are produced through heterogeneous condensation are usually larger in size. However, fine ash particles produced from homogeneous nucleation can further collide and coagulate to form clusters of larger ash particles (Zygarlicke et al., 2001).

To enable the calculations of condensation in this system, firstly the gas phases that are involved are determined from the high temperature thermochemistry method in the first part of this chapter. It was seen that for the biomass fuels studied in the present work, the main vapours to look into are KCl, K_2SO_4, NaCl and Na_2SO_4.

Figure 5.7 summarises the procedure to determine the possibility of homogeneous or heterogeneous condensation occurrence during biomass combustion. It is observed that firstly the saturation ratio is measured using equation (Eq.) 2.1. If the saturation ratio of the gas is much larger than one, the possibility of homogeneous condensation arises, which then suggests that the calculation of the rate of homogeneous nucleation should be included. However, if the saturation ratio is only slightly larger than one, the step proceeds towards the calculation of heterogeneous condensation of the gases on the surface of existing ash particles in the system. The heterogeneous condensation on particle surfaces also faces competition with condensation on tube surfaces of the heat exchanger section. Tube surface condensation can occur when there is low particle surface available for heterogeneous condensation.

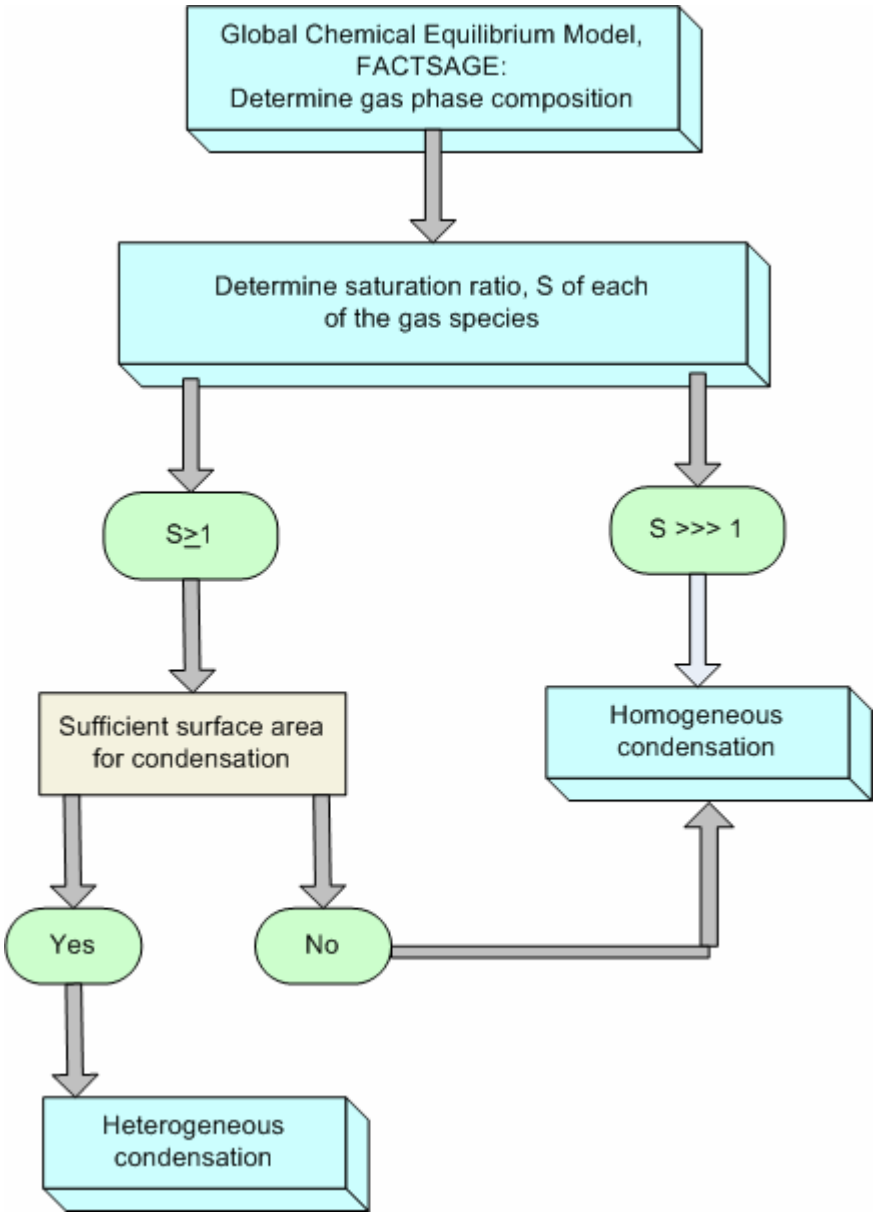

Figure 5.7: Homogeneous and heterogeneous condensation occurrence during fuel combustion

5.2.1 Homogeneous and Heterogeneous Condensation

The rate of homogeneous nucleation, J_{hom} measures the number of nuclei formed per unit volume. The calculations examined in this thesis are based upon the Classical Theory of nucleation whereby the basic assumption is taken from the Capillary Approximation (Peeters, 2002). The classical theory assumes that a cluster can be represented as a droplet and its properties such as density and surface tension are the same as those of bulk liquid. It therefore neglects the inhomogeniety of the density

and the curvature correction of surface tension (Iwamatsu, 1994). The homogeneous nucleation rate expression in Seinfeld and Pandis (1998) is calculated as follows:

$$J_{\text{hom}} = \left(\frac{2\sigma}{\pi M}\right)^{1/2} \frac{vN^2}{S} \exp\left(\frac{-16\pi}{3} \frac{v_1^{\,2}\sigma^3}{(kT)^3 (\ln S)^2}\right) \qquad \text{Eq 5.1}$$

where:

v_1 ≡ volume of one molecule of the condensing gas
M ≡ mass of a molecule of condensing gas
N ≡ number concentration of condensing gas in the system
σ_p ≡ surface tension of particle
S ≡ saturation ratio of condensing gas

Heterogeneous and homogeneous condensation are competing processes and it has been seen that conditions for heterogeneous condensation are more easily achieved (Jacobson, 1999). Therefore, it brings about the question whether homogeneous nucleation does actually occur in boilers. This is necessary to verify in ash formation modeling so that it can be summarised whether the inclusion of homogeneous condensation calculation is necessary for the model. Besides knowing the saturation ratio it is also important to know the rate at which vapor species can condense on pre-existing particles as this will determine whether the critical supersaturation for homogeneous nucleation will exceed during cooling of combustion gases (McNallan et al 1980). This means that when cooling takes place and the flue gas becomes more saturated with vapor, it is necessary to determine if the condensation rate of vapor onto preexisting surfaces in the flue gas is sufficient enough to keep the saturation ratio below the amount required for homogeneous nucleation to commence.

Christensen (1998) suggests a calculation expressing the molecular rate of condensation, J_c, of a gas on a particle of diameter d_p.

$$J_c = \frac{2\pi D_i d_p M (p_i - p_d)}{RT} \qquad \text{Eq 5.2}$$

where:

D_i ≡ diffusion coefficient of condensing gas in flue gas

p_i ≡ partial pressure of the condensing gas in the system

p_d ≡ vapor pressure of the condensing gas

d_p ≡ diameter of each particle available for condensation;

p_i ≡ partial pressure of the condensing gas in the system

p_d ≡ vapor pressure of the condensing gas

M ≡ molecular weight

It has to be noted here that for the case of direct condensation on tube surfaces rather than condensation on particles, the vapour pressure, p_d has to be taken at the temperature of the tube and not the gas temperature as done in Eq 5.2.

5.2.2 Ash particle formation

In order to model the ash formation for a co-fired coal and biomass in pf boilers, the wood chips sample was chosen for calculations. Using the background information from the above mentioned research, the occurrence of homogeneous and heterogeneous condensation was tested. Firstly, saturation ratio calculation was done for the composition in the gas phase to establish conditions under which homogeneous nucleation is possible and when only heterogeneous condensation occurs (Figure 5.7).

The composition or concentration of each of the gases was obtained from FACTSAGE for various temperature ranges. Table 5.1 summarises he results for the three samples, namely woodchips, bark and wood chips co-fired with coal. Based on the table, it is possible to see that most of the gas phases are recorded for temperatures above 700^{o}C and at lower temperature the composition is mostly stable as solids. However, for the combined coal/wood chip blend, the behaviour of the blend matches with coal, whereby gaseous phase is only stable at temperatures higher than 1000^{o}C. The composition obtained above 1000^{o}C for K, Na, Cl and S were similar to experimental work carried out previously by Jimenez and Ballester (2007) in high temperature entrained flow reactors. In order to determine the

saturation ratio of the gases present in the system, it was necessary to determine its partial pressure and vapour pressure. Using the mole concentration of each of these gases against the overall flue gas concentration, it was possible to determine the partial pressure of the gases. The data for the vapour pressure on the other hand, was obtained from the following equation (Knacke, et al., 1991):

$$\log p_d^* = 1000.e/T + f \log T + g \qquad \text{Eq 5.3}$$

where p_d is the vapour pressure of the gas and constant e, f and g are derived from Knacke's constant summary depending on the composition and temperature of the gas.

The diffusivity of the condensing gas is calculated from the diffusivity equation derived from the book entitled Fundamentals of Atmospheric Modeling (Jacobson, 1999). From the saturation ratio calculations results (Appendix F.1), which have been summarised in Table 5.2, it was found that for both K and Na, the alkali sulphates achieved nucleation and condensation before the alkali chlorides. This would mean that the alkali sulphates would become available particles for the alkali chlorides to condense on when they achieve their saturation at a later stage. Similar observations are reported in literature by several researchers during their experimental and modelling work. Jimenez and Ballester found in their work that K_2SO_4 occurs at high temperature whilst Cl reacts with K to produce KCl as the temperature drops (Jimenez and Ballester, 2005). Results obtained by Glarborg and Marshall in their modelling research were comparable for the gas phase of K (Glarborg and Marshall, 2005).

Table 5.2: Homogeneous and heterogeneous temperature occurrence for the main gas phases in biomass

Species	Temperature when S>1 was achieved	Temperature when S>>>1 was achieved
KCl	700^{o}C	500^{o}C
K_2SO_4	1100^{o}C	900^{o}C
NaCl	700^{o}C	700^{o}C
Na_2SO_4	1100^{o}C	900^{o}C

In the case of the saturation ratio being larger than one, it indicates the occurrence of heterogeneous condensation and therefore Eq 5.2 is used to calculate the rate of condensation (Appendix F.1). The usage of this equation requires the derivation of certain parameters. The diffusivity of the condensing vapor was calculated using the method derived from Jacobson (1999) with the assumption that the properties of flue gas were approximately a similar composition to air. A typical particle size distribution (PSD) of coal fly ash was used to represent the particles of diameter, d_p that provides the surface available for condensation. (Figure 5.8). This assumption was based on the notion that during combustion of biomass, a large quantity of the flue gas that will be available for condensation are primarily the coarse fly ash indicating a similar pattern of PSD of a coal fly ash.

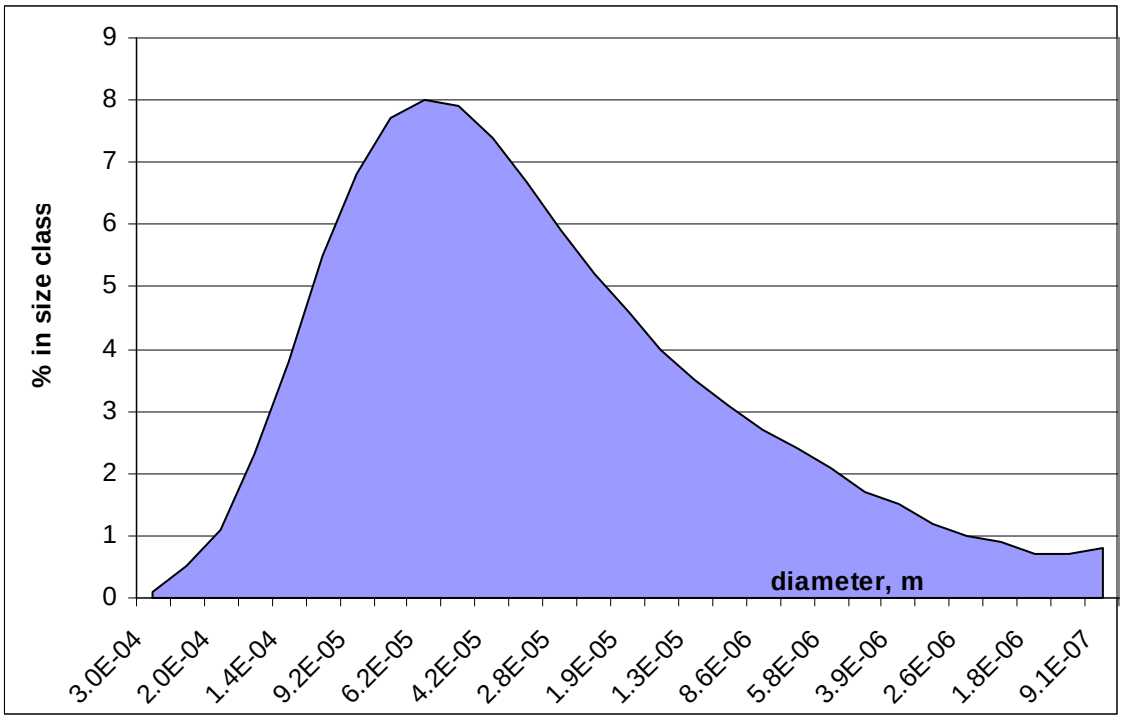

Figure 5.8: Average particle size distribution for coal ash

Further assumptions that were made include:

1) Biomass fuel contains around 2.5% ash and the ash has a bulk density of 2500kg/m^3 (Loo, 2002)
2) In order to approximate the partial pressure of gas in the system, a value for the volume of flue gas that contained the inorganic vapor was used to determine the total or sum of gas in the system. This volume of flue gas produced was obtained assuming the remaining (non-ash) 97.5% of the fuel. Detailed calculations are as shown in Appendix F.2
3) Gas composition was calculated for a typical coal with 20% excess air.

5.2.3 Overall Model

As shown in Chapter Two that when coal is combusted, ash formation depends upon the possibility and extent of fragmentation or coalescence of the coal particle. The same holds true for the behaviour of the mineral matter in a biomass during combustion. As observed in the earlier section of this chapter, the ash formation

behaviour for the vaporised and organically bound inorganics within biomass is completely different.

It is found from the high temperature equilibrium model that at temperatures above 1000^{o}C, that the inorganics were bound mainly as the gaseous phase of KCl, NaCl, KOH and NaOH and when the temperature decreases sulphation occurs producing K_2SO_4 and Na_2SO_4. At this temperature the alkali sulphates have already reached the saturation ratio of above one, and therefore start condensing on the fine particles present in the boiler. The KCl and NaCl start condensing at 700^{o}C, either on the alkali sulphates or tube surfaces or even undergoing homogenous nucleation.

Although the scope of this work does not include the actual PSD calculations of the condensed ash, it was seen that homogeneous nucleation leads to the production of new particles from the gas phase, thus increasing the number and mass of the fine particulate phase formation. Heterogeneous condensation, on the other hand, does not change the number of particles already present in the system, but it does increase the particle size by the transfer of condensed gas phase onto the surface area of present particles. Calculations to derive actual PSD using coagulation and agglomeration processes are recommended for further studies that will be done for biomass combustion. At this stage of the work, it has been possible to derive the type of condensation expected at various temperature ranges and the condensation rate of the gaseous species.

CHAPTER 6

Practical Implications

The motivation to develop a co-firing advisory tool is to deepen the understanding of ash formation during the co-firing of coal and biomass. It is known that the ash forming matter in coal and biomass is responsible for several ash-related issues. The tool that is used in this work can be described as a conceptual model that has five main functions, including:

- To identify a method to determine the speciation of biomass used in co-firing
- To classify the inorganics within the coal and biomass
- To recognise the ash release behaviour of the different classes within the fuels during combustion
- To study the interaction of the inorganics of biomass with the inorganics of coal during combustion
- To model the condensation of the inorganics during the cooling process after combustion

The discussions in this chapter will show the relevance of the results obtained in this research work to arrive at a conceptual model which addresses the above-mentioned functions. Figure 6.1 provides the schematic of the conceptual model whilst the following sections in this chapter go into further details on each of these functions.

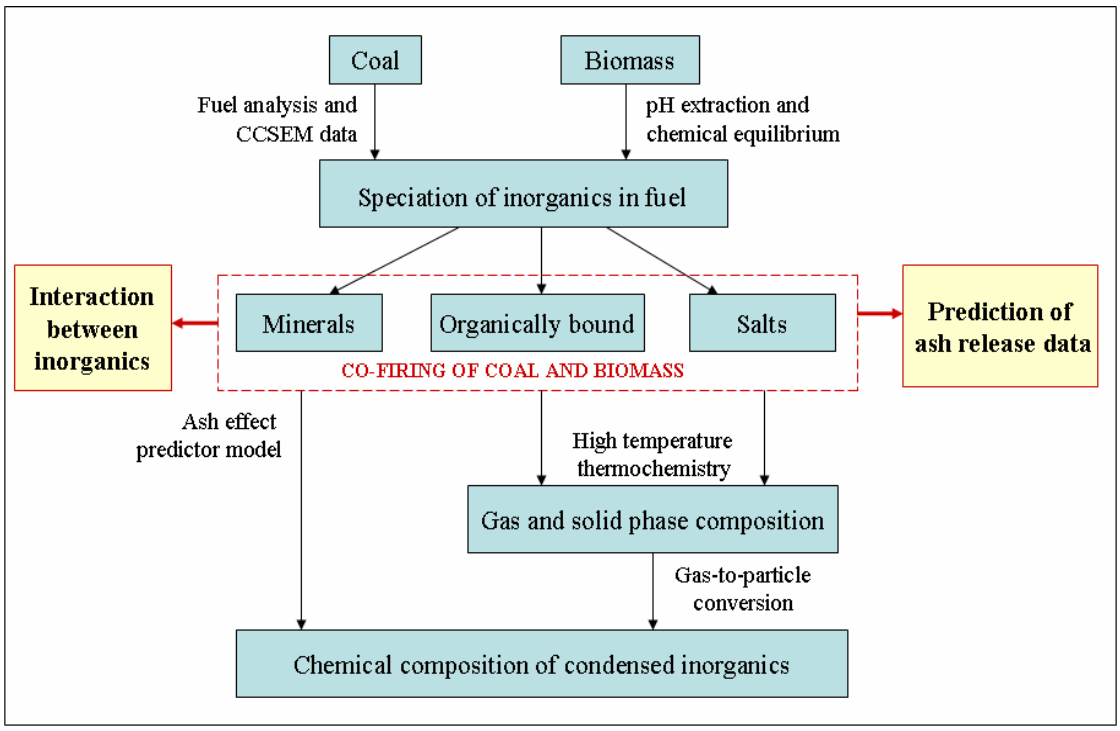

Figure 6.1: Schematic of a conceptual model showing the co-firing advisory tool functions

6.1 Determination of biomass speciation

Several ash formation models to determine the speciation of inorganic matter in coal (<30%) already exist and are available. Therefore for this current research, method of determining speciation of coal was not further studied, but instead a suitable model called the Ash Effect Predictor (AEP) has been adopted for the identification of coal speciation (Yan, et al., 2002; Wu, et al.,1999 and Gupta, 2005). The focus of this section of the study is to establish a reliable method for finding the speciation in biomass, especially for wood and straw samples.

The method proposed in this research is arrived at determining the speciation of biomass with a combination of pH extraction test and chemical equilibrium calculation. The pH extraction test provides the geochemical fingerprint of every element within biomass by observing its leaching curve. The geochemical fingerprint displays the behaviour of elements in various pH ranges, enabling the recognition of the elements just by its leaching curve. The maximum quantity leached is used as an input into the chemical equilibrium model to determine the likely speciation of the

biomass. This model uses equilibrium properties data to predict the biomass speciation.

Taking the steps mentioned above into further detail, it is firstly vital to establish the leachability curves of the main inorganic matter using pH extraction test. The recommended method to determine the leaching is the CEN 292 test (2005) and the leaching pH range is fixed between the range of pH 2 to12. This wide range in pH ensures that all elements are maximally leached out, minimising residues and thereby allowing accurate predictions. The elements analysed to are K, Na, Ca, Mg, Si, Al, Cl, S, N and P.

The maximum leached value for every element is based on the highest peak of its individual leachability curve. For some elements the amount leached is not related to the pH of the leaching solution, there by producing a constant graph. These elements are K, Na, Cl and S. The leaching behaviour of elements most often gives an idea of its chemical speciation even before carrying out the chemical equilibrium calculations. For example for elements with constant leaching behaviour at all pH, it is most likely that the speciation will mostly consists of salts or free ions with a small amount of dissolved organics. For elements that have optimum leaching range at the acidic or pH regions such as Ca, Mg, Al and Si, it is likely that larger speciation of either minerals or solid organics exists.

The concentration of the highest peak is fed into LeachXS, a chemical speciation model. In this research work, the database of LeachXS has been updated with thermodynamic properties of speciation that are relevant to biomass samples. The equilibrium model can be used to predict the free ions, salts, organically bound matter and minerals that are seen in the inorganic matter within biomass. In this way, a large section of the speciation (inorganics) in biomass can be determined, as the extraction method has efficient leachability, enabling a good prediction for its speciation.

6.2 Classification of inorganic matter

Using resources from various literature reviews, the speciation of the inorganics in biomass have been compiled and classified into three main groups. These groups are firstly, the free ions and salts, secondly the organically associated matter and thirdly the minerals. The summary for the classified speciation has been compiled in Table 3.1. It was seen that the results obtained from the biomass speciation using leaching and chemical equilibrium methods are comparable to the classification table from literature review.

For coal, the classification can be done in a similar way to biomass. However, the quantity of salts and organically bound matter in high rank coals are very low (around 1%) compared to the total amount of minerals in the coal. It is known that ash is formed from the inorganic matter in coal and biomass; however the chemical bonding of the inorganic matter to the rest of the fuel determines how the inorganic matter behaves during combustion.

6.3 Ash release behaviour

The main ash forming species in biomass are the salts and the organically associated species. The latter have a weak ionic bond to the carbonaceous material and therefore are expected to be easily vaporised at relatively lower temperatures. The minerals, which are present in larger quantities in coal (rather than in biomass), are the main contributor of ash formation in coal combustion. The formation of ash from minerals depends on characteristics such as the association of minerals (included or excluded) to the carbonaceous material and the coalescence and fragmentation behaviour of the minerals.

In this research, positive linkage was found between the derived speciation of biomass and the ash release data during combustion. The release of inorganics during combustion depends on the way the species is bound to the fuel. Therefore in this work, the speciation of the biomass was categorised into three groups: ionically bound, organically bound and those that exist as minerals. The total of the first two

groups were compared with the ash release data of inorganics in fuels during combustion, as these two groups are more volatile and are easily released during combustion.

6.4 Interaction between coal and biomass ash

Research previously carried out on ash formation during co-firing suggests that interaction between the inorganics in coal and biomass occurs for S, Al and Si from coal with the alkali metals and chloride in biomass. In this work, a high temperature thermochemistry model known as FACTSAGE was used to study the release behaviour of these elements, in addition to studying the interaction between the elements of coal and biomass.

From the high temperature thermochemistry model, it was found that in biomass combustion, the chemically stable gas phases are mainly KCl, NaCl, K_2SO_4 and Na_2SO_4. These are the gases that generally undergo condensation and are responsible for formation of submicron ash. Only a small amount of the remaining material was stable in the form of alkali-silicates and aluminosilicate. When a similar analysis was carried out for coal (80% mass fraction) and biomass (20% mass fraction) blend, it was found for these elements that the gas phase was not the stable phase, as in pure biomass combustion, but instead a higher quantity of alkali-aluminosilicates (>80%) was observed. This indicates that coal has a 'buffering' effect on biomass alkali metals, reducing the release of alkali-gases that can cause deposition and corrosion issues.

It has been previously observed that KCl is the cause for corrosion problems during ash deposition whilst the low melting temperature of K-silicates leads to severe ash deposition (Zheng et al., 2007). The K-aluminosilicates on the other hand, have a higher melting point and therefore leads to the formation of a less troublesome deposition. From equilibrium calculations it can therefore be expected that the chemical composition of the coal may help to reduce the risk of deposit related corrosion.

6.5 Gas-to-particle formation

The final step in this conceptual model is the formation of particles from the gas phase during the cooling stage. As the temperature begins to drop after the radiant section, nucleation and condensation of the gas phase occurs, causing formation of particles of various chemical composition and size. The actual gas phase in the system is firstly determined from FACTSAGE, followed by calculations to determine the particle formation based on the competition between homogeneous and heterogeneous condensation.

Using the saturation ratio, it was possible to identify temperatures/regions for homogeneous or heterogeneous condensation to occur. The summary for this range for various gas phases was given in Table 5.2. It was found that the sulphates, namely K_2SO_4 and Na_2SO_4 condense first followed by KCl and NaCl that condense either on the sulphates or on tube surface. Homogeneous nucleation can also occur at lower temperatures (<900^oC), but this is quite unlikely as homogeneous nucleation only occurs when there is not enough surface area for heterogeneous condensation to occur.

Overall, the main implication obtained from this work is the development of a model that can summarise the behaviour of inorganics in coal and biomass during co-firing. This model can be used as an effective tool to determine the chemical composition and particle size distribution of the ash formed during co-firing of coal with biomass in pf boilers. The information obtained from the model is useful for those involved in the operation and technical planning of pf boilers to determine the ratio of biomass that can be co-fired with coal without causing serious ash deposition issues. The knowledge obtained about the ash properties is also useful for the development of effective Air Pollution Control devices in boilers.

CHAPTER 7

Conclusion and Recommendations

The aim of this research work was to develop a conceptual model for an advisory tool that predicts ash formation during the co-firing of coal with biomass. This chapter summarises the main findings made during this research into two main sections, which are characterisation of the fuel and ash formation modelling. The chapter concludes with recommendations for future work to further refine the co-firing advisory tool.

7.1 Characterisation of fuel

Before being able to determine the behaviour of ash forming matter, it is first vital to understand the chemical speciation and quantity of the inorganics in coal and biomass

- The chemical fractionation method has been used in the past to classify inorganics into three groups based on their behaviour during combustion. The first two groups are those that are ionically and organically bound which vaporise easily during combustion and the third group is the minerals, which do not vaporise easily. However, it is not possible to determine the speciation of biomass using chemical fractionation.

- A pH based extraction method was adopted in this research to study the leaching behaviour of the various elements in a wide range of pH solutions (pH 2-12). Every element was found to have its individual leaching pattern with an optimum pH range that allows maximum leachability. The pH extraction method used was found to have a leaching efficiency of more than 70% for all elements at its optimum pH range, (depending on how the species is bound to the fuel). This indicates that most of the elements in the fuel have been leached out using pH extraction method, thus reducing the possibilities of having high amount of residues that are not analysed.

- A chemical equilibrium model known as LeachXS has been updated with thermodynamic properties of all likely speciation found in biomass. The model uses equilibrium constant / solubility product constant to determine the speciation of biomass inorganic matter by using the leached concentration data from pH extraction test as the input.

- Comparison was made between the inorganic speciation found using the combined method of pH extraction / chemical equilibrium and the inorganic speciation found from literature review. A good comparison was found for the salts, organically associated inorganics and the minerals in biomass.

- The prediction model called the Ash Effect Predictor (AEP) was used to determine the ash formation of coal. Using data from fuel analysis (CCSEM), the model combines the knowledge of coalescence and fragmentation of char, included and excluded mineral within coal to predict ash formation during coal combustion.

7.2 Ash Formation Modelling

- It was found that the speciation of biomass obtained from this work can be linked with ash release data obtained from experimental work. A positive correlation was seen between the total sum of salts and dissolved organics for K-, Na- and the anions speciation with the release of ash from wood chips and wood bark. A good correlation was also seen for the organically bound Ca- and Mg- speciation with the total ash released in wood chips and wood bark.

- A high temperature thermochemical model known as FACTSAGE was used to determine the gas and solid phase of the inorganics after combustion. The stable gases in the high temperature range (>800^{o}C) are KCl, NaCl, K_2SO_4 and Na_2SO_4 whilst alkali-silicates and aluminosilicate are the stable phases at lower temperatures. When the FACTSAGE was used for co-fired samples of coal and biomass, it was seen that a shift in stability phases occurred due to the interaction of coal and biomass, thereby making alkali-aluminosilicate the more stable phase and reducing the stability of the alkali gas phases.

- The gas phase obtained from equilibrium studies is used to determine the formation of ash particles by using gas-to-particle (condensation) calculations. Using partial pressures of gases in the system, the temperature range for the occurrence of homogeneous and heterogeneous condensation was determined from its saturation ratio. It was found that the sulphate gases condensed first (<1000^{o}C) followed by the chlorides (<700^{o}C) that condensed either on the sulphates or on tube surfaces.

7.3 Recommendations for future work

The characterisation technique derived for biomass in this work provides a better overview of the inorganic speciation for various samples. Combined with the existing methods for coal characterisation and interactions between elements of coal and biomass, it was possible to begin the pathway towards producing an efficient ash formation model during co-firing. Recommendations for further improving this model are given below:

- Currently ionic salts and organically bound inorganics are separated into two categories when comparing the speciation of biomass with the ash release data. To determine if this step is necessary, further research will be required to verify if there are kinetic differences in terms of the release of ionic salts and organically associated inorganics during combustion. From the concluding remarks, it is seen that further work is also required to re-evaluate and improve correlations between ash release data and the chemical speciation of the biomass fuels.

- The characterisation technique for biomass requires further work, especially for the organically associated inorganics. At this stage the organics were compared to humic and fulvic acids, which are calculated, using the Nica Donnan model present within ORCHESTRA.

- Interaction between ash of coal and biomass was studied using high temperature equilibrium chemistry model. To further verify the results, experimental work should be carried out to analyse interaction of coal and biomass inorganics by varying the quantity of the coal/biomass in the blend. This way it will also be

possible to determine the ideal ratio of coal to biomass that can be used in order to minimise ash formation from the alkali element in biomass.

- Additional work can also be done for the homogeneous and heterogeneous condensation rate calculations, followed by calculation on agglomeration/coagulation of particles in order to determine the particle size distribution of the ash. This work can also be further extended and combined with ash deposition work to get a complete overview on the fate of the inorganics in coal and biomass after combustion.

Appendix A

Summary of coal and biomass composition

Table A.1: Proximate, ultimate and elemental analysis of wood bark, wood chip, straw and Polish coal used in this research

Fuel name	Units	Wood bark(spruce)	Wood chip (spruce)	Straw (wheat)	Polish coal
Proximate					
ash content	wt.% d.b.	4.90	0.50	8.21	18.92
moisture	wt.% w.b.	0.47	0.40	11.21	3.56
vol. matter	wt.% d.b.	70.31	83.99	74.40	
Ultimate					
C	wt.% d.b.	49.90	48.71	44.71	64.79
H	wt.% d.b.	5.84	6.15	5.83	4.02
N	wt.% d.b.	0.46	0.08	0.59	1.15
O	wt.% d.b.				
Elements					
Si	mg/kg d.b.	3866.0	380.0	20186.0	41601.0
Al	mg/kg d.b.	616.0	102.0	116.0	21217.0
Fe	mg/kg d.b.	377.0	75.0	168.0	10319.0
Ca	mg/kg d.b.	13196.0	1189.0	3483.0	7934.0
Mg	mg/kg d.b.	781.0	165.0	396.0	4527.0
Na	mg/kg d.b.	103.0	32.0	61.0	1403.0
K	mg/kg d.b.	2493.0	425.0	14953.0	3887.0
Ti	mg/kg d.b.	36.0	7.0	7.0	1087.0
P	mg/kg d.b.	361.0	67.0	649.0	351.0
S	mg/kg d.b.	369.0	62.0	1410.0	6014.0
Cl	mg/kg d.b.	165.0	79.0	5625.0	2405.0
Mn	mg/kg d.b.	428.0	167.0	11.3	210.0
Zn	mg/kg d.b.	84.0	9.0	9.2	29.0
Pb	mg/kg d.b.	1.0	0.0	0.39	15.4

Appendix B

Chemical Fractionation Experimental Method

Chemical fractionation method was used to compare results from pH extraction. The method used is described in Figure B.1 below. It is possible to derive the quantity of elements dissolved in water, alkaline and acid, in order to predict the behaviour of the fuel during combustion.

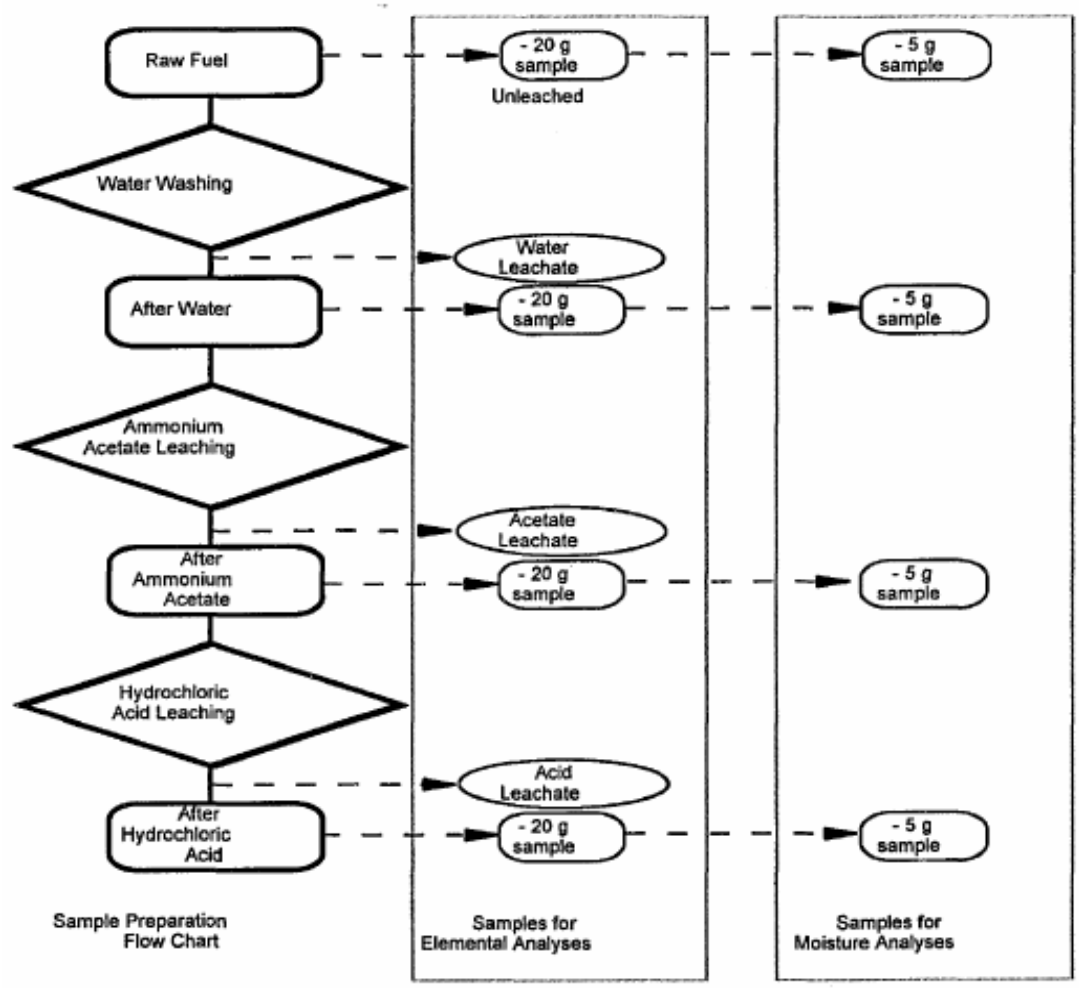

Figure B.1: Chemical fractionation experimental procedure adopted from Miles, et al., 1996

Appendix C

pH Extraction Method

C.1 pH Extraction Experimental Procedure

The method used for these experiments are based on the Leaching behaviour tests – influence of pH on leaching with continuous pH-control, CEN292. The detailed procedures are discussed here (CEN 292, 2005).

Reagents

Distilled water
Demineralised water
Nitric acid (pro analysis), 0,1 mol/l to 5 mol/l.
Sodium hydroxide, NaOH, 0,1 mol/l to 5 mol/l

Equipment

Automatic pH control device with a precision of 0.2 units through acid/base addition
Vacuum filtration device or pressure filtration device
Membrane filters for the filtration device, fabricated from inert material
Sieve with 1 mm nominal screen sizes.
pH meter with a measurement accuracy of at least ± 0,05 pH units
Stirring device
Crushing equipment
Bottles (250 ml for the test portions of 15 g of dry mass, 500 ml for test portions of 30 g dry mass and 1 l for test portions of 60 g dry mass) made of polypropylene (PP), polyethylene (PE) or PTFE

Test Procedure

1. Contact time

The leaching procedure consists of three defined stages:

- Period A (initial acid/base addition) from t_0 up t_0 +4 hours for adjustment of pH;
- Period B (equilibration period) from $t_{0+4\ h}$ up to t_0 +44 hours equilibration period at continuously controlled pH;
- Period C (verification period)from $t_{0+44\ h}$ up to t_0+48 hours for verification of equilibrium condition at continuously controlled pH.

The amount of acid or base added is recorded after each of these periods. The pH in the liquid is recorded after each of these periods. The total contact period (A+B+C) is 48 hours.

2. pH range

The test shall cover the range pH 2 to pH13 with at least 8 pH values tested including the natural pH (without acid or base addition). The maximum difference between two consecutive pH values shall not exceed 1.5 pH units.

3. Leaching test

Carry out the test at a temperature of 20°C ± 5°C.

Select the appropriate bottle size according to the test portion size. For M_d =15 g, bottle sizes of 250 ml is required.

Clean the bottle before use by filling it with 1 mol/l nitric acid, leaving it for at least 24 h and then flushing it out with de-mineralized water. Place one of the test portions in the rinsed bottle. Add the volume of de-mineralised water V_{demin}.

Connect the bottle to the pH control device and insert the pH electrode.To ensure proper suspension of waste particles mixing of the solution is applied throughout the procedure.

Start pH control at the preset pH value with a tolerance of ± 0.1 pH unit at t_0 and continue until t = t_0+48h.

Measure and record the acid or base consumption and the pH at t_{0+4h}. The pH measurement shall be done over a 5 minute interval to avoid incidental deviation due to acid or base addition. The pH at t_{0+4h} shall not deviate more than 0.3 pH unit from the preset pH value.

Measure and record the acid or base consumption and the pH at t_{0+44h} and t_{0+48h}. The pH value measured before filtration at t_{0+48h} will be the one associated to the analysis of the eluate.

The test aims at a final L/S ratio of 10 after acid or base addition. The ultimate L/S shall not deviate more than 10 % from L/S=10.

Report the acid or base consumption t_{0+4h} and t_{0+44h} and between t_{0+44h} and $t_{0+48\ h}$.
The acid or base addition between t_{0+44h} and t_{0+48h} shall not exceed 2% of the total acid or base consumption (Mol/kg) between t_0 and t_{0+48h}. This is the limit for achieving equilibrium condition.

Rinse the part of filtration device which is in contact with the elute, with nitric acid and flush with ultra pure water before any use.
Filter the suspension through a 0.45 μm membrane filter using the filtration device.

C.2 Leaching test reproducibility

pH extraction tests were repeated for the three biomass samples to verify the reproducibility of the leaching data. It was seen that comparable concentrations were found for all leached elements, as shown in Figure C.1.

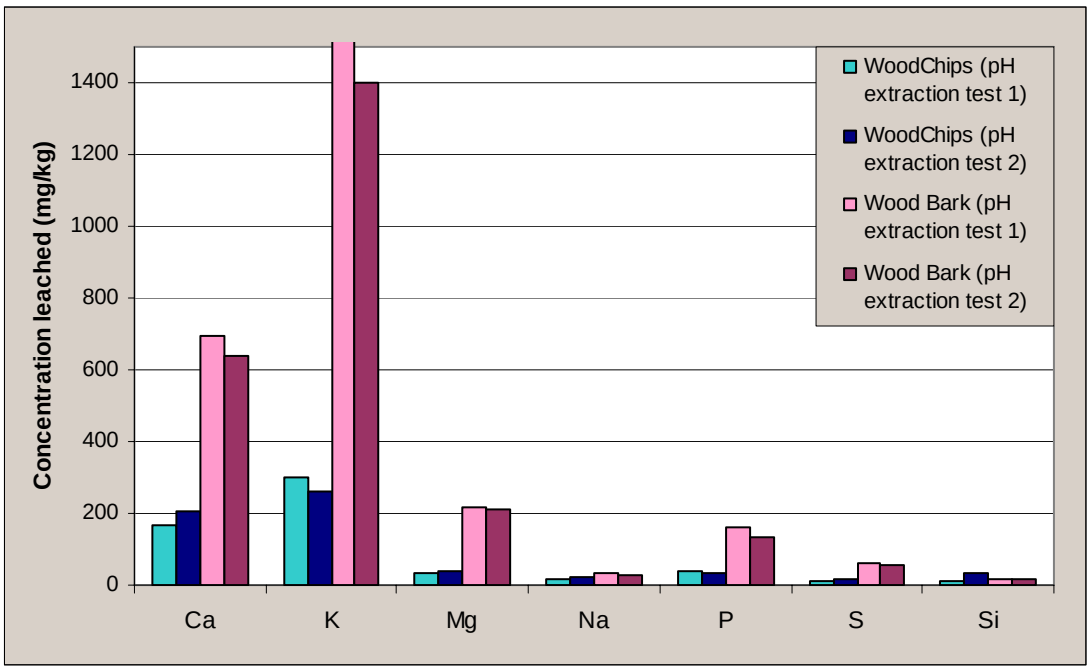

Figure C.1: Reproducibility of leaching data for wood samples

Appendix D

Speciation Modelling

D.1 Equilibrium constant values, K_{sp}

The equilibrium knowledge that is used for the calculation of speciation is the equilibrium constant or the solubility product constant (K_{sp}). These values are determined from various literature sources and thermodynamic calculations. Table D.1 summarises the solubility product constants assembled for biomass speciation

Table D.1: Solubility constant values for the various compounds found in biomass

	Ionic salts		Formula weight	Common name	Charge	T (C)	deltaH (KJ)	deltaS (J/K)	deltaG (KJ)	K	Log K	Source	Solubility Product Equation
	Compound	Formula											
Na	sodium nitrate	NaNO3	84.99	nitratine	+1	25	-20.589	-88.951	5.931	9.14E-02	-1.039	HSC	Na(+a) + NO3(-a) = NaNO3
	sodium chloride	NaCl	58.44	halite		25	-3.7	-	-	2.60E-02	-1.6025	MTQ	
						25	-3.741	-43.012	9.083	2.56E-02	-1.592	HSC	Na(+a) + Cl(-a) = NaCl
K	Potassium nitrate	KNO3	101.10	niter	+1	25	-35.648	-114.934	-1.38	1.75E+00	0.242	HSC	K(+a) + NO3(-a) = KNO3
	Potassium chloride	KCl	74.55	sylvite		25	-17.435	-75.069	4.947	1.36E-01	-0.867	HSC	K(+a) + Cl(-a) = KCl
Ca	Calcium nitrate	Ca(NO3)2	164.09	-	+2	25	19.908	-44.183	33.081	1.60E-06	-5.796	HSC	Ca(+2a) + 2NO3(-a) = Ca(NO3)2
	Calcium chloride	CaCl2	110.99	-		25	81.853	51.382	66.533	2.20E-12	-11.657	HSC	Ca(+2a) + 2Cl(-a) = CaCl2
	calcium phosphate	Ca3(PO4)2	310.18	-	+2	25	-54			8.318E+28	28.92	MTQ	
						25	63.199	848.955	-189.917	1.89E+33	33.275	HSC	3Ca(+2a) + 2PO4(-3a) = Ca3(PO4)2
Mg	magnesium nitrate	Mg(NO3)2	148.31	-	+2	25	88.931	8.188	86.49	7.02E-16	-15.154	HSC	Mg(+2a) + 2NO3(-a) = Mg(NO3)2
	magnesium chloride	MgCl2	95.21	scacchite	+2	25	155.819	114.222	121.764	4.63E-22	-21.334	HSC	Mg(+2a) + 2Cl(-a) = MgCl2
	magnesium phosphate	Mg3(PO4)2	262.86	purpurite	+2	25				1.905E+23	23.28	MTQ	
						25	172.629	1046.92	-139.51	2.78E+24	24.444	HSC	3Mg(+2a) + 2PO4(-3a) = Mg3(PO4)2
Si	amorphous silica	Si(OH)4	96.11	-		25	-1456.961	-500.503	-1307.736	1.31E+229	229.1182	HSC	Si(OH)4(a)
						25	-1612.761	-1253.866	-1238.921	1.18E+217	217.072	HSC	Si + 4OH(g) = Si(OH)4(a)
S	Sulfur tetraoxide -2ion	SO42-	96.06	-	-2	25	-60.14			4.571E+33	33.66	MTQ	SO4(-2a)
P	Phosphate -3ion	PO43-	94.97	-	-3.0	25	-1277.375	-221.752	-1211.26	1.64E+212	212.2154	HSC	
Cl	chloride ion	Cl-	35.45	-	-1	25	-167.08	56.735	-183.995	1.723E+32	32.23632	HSC	Cl(-a)
												HSC	Cl2(g) +2e- = 2Cl(-a)
	Minerals		Formula weight	Common name	Charge	T (C)	deltaH (KJ)	deltaS (J/K)	deltaG (KJ)	K	Log K	Source	Solubility Product Equation
	Compound	Formula											
Ca	Calcium oxalate	$CaC_2O_4.nH_20$	146.11	Whewellite	-2	25	-14			2.32E-09	-8.63451	MTQ	
		CaC2O4*H2O				25	-1675.002	157	-1721.811	1.96×10^{-8}	-7.71	HSC	
		CaC2O4											
Si	Phytolite	$SiO_2.nH_2O$	78.1	silicic acid	0	25	-14			512.86138	2.71	MTQ	
						25	-910.857	41.463	-923.219	5.62E+161	161.75	HSC	

D.2 LeachXS Input Data

The input data for LeachXS was derived from the maximum concentration of the leached elements from the pH extraction test. Table D.2 summarises the input concentrations fed into LeachXS to determine the speciation.

Table D.2: Input concentrations fed into LeachXS

Fuel (per kg)	Al^{3+}	H_3AsO_4	Ca^{2+}	Cl^-	Fe^{3+}	H_2CO_3	K^+	Mg^{2+}	Na^+	NO_3^-	PO_4^{3-}	SO_4^{2-}	H_4SiO_4
Wood chips	1.00E-03	1.00E-09	3.18E-02	2.37E-03	4.31E-04	8.84E-02	1.05E-02	6.64E-03	7.92E-04	4.59E-04	5.59E-04	2.43E-04	2.76E-03
Wood bark	3.87E-03	1.00E-09	2.73E-01	8.30E-03	3.56E-03	1.59E-01	5.26E-02	3.26E-02	1.54E-03	4.84E-04	2.94E-03	1.47E-03	3.34E-02
Straw	1.20E-03	1.00E-09	6.26E-02	1.95E-02	2.17E-03	8.43E-02	1.26E-01	2.36E-02	3.36E-03	4.84E-04	1.03E-02	3.94E-03	4.63E-02

D.3 LeachXS Speciation Results

The results obtained for speciation of wood chips has been described in Section 4.3. The results for wood bark and straw have been illustrated in this section of the Appendix and summarised in Tables 4.3 and 4.4.

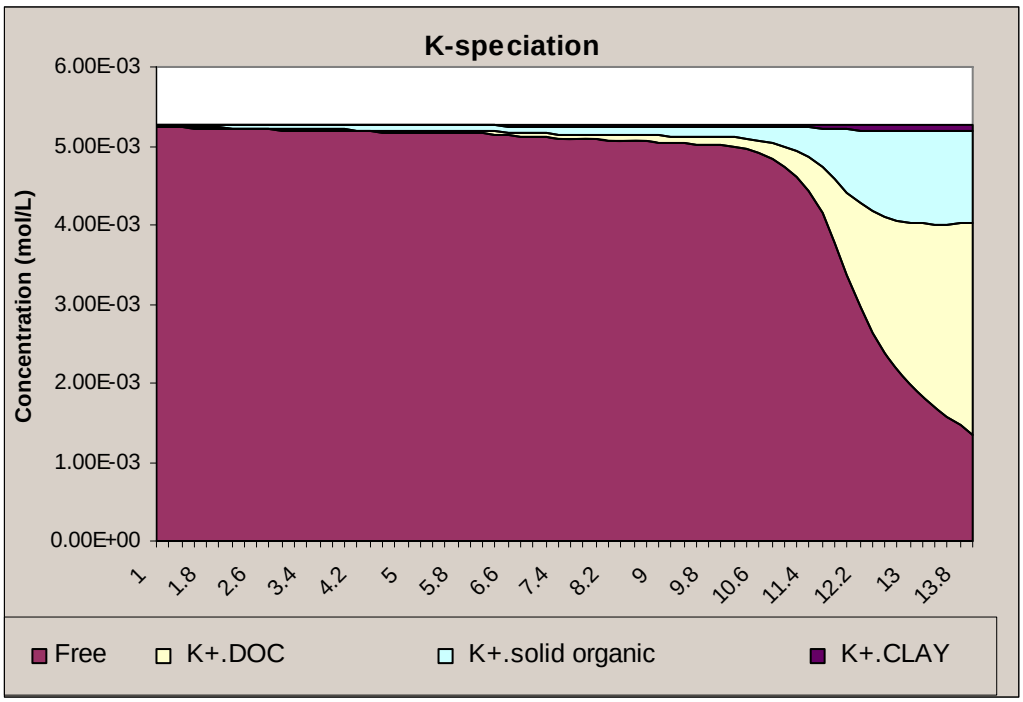

Figure D.1: Speciation for K element in wood bark

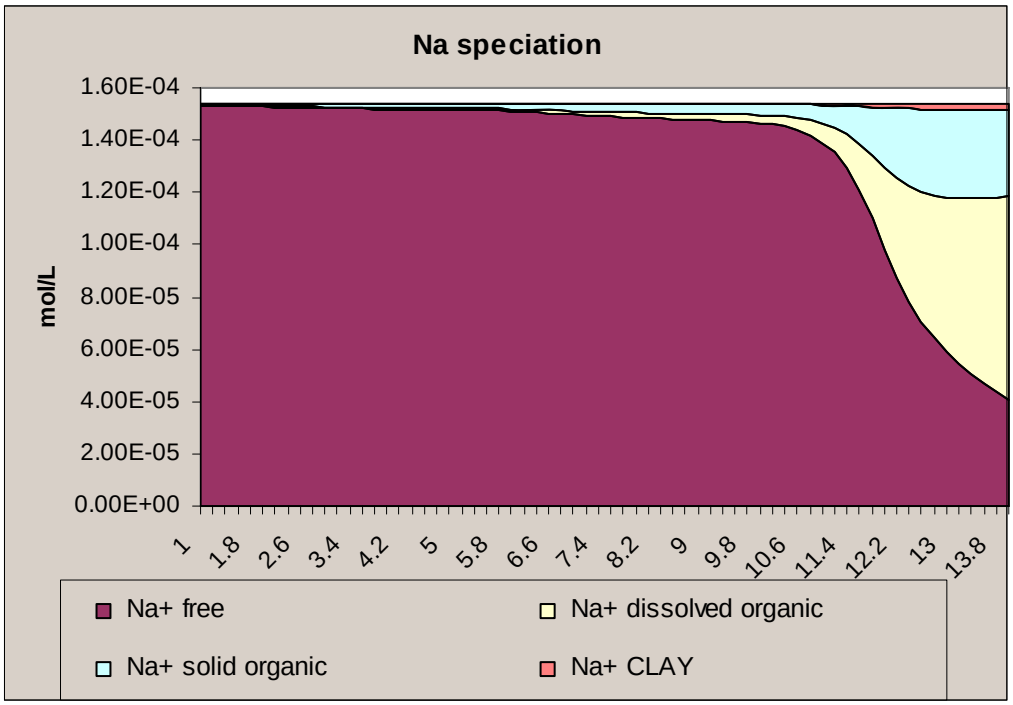

Figure D.2: Speciation for Na element in wood bark

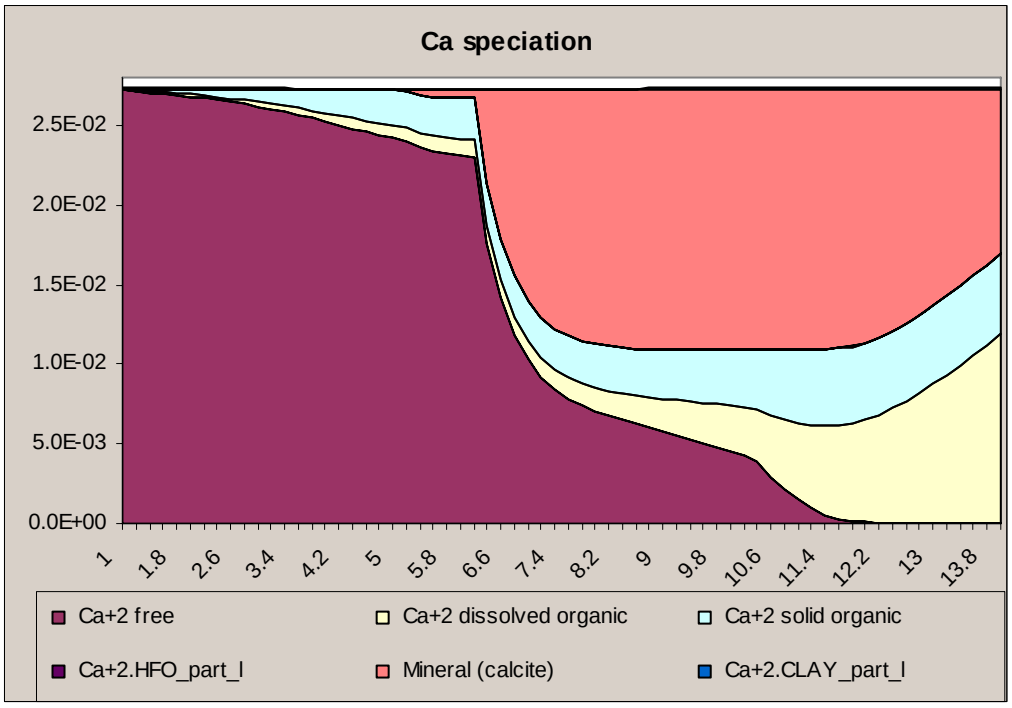

Figure D.3: Speciation for Ca element in wood bark

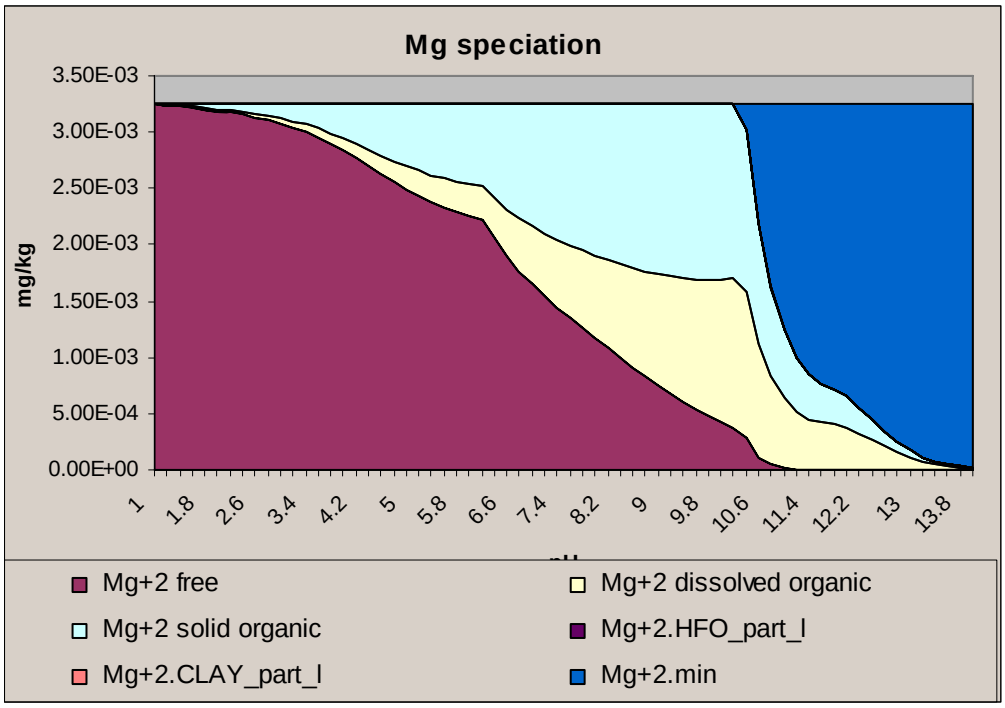

Figure D.4: Speciation for Mg element in wood bark

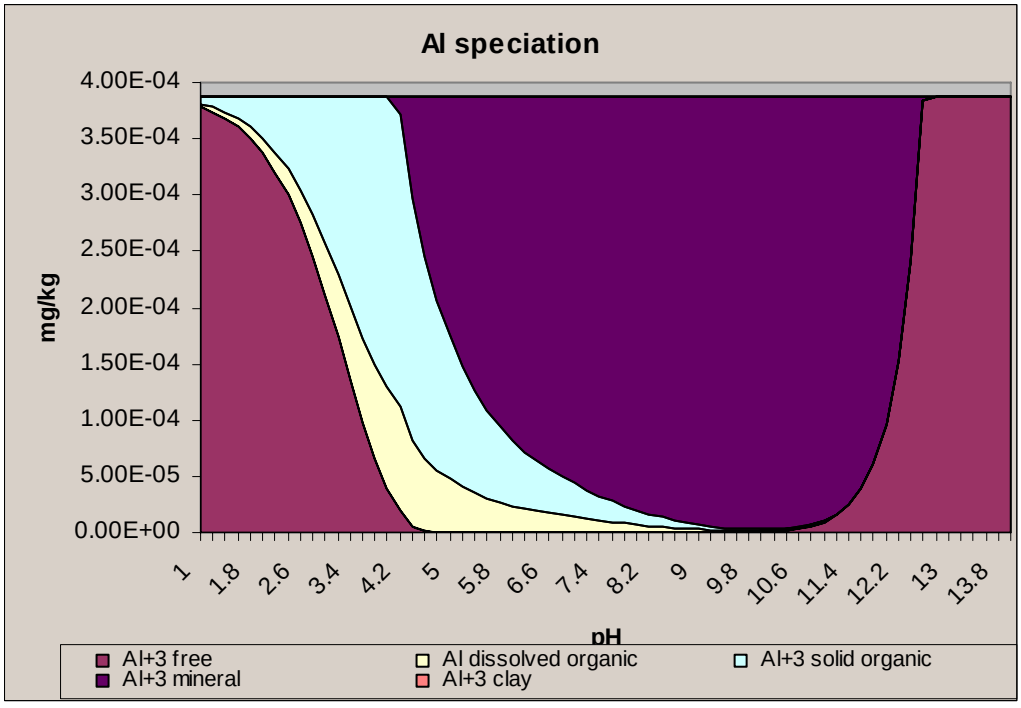

Figure D.5: Speciation for Al element in wood bark

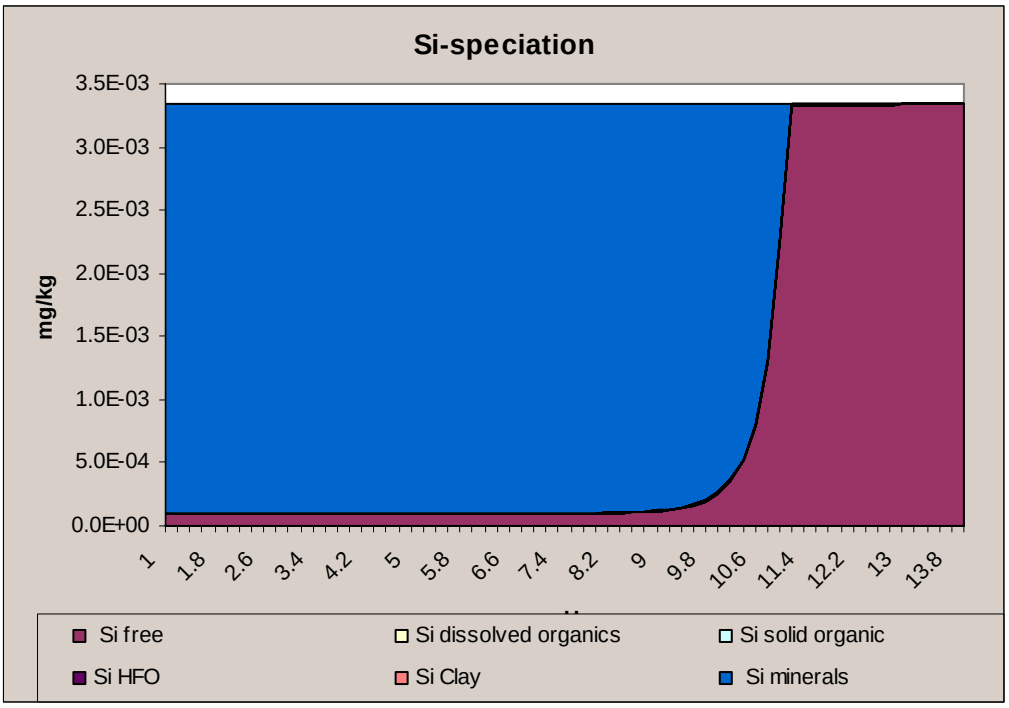

Figure D.6: Speciation for Si element in wood bark

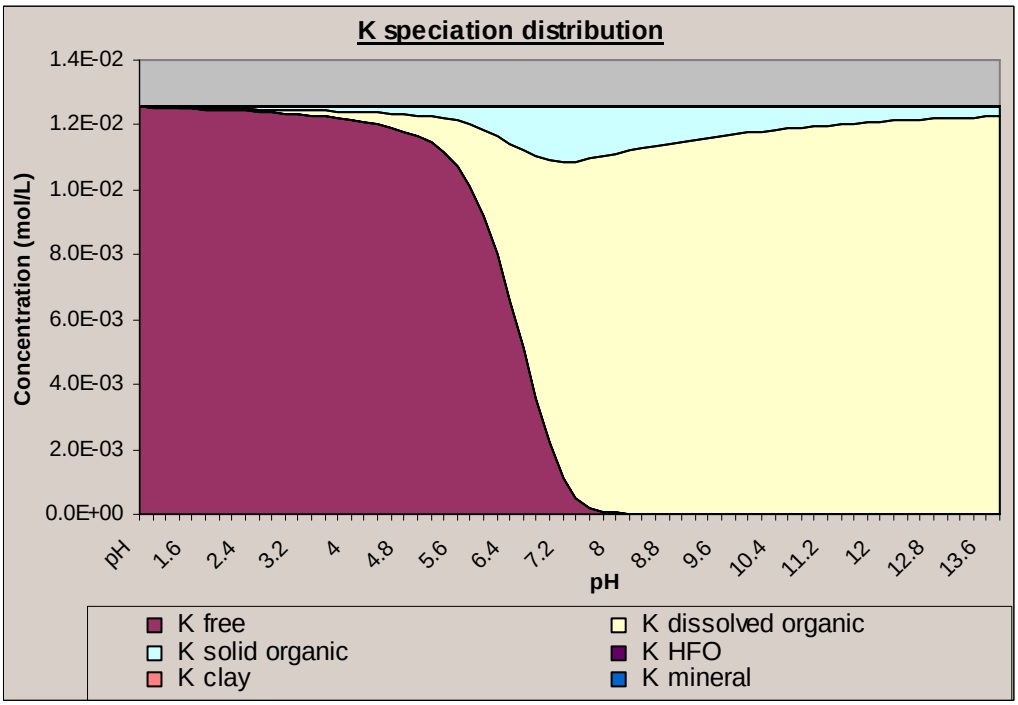

Figure D.7 Speciation for K element in straw

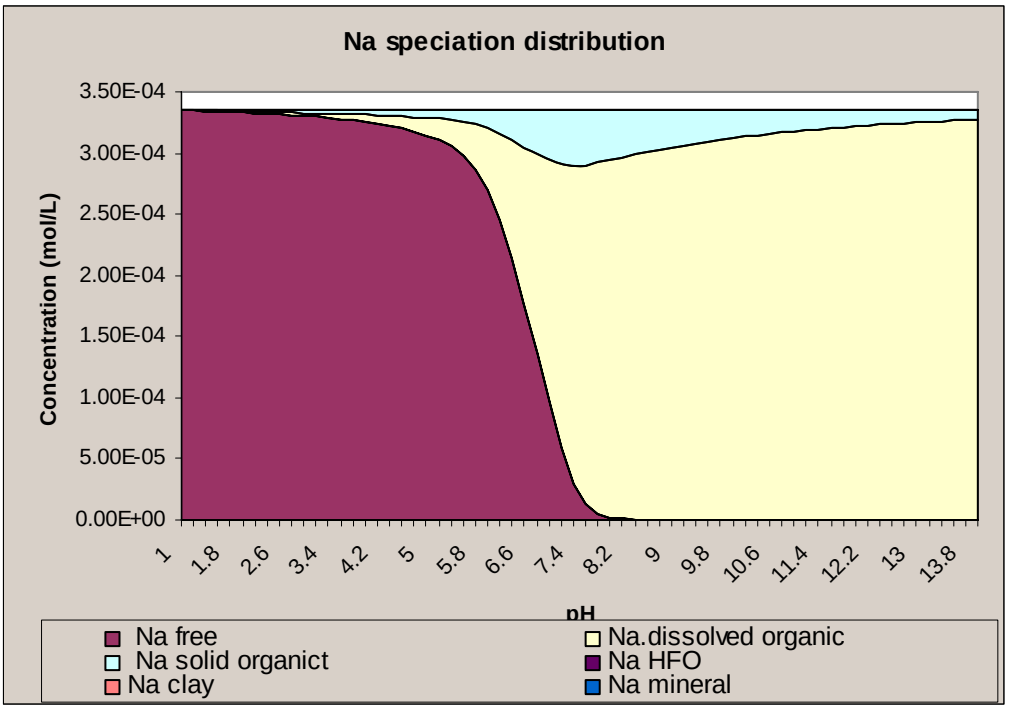

Figure D.8 Speciation for Na element in straw

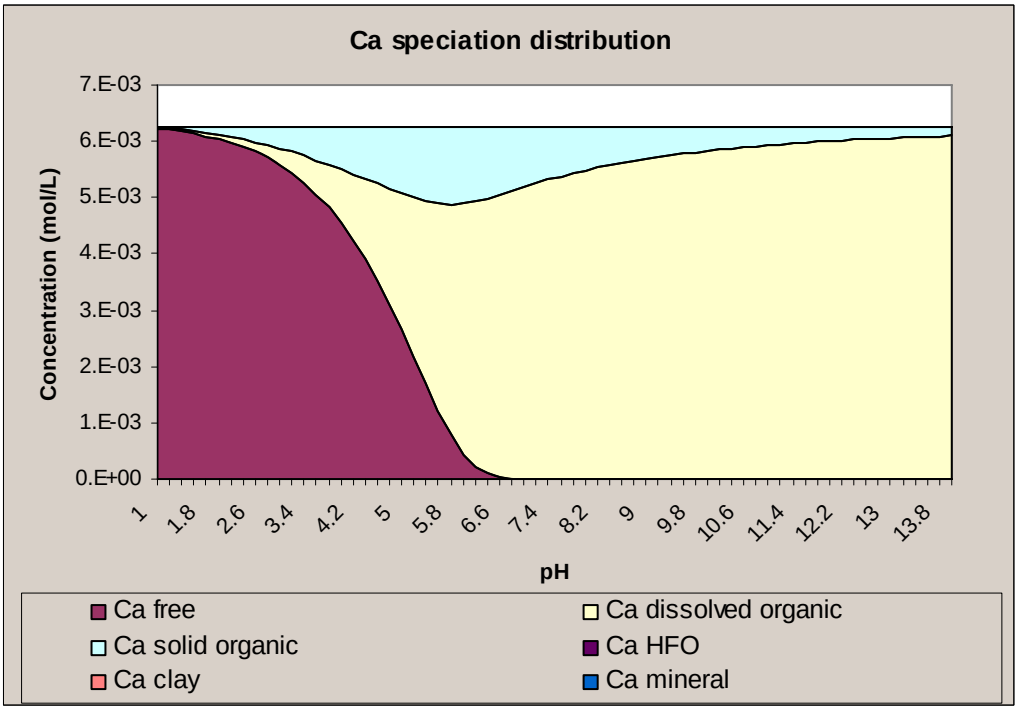

Figure D.9 Speciation for Ca element in straw

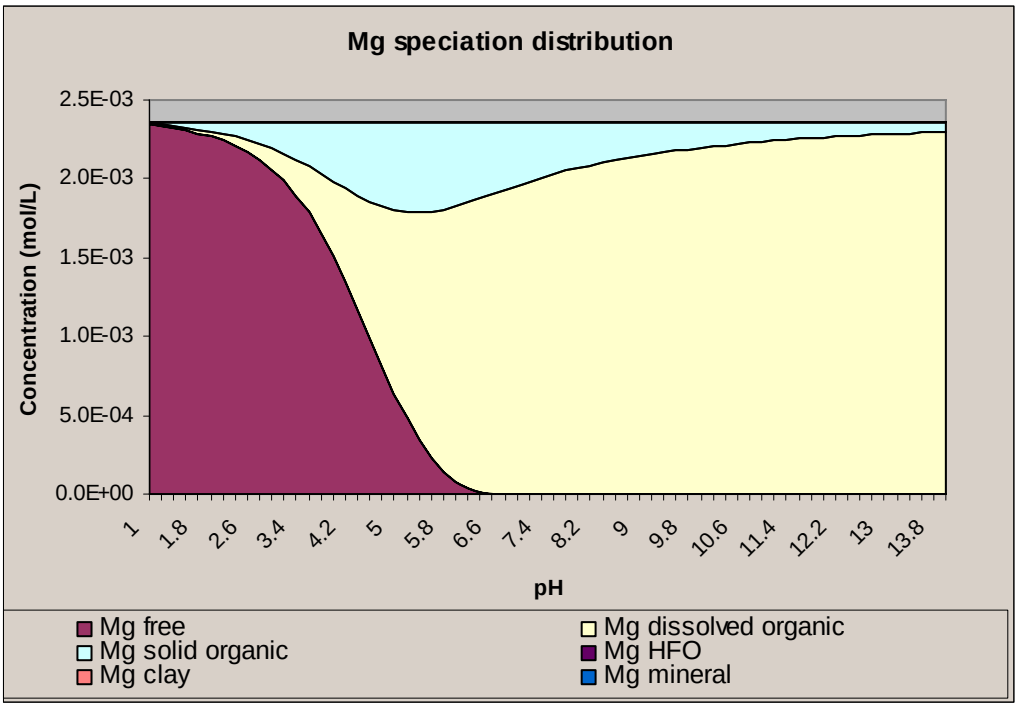

Figure D.10 Speciation for Mg element in straw

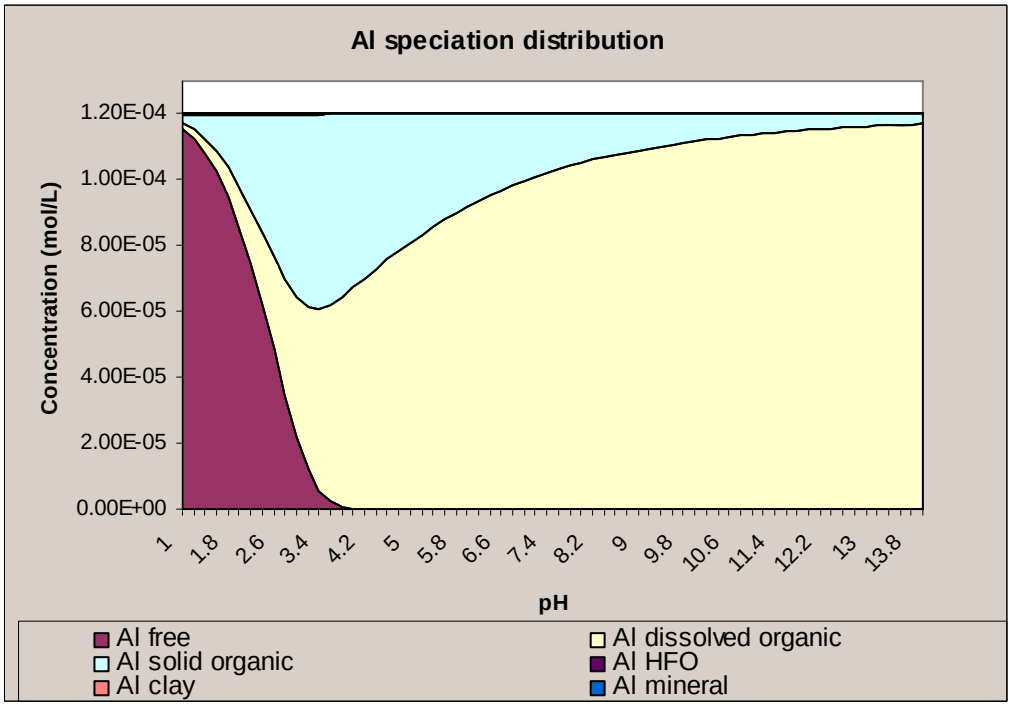

Figure D.11 Speciation for Al element in straw

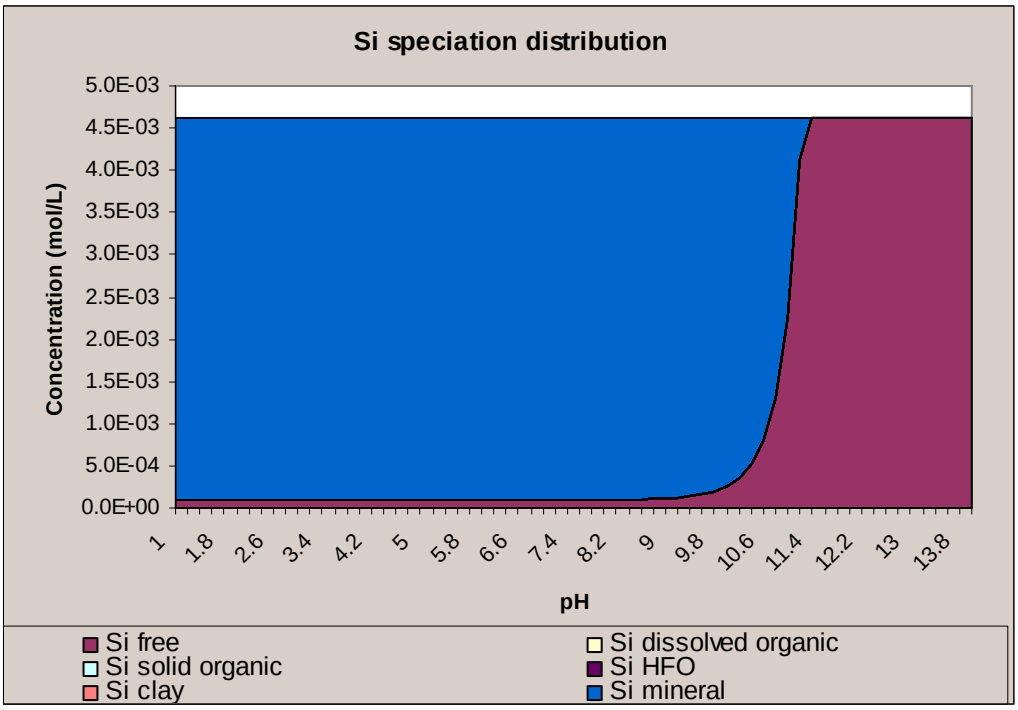

Figure D.12 Speciation for Si element in straw

Appendix E

High temperature thermochemistry

E.1 FACTSAGE input data

The input used for the high temperature thermochemistry model (FACTSAGE) is the concentration of the elements in the fuel. For the complete combustion that is taken into account for the equilibrium calculations, lambda value of 1.04 is taken into account. Table E.1 summarises the input for FACTSAGE calculations determined from the fuel elemental analysis and complete combustion.

Table E.1: Input concentration of fuels fed into FACTSAGE for equilibrium calculations

FACTSAGE input as mol / kg feedstock dry base					
Element	W-chips	Bark	Coal	Straw	80 Coal / 20 W-chips
C	39	41	52	37	50
H	61	59	39	58	43
N	5.7E-02	3.7E-01	8.5E-01	5.71E-02	6.9E-01
O	27	26	7	26	11
Ca	2.3E-02	3.1E-01	2.0E-01	8.3E-02	1.6E-01
Si	9.1E-03	1.0E-01	1.5	6.6E-01	1.2
K	9.0E-03	5.7E-02	9.7E-02	3.6E-01	8.0E-02
Mg	5.1E-03	3.0E-02	1.8E-01	1.5E-02	1.5E-01
Mn	2.6E-03	7.9E-03	3.8E-03	2.2E-04	3.5E-03
Al	2.4E-03	3.2E-02	7.6E-01	4.2E-03	6.1E-01
S	1.9E-03	1.2E-02	1.8E-01	4.2E-02	1.4E-01
P	1.7E-03	1.1E-02	1.0E-02	1.8E-02	8.7E-03
Cl	1.4E-03	3.4E-03	7.6E-02	2.7E-01	6.1E-02
Na	9.1E-04	5.6E-03	6.2E-02	2.2E-03	5.0E-02
Fe	7.9E-04	8.5E-03	1.8E-01	2.1E-03	1.4E-01
O2	43	44	61	40	57
N2	161	167	228	151	214
Lambda	1.04	1.04	1.04	1.04	1.04
Total moles	331	337	391	313	379

E.2 FACTSAGE results

The results obtained for the stable phases during the combustion of wood bark and the co-fired blend (coal and wood chips) have been summarised in Table 5.1 The detailed amount are displayed as graphs in this section of the appendix.

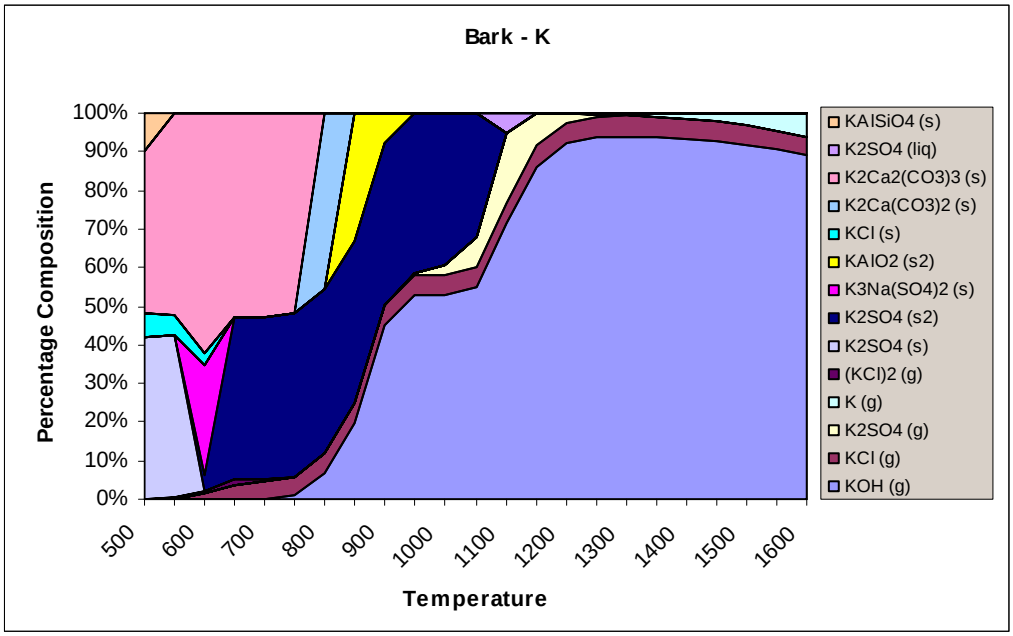

Figure E.1: High temperature distribution for K elements in wood bark

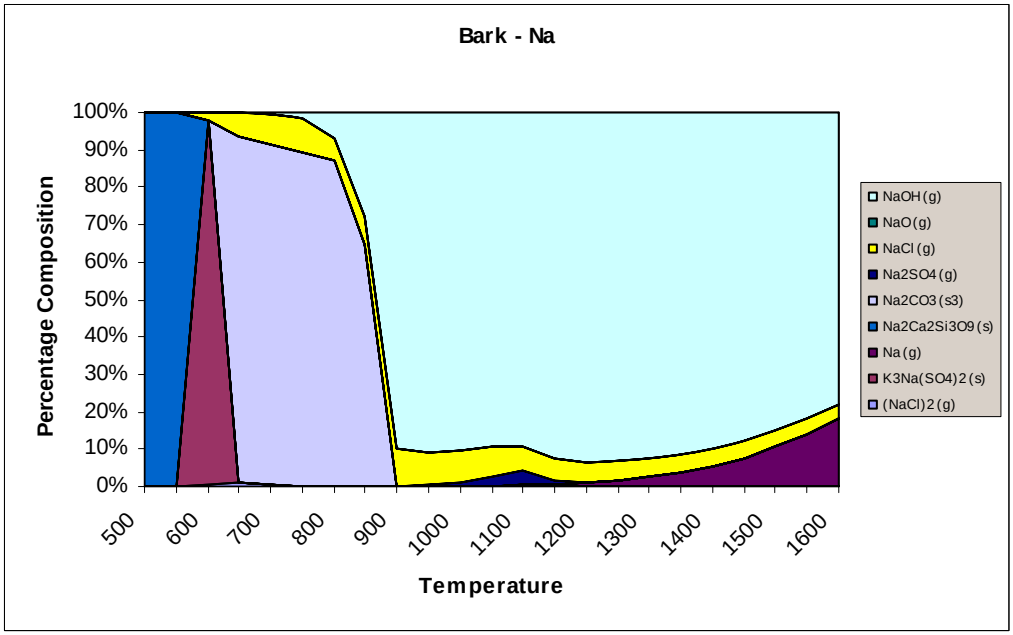

Figure E.2: High temperature distribution for Na elements in wood bark

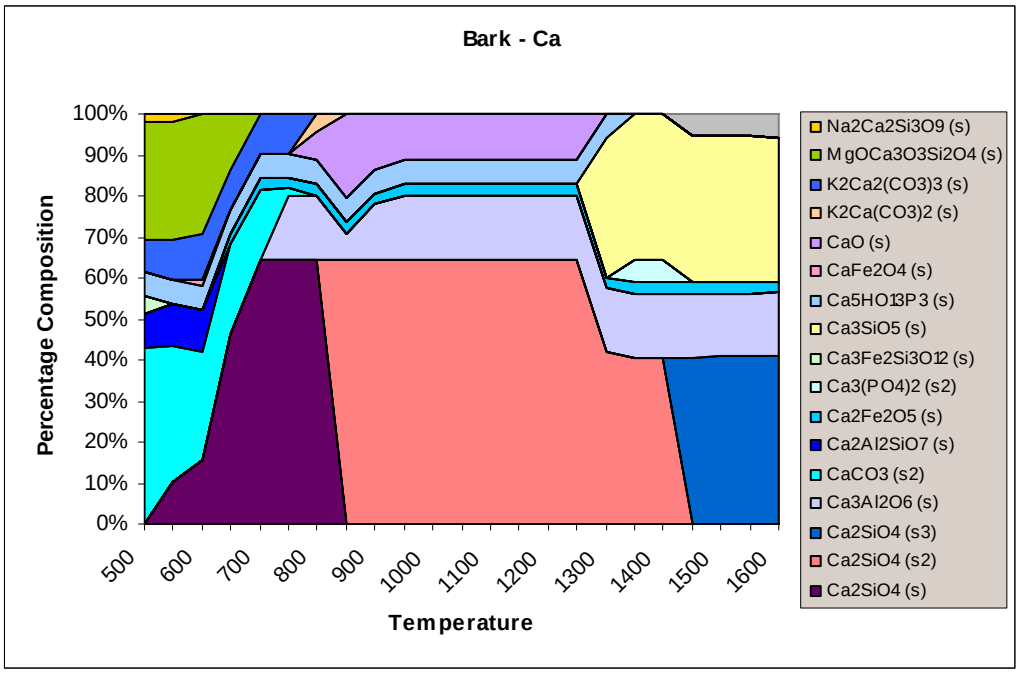

Figure E.3: High temperature distribution for Ca elements in wood bark

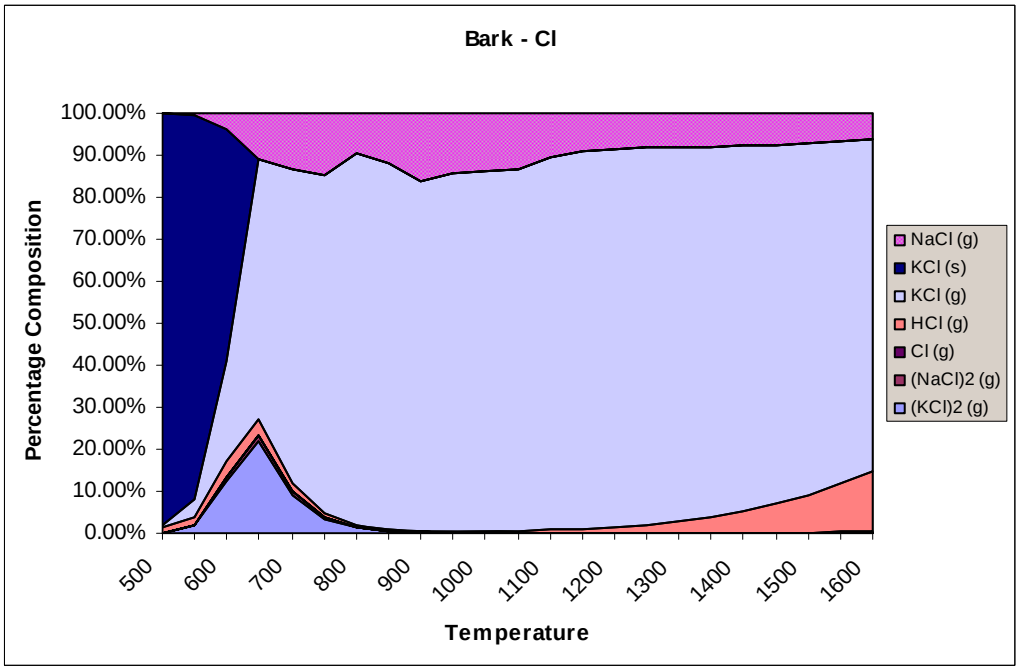

Figure E.4: High temperature distribution for Cl elements in wood bark

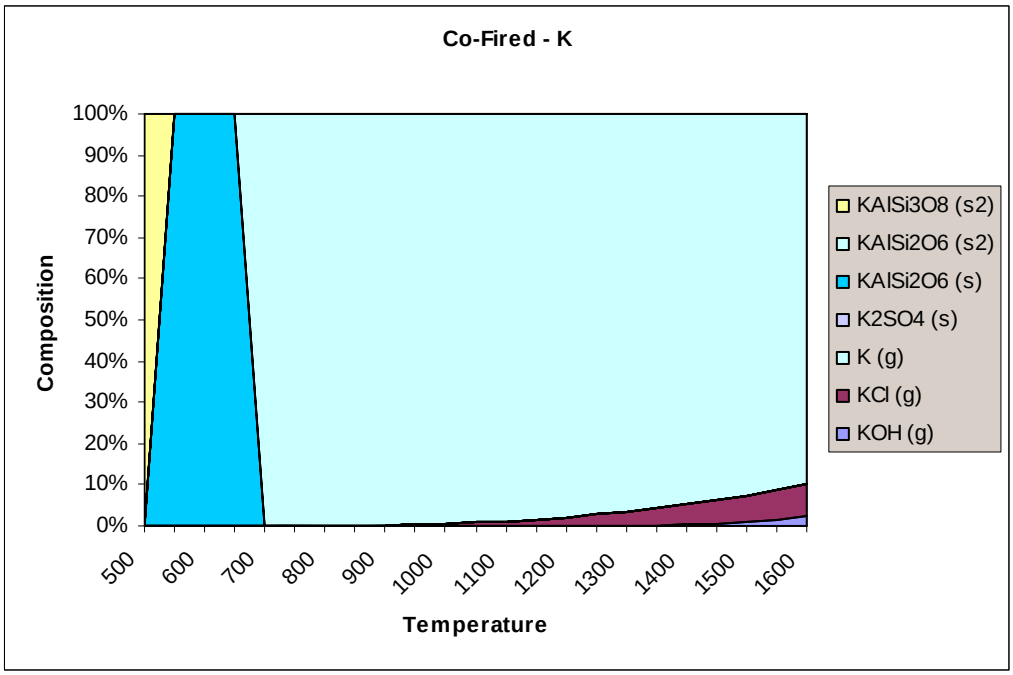

Figure E.5: High temperature distribution for K elements in co-fired blend

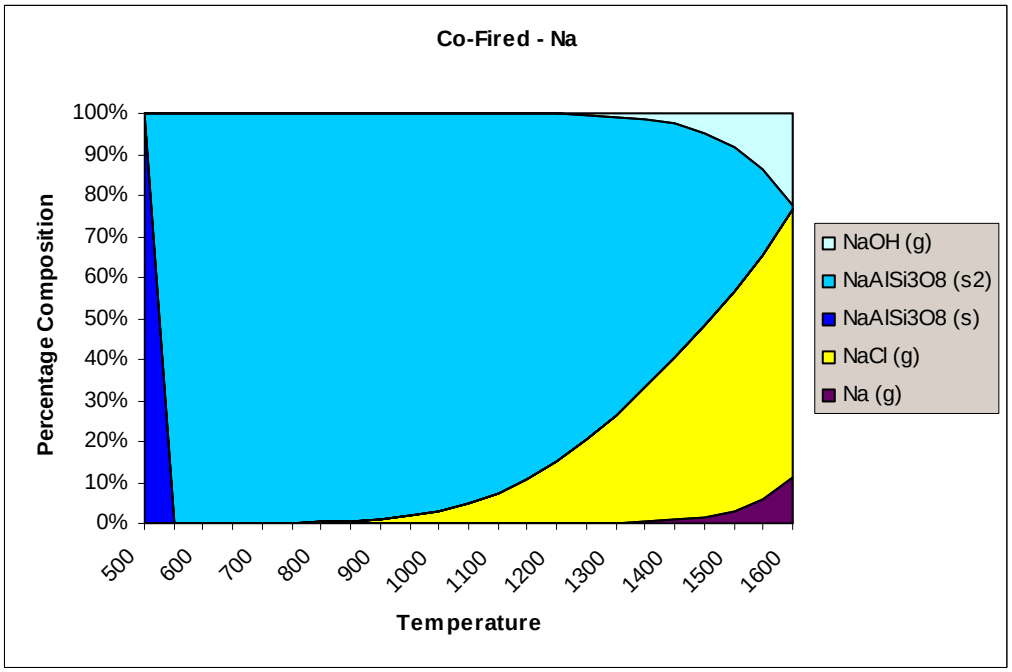

Figure E.6: High temperature distribution for Na elements in co-fired blend

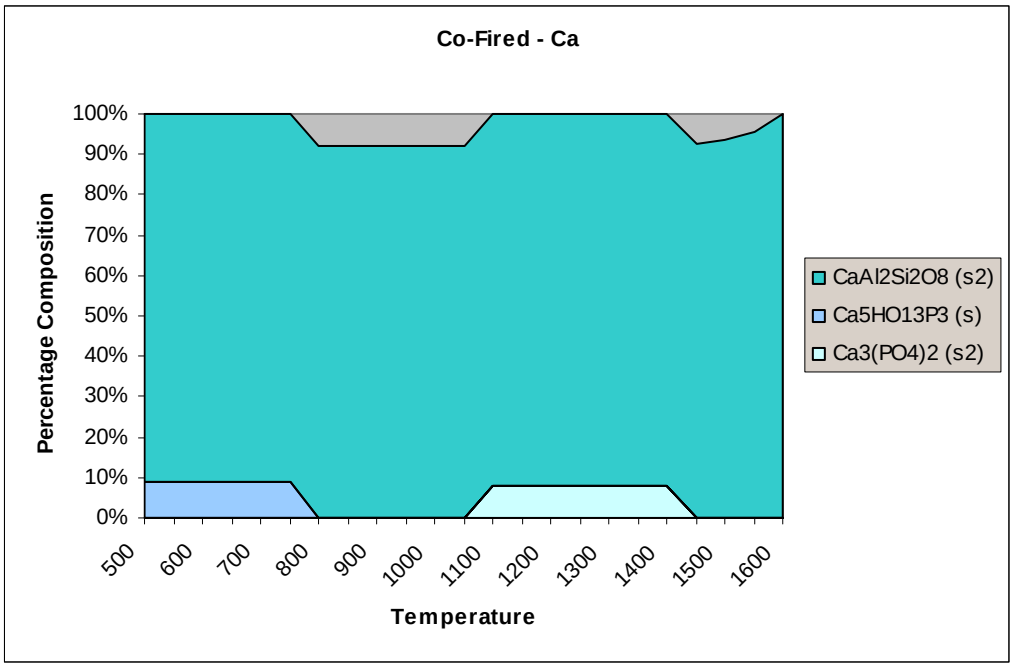

Figure E.7: High temperature distribution for Ca elements in co-fired blend

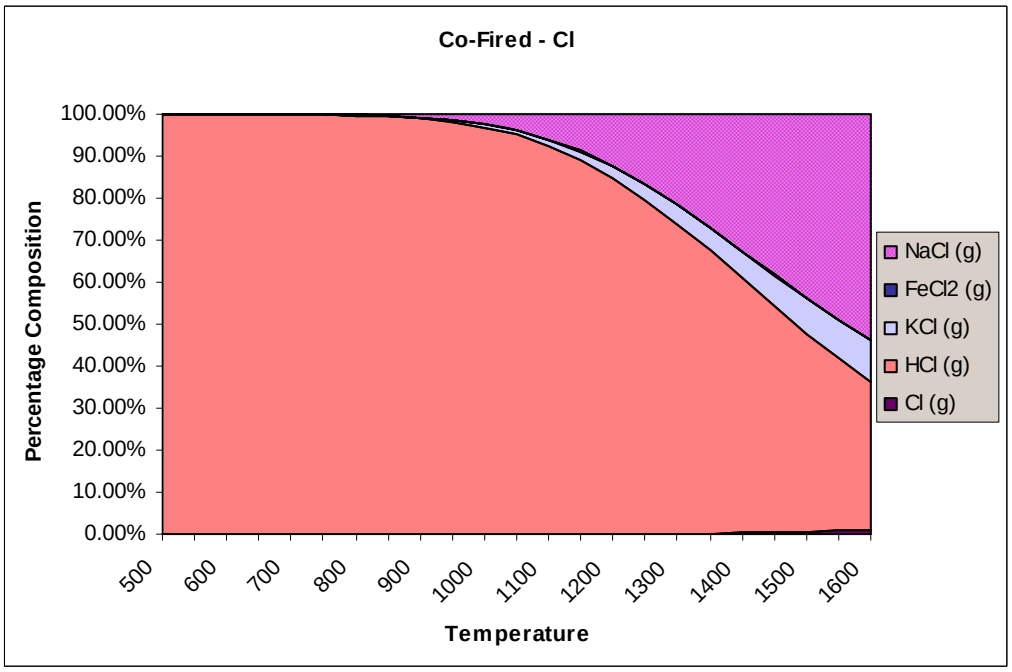

Figure E.8: High temperature distribution for Cl elements in co-fired blend

Appendix F

Condensation calculations

F.1 Homogeneous and heterogeneous condensation

The calculations involved in determining the saturation ratio and condensation rates are appended in this section.

Table F.1: Gas-to-particle conversion calculations for KCl (g)

D (m)	Temperature (K) / Frequency/Diffusivity	773 / 1.25E-05	873 / 1.33E-05	973 / 1.40E-05	1073 / 1.47E-05	1173 / 1.54E-05	1273 / 1.60E-05	1373 / 1.66E-05	1473 / 1.72E-05	1573 / 1.78E-05	1673 / 1.84E-05
3.0E-04	0.1	2.8E+12	2.5E+12	1.1E+12	-1.1E+13	-6.6E+13	-2.6E+14	-8.2E+14	-2.1E+15	-4.9E+15	-9.8E+15
2.5E-04	0.5	1.1E+13	1.0E+13	4.5E+12	-4.4E+13	-2.7E+14	-1.1E+15	-3.4E+15	-8.8E+15	-2.0E+16	-4.0E+16
2.0E-04	1.1	2.0E+13	1.9E+13	8.2E+12	-7.9E+13	-4.9E+14	-1.9E+15	-6.1E+15	-1.6E+16	-3.6E+16	-7.3E+16
1.7E-04	2.3	3.5E+13	3.2E+13	1.4E+13	-1.4E+14	-8.4E+14	-3.3E+15	-1.0E+16	-2.7E+16	-6.2E+16	-1.2E+17
1.4E-04	3.8	4.8E+13	4.4E+13	1.9E+13	-1.8E+14	-1.1E+15	-4.5E+15	-1.4E+16	-3.7E+16	-8.4E+16	-1.7E+17
1.1E-04	5.5	5.7E+13	5.2E+13	2.3E+13	-2.2E+14	-1.3E+15	-5.4E+15	-1.7E+16	-4.4E+16	-1.0E+17	-2.0E+17
9.2E-05	6.8	5.7E+13	5.2E+13	2.3E+13	-2.2E+14	-1.4E+15	-5.5E+15	-1.7E+16	-4.5E+16	-1.0E+17	-2.0E+17
7.6E-05	7.7	5.3E+13	4.9E+13	2.1E+13	-2.1E+14	-1.3E+15	-5.1E+15	-1.6E+16	-4.2E+16	-9.4E+16	-1.9E+17
6.2E-05	8	4.5E+13	4.2E+13	1.8E+13	-1.8E+14	-1.1E+15	-4.3E+15	-1.4E+16	-3.5E+16	-8.0E+16	-1.6E+17
5.1E-05	7.9	3.7E+13	3.4E+13	1.5E+13	-1.4E+14	-8.8E+14	-3.5E+15	-1.1E+16	-2.9E+16	-6.5E+16	-1.3E+17
4.2E-05	7.4	2.8E+13	2.6E+13	1.1E+13	-1.1E+14	-6.7E+14	-2.7E+15	-8.4E+15	-2.2E+16	-5.0E+16	-1.0E+17
3.4E-05	6.7	2.1E+13	1.9E+13	8.4E+12	-8.1E+13	-5.0E+14	-2.0E+15	-6.3E+15	-1.6E+16	-3.7E+16	-7.5E+16
2.8E-05	5.9	1.5E+13	1.4E+13	6.1E+12	-5.9E+13	-3.6E+14	-1.5E+15	-4.5E+15	-1.2E+16	-2.7E+16	-5.4E+16
2.3E-05	5.2	1.1E+13	1.0E+13	4.4E+12	-4.3E+13	-2.6E+14	-1.0E+15	-3.3E+15	-8.6E+15	-1.9E+16	-3.9E+16
1.9E-05	4.6	8.0E+12	7.3E+12	3.2E+12	-3.1E+13	-1.9E+14	-7.6E+14	-2.4E+15	-6.2E+15	-1.4E+16	-2.8E+16
1.6E-05	4	5.7E+12	5.2E+12	2.3E+12	-2.2E+13	-1.4E+14	-5.4E+14	-1.7E+15	-4.4E+15	-1.0E+16	-2.0E+16
1.3E-05	3.5	4.1E+12	3.8E+12	1.6E+12	-1.6E+13	-9.8E+13	-3.9E+14	-1.2E+15	-3.2E+15	-7.2E+15	-1.5E+16
1.1E-05	3.1	3.0E+12	2.7E+12	1.2E+12	-1.2E+13	-7.1E+13	-2.8E+14	-8.9E+14	-2.3E+15	-5.3E+15	-1.1E+16
8.6E-06	2.7	2.1E+12	1.9E+12	8.5E+11	-8.2E+12	-5.1E+13	-2.0E+14	-6.3E+14	-1.7E+15	-3.8E+15	-7.6E+15
7.1E-06	2.4	1.6E+12	1.4E+12	6.2E+11	-6.0E+12	-3.7E+13	-1.5E+14	-4.6E+14	-1.2E+15	-2.7E+15	-5.5E+15
5.8E-06	2.1	1.1E+12	1.0E+12	4.5E+11	-4.3E+12	-2.7E+13	-1.1E+14	-3.3E+14	-8.7E+14	-2.0E+15	-4.0E+15
4.8E-06	1.7	7.4E+11	6.8E+11	3.0E+11	-2.9E+12	-1.8E+13	-7.1E+13	-2.2E+14	-5.8E+14	-1.3E+15	-2.6E+15
3.9E-06	1.5	5.4E+11	4.9E+11	2.1E+11	-2.1E+12	-1.3E+13	-5.1E+13	-1.6E+14	-4.2E+14	-9.5E+14	-1.9E+15
3.2E-06	1.2	3.5E+11	3.2E+11	1.4E+11	-1.4E+12	-8.4E+12	-3.4E+13	-1.1E+14	-2.7E+14	-6.2E+14	-1.3E+15
2.6E-06	1	2.4E+11	2.2E+11	9.6E+10	-9.3E+11	-5.7E+12	-2.3E+13	-7.2E+13	-1.9E+14	-4.3E+14	-8.6E+14
2.2E-06	0.9	1.8E+11	1.6E+11	7.1E+10	-6.9E+11	-4.2E+12	-1.7E+13	-5.3E+13	-1.4E+14	-3.1E+14	-6.3E+14
1.8E-06	0.7	1.1E+11	1.0E+11	4.5E+10	-4.4E+11	-2.7E+12	-1.1E+13	-3.4E+13	-8.8E+13	-2.0E+14	-4.0E+14
1.5E-06	0.7	9.3E+10	8.5E+10	3.7E+10	-3.6E+11	-2.2E+12	-8.9E+12	-2.8E+13	-7.3E+13	-1.6E+14	-3.3E+14
9.1E-07	0.8	6.7E+10	6.1E+10	2.7E+10	-2.6E+11	-1.6E+12	-6.3E+12	-2.0E+13	-5.2E+13	-1.2E+14	-2.4E+14
Saturation ratio		1550.3	35.3	1.8	0.2	0.0	0.0	0.0	0.0	0.0	0.0
Condensation rate		**4.7E+14**	**4.3E+14**	**1.9E+14**	**-1.8E+15**	**-1.1E+16**	**-4.5E+16**	**-1.4E+17**	**-3.7E+17**	**-8.3E+17**	**-1.7E+18**

Table F.2: Gas-to-particle conversion calculations for K_2SO_4 (g)

D (m)	Temperature (K) / Frequency/Diffusivity	773 / 5.8E-06	873 / 6.1E-06	973 / 6.5E-06	1073 / 6.8E-06	1173 / 7.1E-06	1273 / 7.4E-06	1373 / 7.7E-06	1473 / 8.0E-06	1573 / 8.2E-06	1673 / 8.5E-06
3.0E-04	0.1	8.5E+11	8.0E+11	7.6E+11	7.2E+11	6.9E+11	6.3E+11	4.5E+11	-1.9E+11	-2.2E+12	-7.6E+12
2.5E-04	0.5	3.5E+12	3.3E+12	3.1E+12	3.0E+12	2.8E+12	2.6E+12	1.8E+12	-7.8E+11	-9.0E+12	-3.1E+13
2.0E-04	1.1	6.3E+12	5.9E+12	5.6E+12	5.3E+12	5.1E+12	4.7E+12	3.3E+12	-1.4E+12	-1.6E+13	-5.6E+13
1.7E-04	2.3	1.1E+13	1.0E+13	9.6E+12	9.2E+12	8.7E+12	8.1E+12	5.7E+12	-2.4E+12	-2.8E+13	-9.6E+13
1.4E-04	3.8	1.5E+13	1.4E+13	1.3E+13	1.2E+13	1.2E+13	1.1E+13	7.8E+12	-3.3E+12	-3.8E+13	-1.3E+14
1.1E-04	5.5	1.7E+13	1.6E+13	1.6E+13	1.5E+13	1.4E+13	1.3E+13	9.2E+12	-3.9E+12	-4.5E+13	-1.6E+14
9.2E-05	6.8	1.8E+13	1.7E+13	1.6E+13	1.5E+13	1.4E+13	1.3E+13	9.3E+12	-4.0E+12	-4.6E+13	-1.6E+14
7.6E-05	7.7	1.6E+13	1.5E+13	1.5E+13	1.4E+13	1.3E+13	1.2E+13	8.7E+12	-3.7E+12	-4.3E+13	-1.5E+14
6.2E-05	8	1.4E+13	1.3E+13	1.2E+13	1.2E+13	1.1E+13	1.0E+13	7.4E+12	-3.1E+12	-3.6E+13	-1.2E+14
5.1E-05	7.9	1.1E+13	1.1E+13	1.0E+13	9.6E+12	9.2E+12	8.5E+12	6.0E+12	-2.6E+12	-2.9E+13	-1.0E+14
4.2E-05	7.4	8.7E+12	8.2E+12	7.8E+12	7.4E+12	7.1E+12	6.5E+12	4.6E+12	-2.0E+12	-2.3E+13	-7.8E+13
3.4E-05	6.7	6.5E+12	6.1E+12	5.8E+12	5.5E+12	5.2E+12	4.8E+12	3.4E+12	-1.5E+12	-1.7E+13	-5.8E+13
2.8E-05	5.9	4.7E+12	4.4E+12	4.2E+12	4.0E+12	3.8E+12	3.5E+12	2.5E+12	-1.1E+12	-1.2E+13	-4.2E+13
2.3E-05	5.2	3.4E+12	3.2E+12	3.0E+12	2.9E+12	2.7E+12	2.5E+12	1.8E+12	-7.6E+11	-8.8E+12	-3.0E+13
1.9E-05	4.6	2.5E+12	2.3E+12	2.2E+12	2.1E+12	2.0E+12	1.8E+12	1.3E+12	-5.5E+11	-6.4E+12	-2.2E+13
1.6E-05	4	1.8E+12	1.7E+12	1.6E+12	1.5E+12	1.4E+12	1.3E+12	9.3E+11	-3.9E+11	-4.5E+12	-1.6E+13
1.3E-05	3.5	1.3E+12	1.2E+12	1.1E+12	1.1E+12	1.0E+12	9.4E+11	6.7E+11	-2.8E+11	-3.3E+12	-1.1E+13
1.1E-05	3.1	9.2E+11	8.7E+11	8.2E+11	7.8E+11	7.4E+11	6.9E+11	4.9E+11	-2.1E+11	-2.4E+12	-8.2E+12
8.6E-06	2.7	6.6E+11	6.2E+11	5.8E+11	5.6E+11	5.3E+11	4.9E+11	3.5E+11	-1.5E+11	-1.7E+12	-5.8E+12
7.1E-06	2.4	4.8E+11	4.5E+11	4.3E+11	4.1E+11	3.9E+11	3.6E+11	2.5E+11	-1.1E+11	-1.2E+12	-4.3E+12
5.8E-06	2.1	3.4E+11	3.2E+11	3.1E+11	2.9E+11	2.8E+11	2.6E+11	1.8E+11	-7.7E+10	-8.9E+11	-3.1E+12
4.8E-06	1.7	2.3E+11	2.1E+11	2.0E+11	1.9E+11	1.8E+11	1.7E+11	1.2E+11	-5.1E+10	-5.9E+11	-2.0E+12
3.9E-06	1.5	1.7E+11	1.6E+11	1.5E+11	1.4E+11	1.3E+11	1.2E+11	8.7E+10	-3.7E+10	-4.3E+11	-1.5E+12
3.2E-06	1.2	1.1E+11	1.0E+11	9.7E+10	9.2E+10	8.8E+10	8.1E+10	5.7E+10	-2.4E+10	-2.8E+11	-9.7E+11
2.6E-06	1	7.4E+10	7.0E+10	6.6E+10	6.3E+10	6.0E+10	5.5E+10	3.9E+10	-1.7E+10	-1.9E+11	-6.6E+11
2.2E-06	0.9	5.5E+10	5.2E+10	4.9E+10	4.7E+10	4.4E+10	4.1E+10	2.9E+10	-1.2E+10	-1.4E+11	-4.9E+11
1.8E-06	0.7	3.5E+10	3.3E+10	3.1E+10	3.0E+10	2.8E+10	2.6E+10	1.8E+10	-7.9E+09	-9.1E+10	-3.1E+11
1.5E-06	0.7	2.9E+10	2.7E+10	2.6E+10	2.4E+10	2.3E+10	2.1E+10	1.5E+10	-6.5E+09	-7.4E+10	-2.6E+11
9.1E-07	0.8	2.0E+10	1.9E+10	1.8E+10	1.7E+10	1.7E+10	1.5E+10	1.1E+10	-4.6E+09	-5.3E+10	-1.8E+11
Saturation ratio		4153626191.9	13749492.9	160167.8	4582.4	254.4	23.3	3.4	0.8	0.2	0.1
Condensation rate		**1.4E+14**	**1.4E+14**	**1.3E+14**	**1.2E+14**	**1.2E+14**	**1.1E+14**	**7.7E+13**	**-3.3E+13**	**-3.7E+14**	**-1.3E+15**

Table F.3: Gas-to-particle conversion calculations for NaCl (g)

D (m)	Temperature (K) / Frequency/Diffusivity	773 / 1.60E-05	873 / 1.70E-05	973 / 1.80E-05	1073 / 1.89E-05	1173 / 1.97E-05	1273 / 2.05E-05	1373 / 2.13E-05	1473 / 2.21E-05	1573 / 2.28E-05	1673 / 2.35E-05
3.0E-04	0.1	3.6E+11	2.4E+11	-1.4E+12	-1.6E+13	-8.0E+13	-3.0E+14	-8.8E+14	-2.2E+15	-4.9E+15	-9.6E+15
2.5E-04	0.5	1.5E+12	9.8E+11	-5.6E+12	-6.6E+13	-3.3E+14	-1.2E+15	-3.6E+15	-9.1E+15	-2.0E+16	-4.0E+16
2.0E-04	1.1	2.6E+12	1.8E+12	-1.0E+13	-1.2E+14	-5.9E+14	-2.2E+15	-6.6E+15	-1.7E+16	-3.6E+16	-7.2E+16
1.7E-04	2.3	4.5E+12	3.0E+12	-1.7E+13	-2.1E+14	-1.0E+15	-3.8E+15	-1.1E+16	-2.8E+16	-6.2E+16	-1.2E+17
1.4E-04	3.8	6.2E+12	4.1E+12	-2.4E+13	-2.8E+14	-1.4E+15	-5.1E+15	-1.5E+16	-3.9E+16	-8.5E+16	-1.7E+17
1.1E-04	5.5	7.3E+12	4.9E+12	-2.8E+13	-3.3E+14	-1.6E+15	-6.1E+15	-1.8E+16	-4.6E+16	-1.0E+17	-2.0E+17
9.2E-05	6.8	7.4E+12	5.0E+12	-2.9E+13	-3.4E+14	-1.7E+15	-6.1E+15	-1.8E+16	-4.6E+16	-1.0E+17	-2.0E+17
7.6E-05	7.7	6.9E+12	4.6E+12	-2.7E+13	-3.1E+14	-1.5E+15	-5.7E+15	-1.7E+16	-4.3E+16	-9.5E+16	-1.9E+17
6.2E-05	8.0	5.9E+12	3.9E+12	-2.3E+13	-2.7E+14	-1.3E+15	-4.9E+15	-1.5E+16	-3.7E+16	-8.1E+16	-1.6E+17
5.1E-05	7.9	4.8E+12	3.2E+12	-1.8E+13	-2.2E+14	-1.1E+15	-4.0E+15	-1.2E+16	-3.0E+16	-6.5E+16	-1.3E+17
4.2E-05	7.4	3.7E+12	2.5E+12	-1.4E+13	-1.7E+14	-8.2E+14	-3.0E+15	-9.1E+15	-2.3E+16	-5.0E+16	-9.9E+16
3.4E-05	6.7	2.7E+12	1.8E+12	-1.0E+13	-1.2E+14	-6.1E+14	-2.3E+15	-6.7E+15	-1.7E+16	-3.7E+16	-7.4E+16
2.8E-05	5.9	2.0E+12	1.3E+12	-7.6E+12	-8.9E+13	-4.4E+14	-1.6E+15	-4.9E+15	-1.2E+16	-2.7E+16	-5.3E+16
2.3E-05	5.2	1.4E+12	9.6E+11	-5.5E+12	-6.5E+13	-3.2E+14	-1.2E+15	-3.5E+15	-8.9E+15	-2.0E+16	-3.9E+16
1.9E-05	4.6	1.0E+12	6.9E+11	-4.0E+12	-4.7E+13	-2.3E+14	-8.6E+14	-2.6E+15	-6.4E+15	-1.4E+16	-2.8E+16
1.6E-05	4.0	7.4E+11	4.9E+11	-2.8E+12	-3.3E+13	-1.7E+14	-6.1E+14	-1.8E+15	-4.6E+15	-1.0E+16	-2.0E+16
1.3E-05	3.5	5.3E+11	3.6E+11	-2.0E+12	-2.4E+13	-1.2E+14	-4.4E+14	-1.3E+15	-3.3E+15	-7.3E+15	-1.4E+16
1.1E-05	3.1	3.9E+11	2.6E+11	-1.5E+12	-1.7E+13	-8.7E+13	-3.2E+14	-9.6E+14	-2.4E+15	-5.3E+15	-1.0E+16
8.6E-06	2.7	2.8E+11	1.8E+11	-1.1E+12	-1.2E+13	-6.2E+13	-2.3E+14	-6.8E+14	-1.7E+15	-3.8E+15	-7.4E+15
7.1E-06	2.4	2.0E+11	1.3E+11	-7.7E+11	-9.1E+12	-4.5E+13	-1.7E+14	-5.0E+14	-1.3E+15	-2.8E+15	-5.4E+15
5.8E-06	2.1	1.4E+11	9.7E+10	-5.6E+11	-6.5E+12	-3.2E+13	-1.2E+14	-3.6E+14	-9.0E+14	-2.0E+15	-3.9E+15
4.8E-06	1.7	9.6E+10	6.4E+10	-3.7E+11	-4.3E+12	-2.1E+13	-8.0E+13	-2.4E+14	-6.0E+14	-1.3E+15	-2.6E+15
3.9E-06	1.5	6.9E+10	4.7E+10	-2.7E+11	-3.1E+12	-1.6E+13	-5.8E+13	-1.7E+14	-4.3E+14	-9.5E+14	-1.9E+15
3.2E-06	1.2	4.6E+10	3.1E+10	-1.8E+11	-2.1E+12	-1.0E+13	-3.8E+13	-1.1E+14	-2.8E+14	-6.3E+14	-1.2E+15
2.6E-06	1.0	3.1E+10	2.1E+10	-1.2E+11	-1.4E+12	-7.0E+12	-2.6E+13	-7.7E+13	-1.9E+14	-4.3E+14	-8.4E+14
2.2E-06	0.9	2.3E+10	1.5E+10	-8.9E+10	-1.0E+12	-5.2E+12	-1.9E+13	-5.7E+13	-1.4E+14	-3.2E+14	-6.2E+14
1.8E-06	0.7	1.5E+10	9.8E+09	-5.7E+10	-6.6E+11	-3.3E+12	-1.2E+13	-3.6E+13	-9.2E+13	-2.0E+14	-4.0E+14
1.5E-06	0.7	1.2E+10	8.1E+09	-4.7E+10	-5.5E+11	-2.7E+12	-1.0E+13	-3.0E+13	-7.5E+13	-1.7E+14	-3.3E+14
9.1E-07	0.8	8.6E+09	5.8E+09	-3.3E+10	-3.9E+11	-1.9E+12	-7.1E+12	-2.1E+13	-5.4E+13	-1.2E+14	-2.3E+14
Saturation ratio		136.2	3.4	0.2	0.0	0.0	0.0	0.0	0.0	0.0	0.0
Condensation rate		**6.1E+13**	**4.1E+13**	**-2.3E+14**	**-2.8E+15**	**-1.4E+16**	**-5.1E+16**	**-1.5E+17**	**-3.8E+17**	**-8.3E+17**	**-1.6E+18**

Table F.4: Gas-to-particle conversion calculations for Na_2SO_4 (g)

D (m)	Temperature (K) / Frequency/Diffusivity	773 / 6.86E-06	873 / 7.29E-06	973 / 7.70E-06	1073 / 8.08E-06	1173 / 8.45E-06	1273 / 8.81E-06	1373 / 9.15E-06	1473 / 9.47E-06	1573 / 9.79E-06	1673 / 1.01E-05
3.0E-04	0.1	7.7E+10	7.3E+10	6.9E+10	6.5E+10	6.2E+10	5.2E+10	7.7E+09	-1.9E+11	-9.2E+11	-3.1E+12
2.5E-04	0.5	3.2E+11	3.0E+11	2.8E+11	2.7E+11	2.5E+11	2.2E+11	3.1E+10	-7.9E+11	-3.8E+12	-1.3E+13
2.0E-04	1.1	5.7E+11	5.4E+11	5.1E+11	4.8E+11	4.6E+11	3.9E+11	5.7E+10	-1.4E+12	-6.8E+12	-2.3E+13
1.7E-04	2.3	9.8E+11	9.2E+11	8.7E+11	8.3E+11	7.9E+11	6.7E+11	9.8E+10	-2.4E+12	-1.2E+13	-4.0E+13
1.4E-04	3.8	1.3E+12	1.3E+12	1.2E+12	1.1E+12	1.1E+12	9.1E+11	1.3E+11	-3.3E+12	-1.6E+13	-5.4E+13
1.1E-04	5.5	1.6E+12	1.5E+12	1.4E+12	1.3E+12	1.3E+12	1.1E+12	1.6E+11	-3.9E+12	-1.9E+13	-6.4E+13
9.2E-05	6.8	1.6E+12	1.5E+12	1.4E+12	1.4E+12	1.3E+12	1.1E+12	1.6E+11	-4.0E+12	-1.9E+13	-6.5E+13
7.6E-05	7.7	1.5E+12	1.4E+12	1.3E+12	1.3E+12	1.2E+12	1.0E+12	1.5E+11	-3.7E+12	-1.8E+13	-6.0E+13
6.2E-05	8.0	1.3E+12	1.2E+12	1.1E+12	1.1E+12	1.0E+12	8.6E+11	1.3E+11	-3.2E+12	-1.5E+13	-5.1E+13
5.1E-05	7.9	1.0E+12	9.7E+11	9.2E+11	8.7E+11	8.2E+11	7.0E+11	1.0E+11	-2.6E+12	-1.2E+13	-4.2E+13
4.2E-05	7.4	7.9E+11	7.4E+11	7.1E+11	6.7E+11	6.3E+11	5.4E+11	7.9E+10	-2.0E+12	-9.4E+12	-3.2E+13
3.4E-05	6.7	5.9E+11	5.5E+11	5.2E+11	5.0E+11	4.7E+11	4.0E+11	5.9E+10	-1.5E+12	-7.0E+12	-2.4E+13
2.8E-05	5.9	4.3E+11	4.0E+11	3.8E+11	3.6E+11	3.4E+11	2.9E+11	4.2E+10	-1.1E+12	-5.1E+12	-1.7E+13
2.3E-05	5.2	3.1E+11	2.9E+11	2.7E+11	2.6E+11	2.5E+11	2.1E+11	3.1E+10	-7.6E+11	-3.7E+12	-1.2E+13
1.9E-05	4.6	2.2E+11	2.1E+11	2.0E+11	1.9E+11	1.8E+11	1.5E+11	2.2E+10	-5.5E+11	-2.7E+12	-9.0E+12
1.6E-05	4.0	1.6E+11	1.5E+11	1.4E+11	1.4E+11	1.3E+11	1.1E+11	1.6E+10	-4.0E+11	-1.9E+12	-6.4E+12
1.3E-05	3.5	1.1E+11	1.1E+11	1.0E+11	9.7E+10	9.2E+10	7.8E+10	1.1E+10	-2.8E+11	-1.4E+12	-4.6E+12
1.1E-05	3.1	8.3E+10	7.9E+10	7.4E+10	7.1E+10	6.7E+10	5.7E+10	8.3E+09	-2.1E+11	-9.9E+11	-3.4E+12
8.6E-06	2.7	5.9E+10	5.6E+10	5.3E+10	5.0E+10	4.8E+10	4.0E+10	5.9E+09	-1.5E+11	-7.1E+11	-2.4E+12
7.1E-06	2.4	4.3E+10	4.1E+10	3.9E+10	3.7E+10	3.5E+10	3.0E+10	4.3E+09	-1.1E+11	-5.2E+11	-1.8E+12
5.8E-06	2.1	3.1E+10	2.9E+10	2.8E+10	2.6E+10	2.5E+10	2.1E+10	3.1E+09	-7.7E+10	-3.7E+11	-1.3E+12
4.8E-06	1.7	2.1E+10	1.9E+10	1.8E+10	1.8E+10	1.7E+10	1.4E+10	2.1E+09	-5.1E+10	-2.5E+11	-8.3E+11
3.9E-06	1.5	1.5E+10	1.4E+10	1.3E+10	1.3E+10	1.2E+10	1.0E+10	1.5E+09	-3.7E+10	-1.8E+11	-6.0E+11
3.2E-06	1.2	9.9E+09	9.3E+09	8.8E+09	8.4E+09	7.9E+09	6.7E+09	9.8E+08	-2.4E+10	-1.2E+11	-4.0E+11
2.6E-06	1.0	6.7E+09	6.3E+09	6.0E+09	5.7E+09	5.4E+09	4.6E+09	6.7E+08	-1.7E+10	-8.0E+10	-2.7E+11
2.2E-06	0.9	5.0E+09	4.7E+09	4.4E+09	4.2E+09	4.0E+09	3.4E+09	4.9E+08	-1.2E+10	-5.9E+10	-2.0E+11
1.8E-06	0.7	3.2E+09	3.0E+09	2.8E+09	2.7E+09	2.5E+09	2.2E+09	3.2E+08	-7.9E+09	-3.8E+10	-1.3E+11
1.5E-06	0.7	2.6E+09	2.5E+09	2.3E+09	2.2E+09	2.1E+09	1.8E+09	2.6E+08	-6.5E+09	-3.1E+10	-1.1E+11
9.1E-07	0.8	1.9E+09	1.7E+09	1.7E+09	1.6E+09	1.5E+09	1.3E+09	1.8E+08	-4.6E+09	-2.2E+10	-7.5E+10
Saturation ratio		471017643.7	2240012.0	34014.1	1185.2	76.3	7.8	1.2	0.2	0.1	0.0
Condensation rate		**1.3E+13**	**1.2E+13**	**1.2E+13**	**1.1E+13**	**1.1E+13**	**8.9E+12**	**1.3E+12**	**-3.3E+13**	**-1.6E+14**	**-5.3E+14**

F.2: Flue gas calculations

Flue Gas Molecular Weight Calculation							
Element	Moles	Product	mol O2	mol	% of gas	MW	Gas weight
C	6.535179	CO2	6.535179	6.535179	0.59513	44.01	26.19166723
H	4.449405	H2O	2.224702	2.224702	0.202594	18.016	3.649930373
O	0.749531	O2	0	2.132344	0.194183	3.20E+01	6.213860926
N	0.125357	NO2	0.003635	0.003635	0.000331	46	0.015228573
S	0.024375	N2	0	0.060861	0.005542	28	0.155185321
	11.88385	SO2	0.024375	0.024375	0.00222	64.06	0.142195498
Total			8.787892	10.9811			36.36806791

References

Allison, J., Brown, D. and Novo-Gradac, K. (1991). *MINTEQA2/PRODEFA2, A Geochemical Assessment Model for Environmental Systems: User's Manual* Environmental Research Laboratory, Georgia

Bale, C. W., Chartrand, P., Degterov, P. A., Eriksson, G., Hack, K., Ben Mahfoud, R., J., M., Pelton, P. A. and Petersen, S. (2002). *FactSage Thermochemical Software and Databases* [WWW] http://www.crct.polymtl.ca (30 July 2005)

Baxter, L., Miles, T., Jenkins, B., Dayton, D., Milne, T., Bryers, R. and Oden, L. (1996). *Alkali Deposits Found in Biomass Power Plants*. Sandia National Laboratories, US Department of Energy

Baxter, L., Miles, T., Jenkins, B., Dayton, D., Milne, T., Bryers, R. and Oden, L. (1998). "The Behaviour of Inorganic Material in Biomass-fired Power Boilers." *Fuel Processing Technology,* 54, 47-78

Baxter, L. (2005). "Biomass-coal Co-combustion: Opportunity for Affordable Renewable Energy." *Fuel*, 84(10), pp 1295-1302

Benson, S. and Holm, P. (1985). "Comparison of Inorganic Constituents in Three Low-rank Coals." *Industrial and Engineering Chemistry Product Research and Development,* 24, pp 145-149

Benson, S., Steadman, E., Zygarlicke, C. and Erickson, T. (1996). *Applications of Advanced Technology to Ash-Related Problems in Boilers*. Plenum Publishing Corporation, Portland

Biagini, E., Lippi, F., Petarca, L. and Tognotti, L. (2002). "Devolatilisation Rate of Biomasses and Coal-biomass Blends: An Experimental Investigation." *Fuel,* 81, pp 1041-1050

Blakemore, L., Searle, P. and Daly, B. (1987). *Methods for Chemical Analysis of Soils*. Scientific report 80, NZ Soil Bureau, New Zealand

Blander, M., Milne, T.A., Dayton, D.C., Backman, R., Blake, D., Kuhnel, V., Linak, W., Nordin, A.and Ljung, A. (2001). "Equilibrium Chemistry of Biomass Combustion: A Round-robin Set of Calculations using Available Computer Programs and Databases." *Energy and Fuels*, 15(2), pp 344-349

Bryers, R. (1996). "Fireside Slagging, Fouling and High Temperature Corrosion of Heat Transfer Surface Due to Impurities in Steam-Raising Fuels." *Progress in Energy Science Combustion*, 22(120), pp 29

Buhre, B., Hinkley, J., Gupta, R., Wall, T. F. and Nelson, P. (2003). "Submicron Ash Formation from Vaporisation of Minerals in Coal." *12th International Conference on Coal Science,* Cairns, Australia

Buhre, B., Hinkley, J, Gupta, R., Wall, T. and Nelson, P. (2005). "Submicron Ash Formation from Coal Combustion." *Fuel*, 84(10) pp 1206-1214

CEN/TC 292 (2005). *European Committee of Standardisation.* "Characterisation of Waste Leaching Behaviour Tests - Influence of pH on Leaching with Continuous pH-control TS14997." [WWW] http://www.cen.eu/cenorm/index.htm (20 October 2005)

Christensen, K., Stenholm, M. and Livbjerg, H. (1998). "The Formation of Submicron Aerosol Particles, HCl and SO_2 in Straw-Fired Boilers." *Journal of Aerosol Science,* 29, pp 421–444

Couch, G. (1994). *Understanding Slagging and Fouling During PF Combustion.* IEA Coal Research, London

Dayton, D., Belle-Oudrey, D. and Nordin, A. (1999). "Effect of Coal Minerals on Chlorine and Alkali Metals Released during Biomass/Coal Cofiring." *Energy & Fuels,* 13, 1203-1211

Dijkstra, J., van der Sloot, H. and Comans, R. (2006). "The Leaching of Major and Trace Elements from MSWI Bottom Ash as A Function of pH and Time*." Applied Geochemistry,* 21 (2), pp 335 – 351

Dios de, A. (not dated). *Chemical Equilibria.* [WWW] http://bouman.chem.georgetown.edu/S02/lect8/lect8 (28 February 2005)

Dzombak, D.A., Morel, F.(1990). *Surface Complexation Modelling: Hydrous Ferric Oxide.* John Wiley & Sons, Inc, New York

Frandsen, F., Lith van, S., Korbee, R., Yrjas, P., Backman, R., Obenberger, I., Brunner, T. And Joller, M. (2006). "Quantification of the Release of Inorganic Elements from Biofuel." *Ash Deposition Conference*, Snowbird, Utah

Freidlander, S. (2000). *Smoke, Dust and Haze: Fundamentals of Aerosol Dynamics.* Second Edition, Oxford University Press, New York

Glarborg, P. and Marshall, P. (2005). "Mechanism and Modelling of the Formation of Gaseous Alkali Sulfates." *Combustion and Flame*, 141(1), pp 22-39

Gupta, R. P., Beacher, C., Bhargava, A. and Wall, T. F. (2002). "The Fate of Inorganic Matter in Biomass during Combustion." *19th Annual Pittsburgh Coal Science Conference*, Pittsburgh

Gupta, R. (2005). "Coal Research in Newcastle—Past, Present and Future" *Fuel* 84(10), pp 1176-1188

Hiemstra, T., Riemsdijk, van W., Bolt, G. (1989). "Multisided Proton Adsorption Modelling at the Solid/solution Interface of (Hydr)oxides: A New Approach (I) - Model Description and Evaluation of Intrinsic Reaction Constants." *Journal of Colloid Interface Science,* 133, pp 91-104

Iwamatsu, M. (1994). "Homogeneous Nucleation of Spherical Droplets and Bubbles." *Chinese Journal of Physics*, 33 (2)

Jacobson, M. (1999). *Fundamentals of Atmospheric Modelling*, Cambridge Press, UK

Jak, E. and Saulov, D. *Prediction of ash phase equilibria using FACT models.* Research Report 54. CRC for Coal in Sustainable Development, Australia

Jenkins, B., Baxter, L., Miles, T. and Miles, T. J. (1998). "Combustion Properties of Biomass." *Fuel Processing Technology,* 54, pp 17–46

Jimenez, S. and Ballester, J. (2005). "Influence of Operating Conditions and the Role of Sulfur in the Formation of Aerosols from Biomass Combustion." *Combustion and Flame*, 140(4), pp 346-358

Jimenez, S. and Ballester, J. (2007). "Formation of Alkali Sulphate Aerosols in Biomass Combustion." *Fuel,* 86, 486–493

Joller, M., Brunner, T. and Obernberger, I. (2005). "Modelling of Aerosol Formation during Biomass Combustion in Grate Furnaces and Comparison with Measurements". *Energy & Fuels,* 19, pp 311-323

Kinniburgh, D., Riemsdijk van, W., Koopal,L. Borkovec, M., Benedetti, M. and Avena, M. (1999). "Ion binding to natural organic matter: competition, heterogeneity, stoichiometry and thermodynamic consistency." *Colloids and Surfaces: Physicochemical and Engineering Aspects*, 151, pp 147-166

Knacke, O., Kubaschewski, O. and Hesselmann, K. (1991). *Thermochemical Properties of Inorganic Substances* 2nd Edition, Springer-Verlag, Berlin

Knudsen, J., Jensen, P., Weigang, L., Frandsen, F. and Dam-Johanes, K. (2004). "Sulfur Transformations during Thermal Conversion of Herbaceous Biomass." *Energy & Fuels,* 18, pp 810-819

Knudsen, J., Jensen, P. and Dam-Johanes, K. (2004). "Transformation and Release to the Gas-phase of Cl, K and S during Combustion of Annual Biomass." *Energy & Fuels*, 18(5), pp 1385-1399

Korbee, R., Eenkhoorn, S., Heere, P. and Kiel, J. (2002). *Prediction of Ash and Deposit Formation for Biomass Co-combustion*. Report. Energy Research Centre, Netherlands

Korbee, R., Kiel, J. H. A., Zevenhoven, M., Skrifvars, B., Jensen, P. and Frandsen, F. (2003). *Investigation of biomass inorganic matter by advanced fuel analysis and conversion experiments*. Report BioAerosol Project, Energy Research Centre of Netherlands

Korbee, R. and Cieplik, M. (2006). "Ash Formation from Biofuels and Coal in pf Systems." *Ash Deposition Conference*, Snowbird, Utah

Kostka, J. and Luther III, G. (1994). "Partitioning and Speciation of Solid Phase Iron in Salt Marsh Sediments." *Geochimica Et Cosmochimica Acta*, 58(1), pp 1701-1710

Loo, S. van. (2002). *Handbook of Biomass Combustion and Co-Firing.* Twente University Press, Enschede

Marschener, H. (1995). *Mineral Nutrition of Higher Plants*, Academic Press, 2nd Edition

Mc Nallan, M., Yurek, G. and Elliott, J. (1980). "The Formation of Inorganic Particulates by Homogeneous Nucleation in Gases Produced by the Combustion of Coal." *Combustion and Flame*, 42, pp 45-60

Monroe, L. (1989). *An Experimental Study of Residual Fly ash Formation in Combustion of a Bituminous Coal*. Doctor of Philosophy. Chemical Engineering, Cambridge, Massachusetts Institute of Technology

Nussbaumer, T. (2003). *Combustion and Co-combustion of Biomass: Fundamentals, Technologies and Primary Measures for Emission Reduction.* Verenum Technology, Zurich

Peeters, P. (2002). *Nucleation and Condensation in Gas-Vapor Mixtures of Alkanes and Water.* Doctor of Philosophy. Eindhoven University of Technology, The Netherlands.

Pronobis, M. (2005). "Evaluation of the Influence of Biomass Co-combustion on Boiler Furnace Slagging by Means of Fusibility Correlations." *Biomass and Bioenergy* 28, pp 375–383

Robinson, A., Baxter, L., Junker, H. and Shaddix, C. (1998). *Fireside Issues Associated with Coal-Biomass Co-firing.* Sandia National Laboratories, USA.

Robinson, A., Junker, H. and Baxter, L. (2002). "Pilot-Scale Investigation of the Influence of Coal-Biomass Co firing on Ash Deposition." *Energy and Fuels,* 16, 343-355

Sami, M., Annamalai, K. and Wooldrigde, M. (2001). "Co-firing of Coal and Biomass Fuel Blends." *Progress in Energy and Combustion Science* 27, pp171–214

Sarofim, A., Padia, A. and Howard, J. (1977). "The Physical Transformation of the Mineral Matter in Pulverized Coal Under Simulated Combustion Conditions," *Combustion Science Technology*, 16, pp187-204

Skrifvars, B.O. and Backman, R. (2001). "Thermodynamic stability calculations in predicting corrosion behaviour at elevated temperature." *Materials Science Forum*, 369-372, pp 923-930

Seinfeld, J. and Pandis, S. (1998). *Atmospheric Chemistry and Physics,* Wiley Interscience, Canada

Sloot, van der H., Zomeren van, A., Siegnette, P., Dijkstra, J., Comans, R. and Meussen, H. (2003). "Evaluation of Environmental Aspects of Alternative Materials using an Integrated Approach Assisted by a Database/Expert System." Keynote paper. *Conference of Advances in Waste Management and Recycling*, Dundee

Sloot van der, H. and Zomeren van, A. (2005). "Prediction of the Leaching Behaviour of Waste Mixtures by Chemical Speciation Modelling Based on a Limited Set of Key Parameters." *10th International waste management and landfill symposium,* Sardinia, Italy

Strand, M. Bohgard, M. Sweitlicki, E. Gharibi, A. & Sanati, M. (2004). "Laboratory and Field Test of a Sampling Method for Characterization of Combustion Aerosols at High Temperatures." *Journal of Aerosol Science and Technology,* 38, pp 757-765

Swift, R. S. (1996). *Organic matter characterization, in Methods of Soil Analysis: Chemical Methods*. Soil Science Society. America. pp 1011-1069

Thurman, E. and Malcolm, R. (1981). "Preparative Isolation of Aquatic Humic Substances." *Environment Science Technology,* 15, pp 463-466

Williams, A., Pourkashanian, M. and Jones, J. (2001). "Combustion of Pulverised Coal and Biomass." *Progress in Energy and Combustion Science*, 27, pp 587-610.

Wei, X., Schnellb, U. and Hein, K. (2005). "Behaviour of Gaseous Chlorine and Alkali Metals during Biomass Thermal Utilisation." *Fuel,* 84, pp 841-848

Werkelin, J. (2005). "Chemical Forms of Ash-forming Matter in Woody Fuels for FBC." *18th International Conference on Fluidized Bed Combustion*, Toronto, Canada

Wu, H., Wall, T., Liu, G. and Bryant, G. (1999). "Ash Liberation from Included Minerals during Combustion of Pulverised Coal: the Relationship with Char Structure and Burnout." *Energy and Fuels*, 13, pp 1197-1202

Yamashita, T., Teramae, T. And Tominaga, H. (1998). "Fly Ash Formation Behaviour in Pulverised Coal Combustion." *19th Annual Pittsburgh Coal Science Conference*, Pittsburgh

Yan, L. (2000). *CCSEM Analysis of Minerals in Pulverised Coal and Ash Formation Modelling,* Doctor of Philosophy, University of Newcastle, Newcastle, Australia

Yan, L., Gupta, R. and Wall, T. (2001). "The Implication of Mineral Coalescence Behaviour on Ash Formation and Ash Deposition during Pulverised Coal Combustion." *Fuel*, 80, pp 1333-1340

Yan, L., Gupta, R. and Wall, T. (2002). "A Mathematical Model of Ash Formation during Pulverised Coal Combustion." *Fuel,* 81, 337-344

Zevenhoven, M., Blomquist, J., Skrifvars, B., Backman, R. and Hupa, M. (2000). "The Ash Chemistry in Fluidised Bed Gasification of Biomass Fuels." *Fuel*, 79, 1353-1361.

Zevenhoven, M., Skrifvars, B., Yrjas, P., Hupa, M., Nuutinen, L. And Laitinen, R. (2001). "Searching for Improved Characterization of Ash Forming Matter in Biomass." *16th International Conference on Fluidized Bed Combustion,* Nevada

Zevenhoven, M., Backman, R., Skrifvars, B. and Hupa, M. (2005). " Appearance of Trace Elements." *18th International Conference on Fluidised Bed Combustion*. Toronto, Canada

Zheng, Y., Jensen, P., Jensen, A., Sander, B.and Junker, H. (2007). "Ash Transformation during Co-firing Coal and Straw" *Fuel*, 86, pp 1008-1020

Zomeren van, A. (Submitted for publication, 2006). "Measurement of Humic and Fulvic Acid Concentrations and Dissolution Properties by a Rapid Batch Procedure." *Environment Science Technology*

Zygarlicke, C., McCollor, D., Eylands, K., Hetland, M., Musich, M., Crocker, C., Dahl, J. and Laducer, S. (2001). *Impacts of Co firing Biomass with Fossil Fuels.* U.S. Department of Energy, National Energy Technology Laboratory, Pittsburgh

List of Publications

Doshi, V., Vuthaluru, H., Korbee, R. and Kiel, J. (2005). "Prediction of Ash Formation Behaviour of Biomass during Combustion through Characterisation of Inorganic Matter." *Chemeca*, Queensland

Doshi, V., Vuthaluru, H., Korbee, R., Lensselink, J. and Kiel, J. (2005). "Investigations into the Performance of Electrostatic Precipitators for Co-fired Boilers." *Chemeca*, Queensland

Coleman, H., Doshi, V., Vuthaluru, H., Korbee, R., Lensselink, J. and Kiel, J. (2005)."Investigations into the Effects of Biomass Co-firing on Fly Ash Resistivity." *7th World Congress in Chemical Engineering,* Glassgow

Doshi, V., Vuthaluru, H., Korbee, R., Lensselink, J. and Kiel, J. (2005). "Preliminary Studies on the Effects of Biomass Co-firing on Fly Ash Resistivity." *5th Asia-Pacific Conference on Combustion*, The University of Adelaide, South Australia

Doshi, V., Vuthaluru, H., Korbee, R. and Kiel, J. (*to be submitted for publication in Fuels*). " Ash formation model during co-firing of coal and biomass."

Doshi, V., Vuthaluru, H., Korbee, R. and Kiel, J. (*to be submitted for publication in Fuel Processing Technology*). "Determination of biomass speciation for ash formation modelling in biomass combustion."